sediments) and slopes at water depths of more than 2,500m where the sound pressure starts to rise (part of outcropping rocks). In this part, several parts of outcropping rock that divide the gently inclined taluses into two tiers, the upper and lower tiers, are recognized as steep inclines of about 100m wide and 1,000m long along the isobathymetric lines. This is considered to be the part with ore indications recognized by FDC images.

(94SSS02)

At track line 94SFDC01 on the central ridge that faces the northern ridge- on which track line 94SSS01 was established- across the central graben, ore indications were observed at several points on the slaggy lava part located on the southern ridge of the top. At track line 94SSS02, we conducted the survey along the FDC track line around the southern ridge.

Ranges presumed to be sediments with low reflexion sound pressure stretch on the eastern part of the topographic rise and the northern ridge part. A part with high reflexion sound pressure presumed to be outcropping rocks, which embraces a part with low sound pressure presumed to be sediments, is recognized as a linear part, which indicates the existence of step slopes. The distribution range of ore indications should be around this southern ridge part, but it is not clearly identified. This might be caused by the topography full of variety on which we established our towing route, which made the SSS-fish rise and fall extensively, resulting in blurred images.

From the above, the parts corresponding to the ore indications obtained by FDC observation are recognized at the fractures that are affected by the tectonic lines and at the mound-shaped structures on SSS images, but these are obtained as groups of small structures of less than 100m. Thus it is inferred that these ore indications obtained exist as an assembly of such small structures.

5-4 Characteristics of samples collected

Based on the results of FDC and SSS surveys, we conducted sampling by LC, CB and PG in three sea areas:

The 94S01 Seamount,the central part of the Erromango Basin and the 94S02 Seamount from where relatively extensive ore indications had been observed.

The LC is the same unit as we used for the Base-line Geochemical Exploration. The CB is a steel net fitted with pipes for sampling muddy substances. We collected samples by dredging the CB on the sea-floor. On the other hand, the finder mounted power grab (PG) can observe the sea-floor and collect samples simultaneously.

Some rock samples were collected from the FDC frame during the FDC survey conducted at the central part of the Vate Trough. These samples and samples collected from the three sea areas were included in our subjects for discussion.

Collected samples were listed and weighed rouguly. A portion was collected for laboratory tests (chemical analysis, powder X-ray diffraction tests and others) and the remainder was preserved.

Sampling locations, water depths, amount collected and others are shown in Appendix Table 4.

Sampling locations are shown in Annexed Figure 2; LC columnar charts are shown in Annexed Figure 3.

Samples were mainly manganese oxides, iron oxides, rocks and their altered substances. Muddy substances composed of clay, calcareous shells of foraminifera and clastic minerals were also collected at the same time.

Properties of muddy substances collected from these sea areas are already discussed in the section "Properties of samples collected" of the Base-line Geochemical Survey, so we will not discuss them here.

Properties of samples discussed by each sea area are described here.

(1) 94S01 Seamount

As chimneys and hydrothermal biotic communities on the eastern side of this Seamount had been identified by FDC, the sampling survey was conducted around this place. Ten rounds of LC (94SDLC01 ～ 07, 19 ～ 21) and five rounds of PG (94SDPG04 ～ 08) were carried out. Muddy substances were collected by four rounds of LC. Yellowish brown precipitates presumed to be iron oxides were contained in the general stratigraphic succession of these muddy substances. Most of these precipitates were in direct contact with rocks but, sometimes, brown or green sediments exist between them. Samples of 11kg and 400kg were collected by PG05 and PG07, respectively, but only rocks were collected in these two rounds. Gossan of about 0.5cm is developed on the surface of the rocks. Vitric film of about 1.5cm is concomitant under the gossan. Magnetism is normal and abundant dark gray porous, spheroidal exuviae of about from 1

to 2mm presumed to be phenocrysts are recoginzed (see Fig. 5-4-1 (1).

(2) Central part of the Vate Trough

15kg of rocks were collected from track line FDC08-1 at the central part of the Vate Trough. Only a part of these rocks is concomitant with gossan. These rocks are pillow lava usually developed with about 1cm thick, and black vitric film is developed on the surface. The inner side of these rocks is gray and compact with strong magnetism and a small amount of phenocrysts of about 3mm and a number of long columnar crystal with major axes of about 2mm are recognized (see Fig. 5-4-1 (1)).

(3) Central part of the Erromango Basin

Eight rounds of LC (94SDLC08 ～ 15) and three rounds of PG (94SDPG01 ～ 03) were conducted. Muddy substances were collected by six rounds of LC operation and the operation at PG01. General stratigraphic succession of the muddy ous substances is composed of a few centimeters thick surface layer of brown foraminiferan ooze, sometimes interlayered with about 2cm thick, black volcanic glass. Black manganese oxides of about from 3 to 20cm thick exist under the surface layer. Dark brown to light green semiconsolidated sediments develop under the black manganese oxides.

150kg and 315kg samples were collected at PG02 and PG03, respectively. Samples were mainly composed of black manganese oxides and semiconsolidated sediments,but rocks were also obtained. There are two kinds of manganese oxides: one is a few cm thick platy type and the other is a massive type. The surface of the platy type manganese oxides assumes fatty luster, a number of about from 1 to 2mm thick layers develop under the surface layer, and the under surface is coarse-grained.

Massive manganese oxides are, on the whole, coarse-grained and it is difficult to discern between the upper side and lower side.

Semiconsolidated sediments are not abundant, but there are brown and light green types. The surface of rocks is thinly covered with manganese oxides but not concomitant with vitric film. Magnetism is normal, and gray, compact phenocrysts (presumed to be pyroxene) of about from 1 to 2mm and long columnar crystals with about 2mm major axis are abundantly recognized (see Fig. 5-4-1 (2)).

(4) 94S02 Seamount

Three rounds of LC(94SDLC16 ～ 18) and two rounds of CB (94SDCB01 ～ 02) were

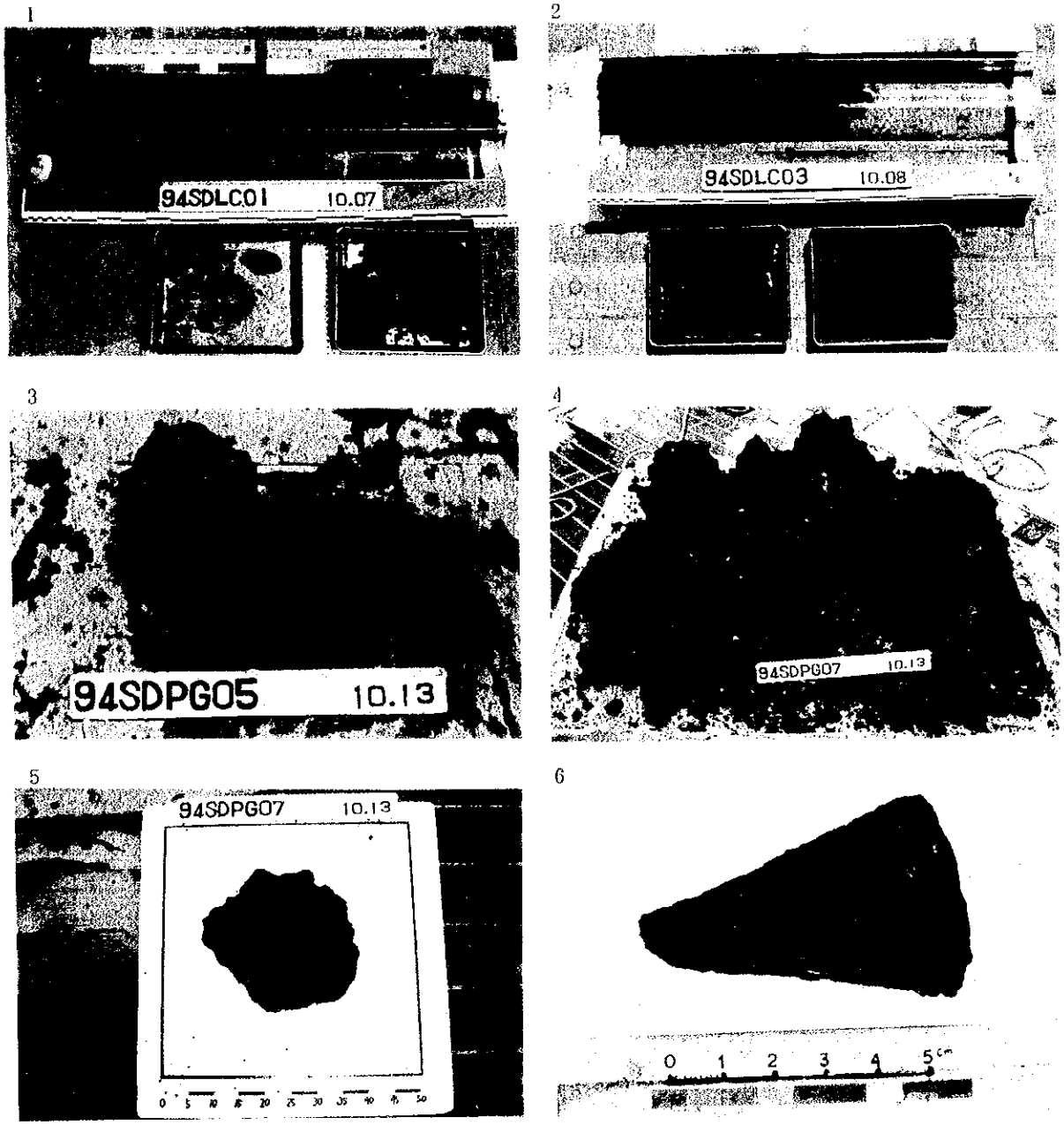

1. Sectional Plane of 94SDLC01 Sample (Core Length 50cm)
2. Sectional Plane of 94SDLC03 Sample (Core Length 86cm)
3. 94SDPG05 Sample (Recovery 10.5kg)
4. 94SDPG07 Sample (Recovery 400 kg)
5. Yellowish brown colured deposit [Iron Oxide] (94SDPG07)
6. Sectional Plane of Hypersthene-Augite Basalt (94SFDC08-1)

Figure 5-4-1 Photos of Samples Collected during Ore Deposit Investigation (94S01 Seamount, Central Part of the Vate Trough) (1)

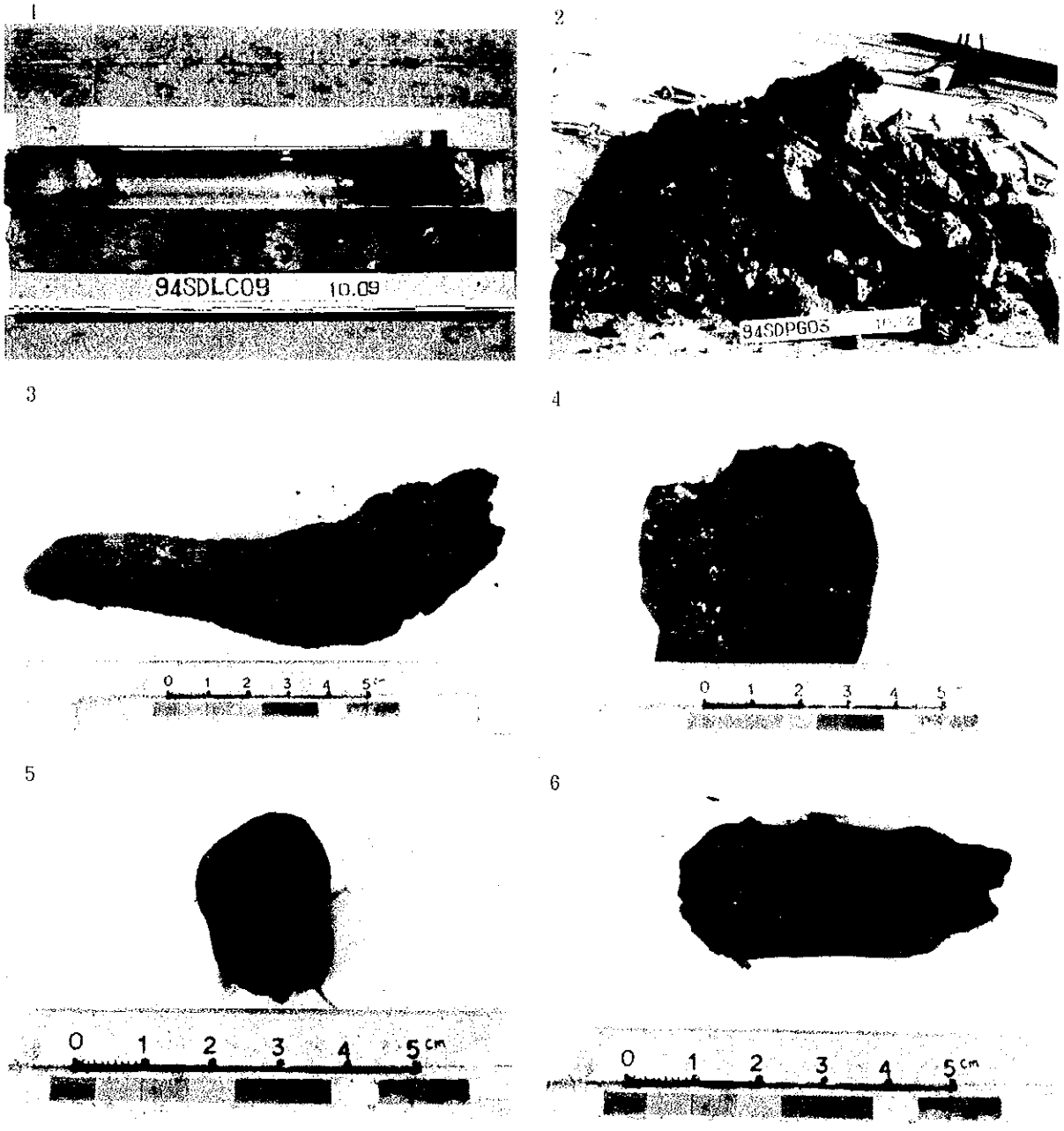

1. Sectional Plane of 94SDLC09 Sample (Core Length 146cm)
2. 94SDPG03 Sample (Recovery 315kg)
3. Sectional Plane of Muganese Oxide (94SDPG03)
4. Basaltic Pock (94SDPG03)
5. Maganese Chimney (Whole view) (94SDLC09)
6. Maganese Chimney (Whole view) (94SDLC09)

Figure 5-4-1 Photos of Samples Collected during Ore Deposit Investigation (Central Part of the Erromango Basin) (2)

conducted in this sea area. Reddish brown precipitates presumed to contain iron oxides (65cm) were collected from 94SDLC18. Precipitates assume partly green with small rock fragments at depths of more than 50cm, so the existence of rocks under this level is inferred. 59kg and 100kg samples were collected from 94SDCB01 and 94SDCB02, respectively. These samples are reddish brown, like the samples of LC18, and mainly classified into manganese oxides and rocks. Reddish brown precipitates are semiconsolidated substances with the maximum diameter of about 30cm, the surface of which is covered with thin manganese oxides (about 1mm thick). Manganese oxide veinlets (about from 1 to 2mm wide) are developed in the inner part of the substances which are fragile and can be easily broken by hand. These manganese oxides are crust with a maximum thickness of 4cm, and their inner part is filled with accidental substances like rock fragments. The surface of the rocks is concomitant with thin, reddish brown gossan (about from 1 to 2mm thick) but not vitric film.

These rocks are vesicular and assume dark gray with weak magnetism. A number of spheroidal, altered phenocrysts (presumed to be pyroxene) of about from 1 to 3mm are identified in these rocks (see Fig. 5-4-1 (3)).

<Thin section appraisal and powder X-ray diffraction test>

Thin section and X-ray diffraction on typical rock samples are discussed here. Figure 5-4-2 (1), (2) shows microphotographs. Results of thin section and X-ray diffraction are shown at the end of this report.

- (94SDLC01B)

  Rock: Non-porphyritic hypersthene augite Basalt

  Phenocryst is not recognized and plagioclase, glass and a small amount of hypersthene and augite are recognized in the matrix. Plagioclase assumes idiomorphic form and a moderate amount of plagioclase smaller than 0.3mm is recognized. Hypersthene and augite also assume an idiomorphic forms and a small amount smaller than 0.1mm is recognized. A great amount of glass is recognized.Glass has a large amount of pore spaces of from 0.5 to 4mm. It is very porous. It shows the variolitic or hyalopilitic texture. We did not conduct X-ray diffraction on this sample but a great amount of plagioclase and a trace amount of hypersthene and augite are detected from other samples (94SDLC03-7) collected from the 94S01 Seamount.

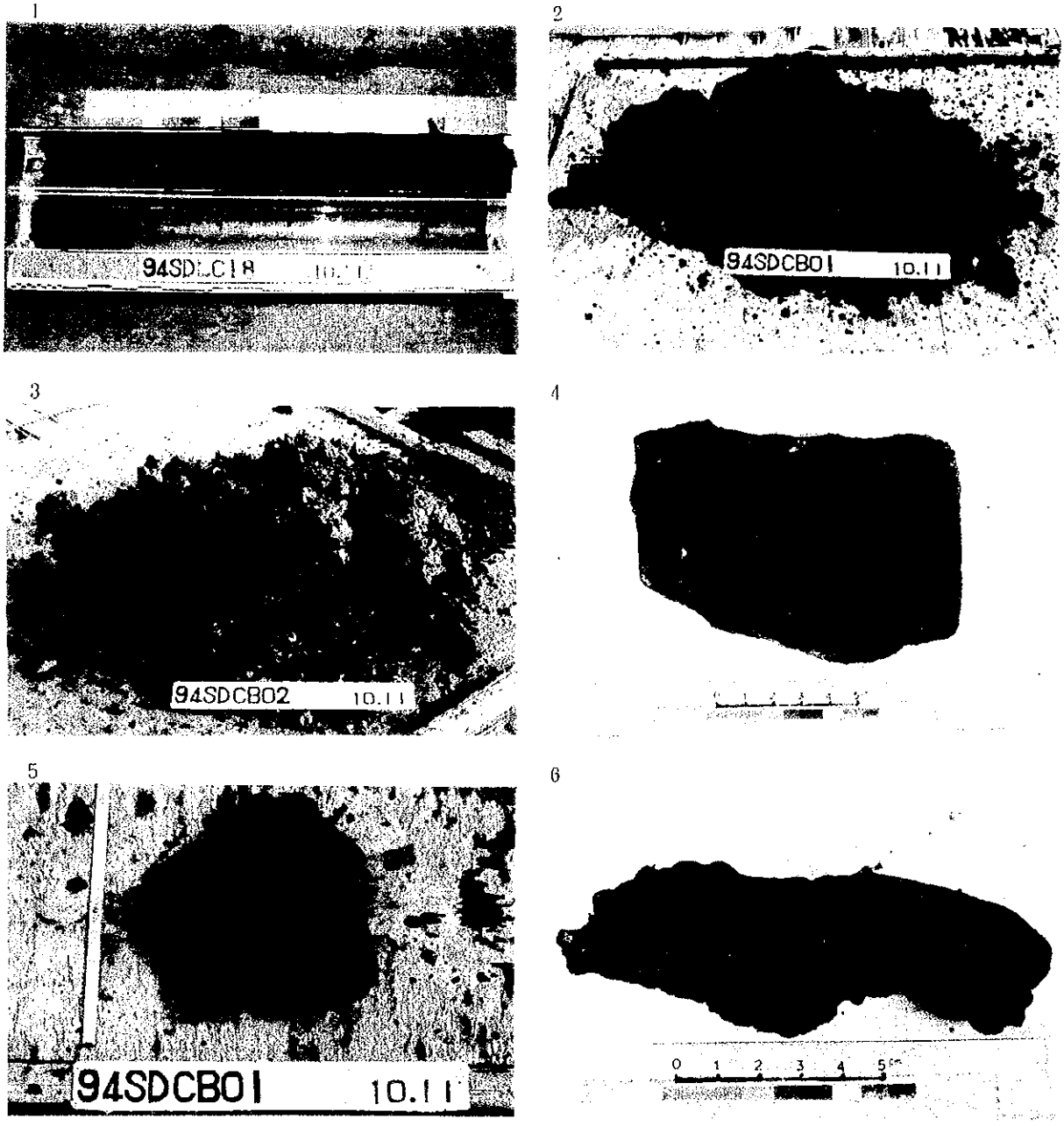

1. Sectional Plane of 94SDLC18 Sample (Core Length 65cm)
2. 94SDCB01 Sample (Recovery 59kg)
3. 94SDCB02 Sample (Recovery 100kg)
4. Sectional Plane of Hypersthene-Augite Andesite (94SDCB01)
5. Reddish Brown colured deposit [Fe-oxide] (94SDCB01)
6. Section Plane of Crust-type Mngabese Oxide (94SDCB02)

Figure 5-4-1 Photos of Samples Collected during Ore Deposit Investigation (94S02 Seamount) (3)

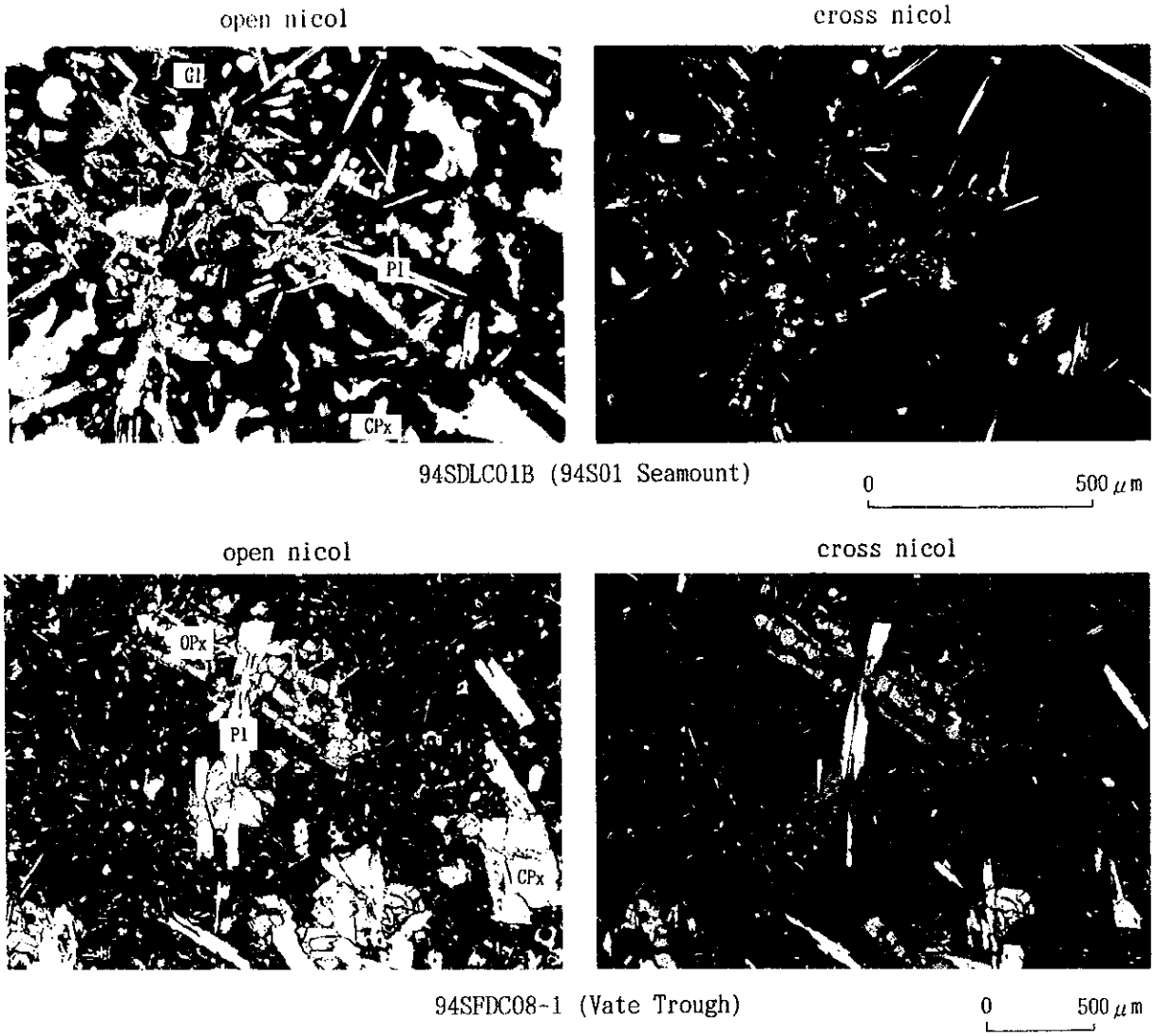

Figure 5-4-2 Microscopic Photos (Thin Section) (1)

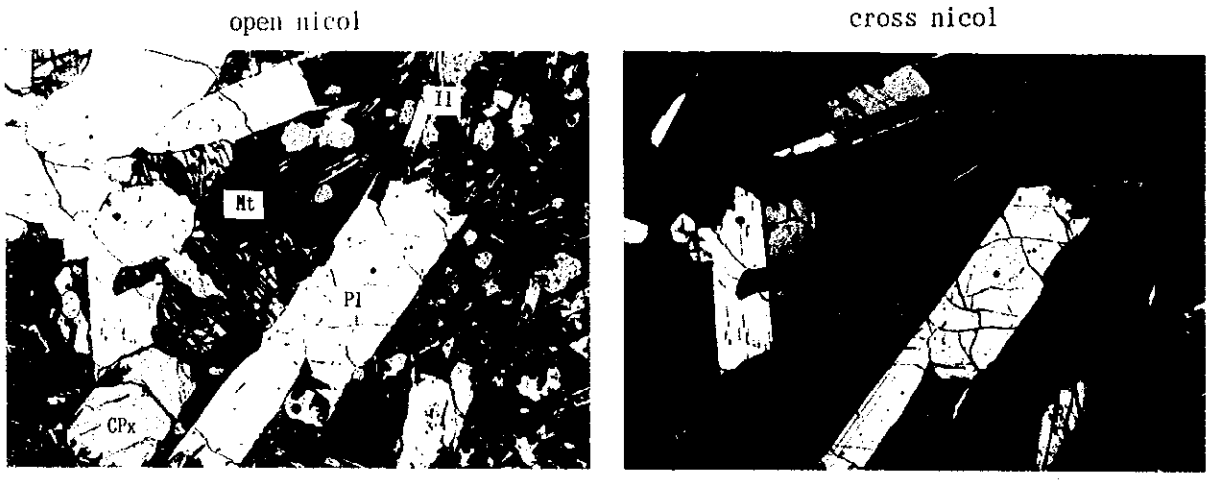

94SDPG02H (Erromango Basin)

0 500 μm

94SDCB02 (94S02 Seamount)

0 500 μm

Abbreviation

Fo : Foraminifera
Gc : Gas cavity
Gℓ : Glass
Iℓ : Ilmenite
Mt : Magnetite
Pℓ : Plagioclase
Px : Pyroxene
CPx : Clinopyroxene
OPx : Orthopyroxene
Sc : Scoria

Figure 5-4-2 Microscopic Photos (Thin Section) (2)

· (94SFDC08-1)

Rock: Hypersthene augite Basalt

This is a rock collected from the central part of the Vate Trough.

Plagioclase, augite and hypersthene are recognized in its phenocryst, and a moderate amount of plagioclase and augite as well as a small amount of hypersthene and glass are recognized in its matrix. Plagioclase, hypersthene and augite in the phenocryst assume idiomorphic forms and respective sizes are from 0.25 to 2mm, from 0.1 to 1mm and from 0.1 to 0.7mm. The matrix part is smaller than 0.1mm and indicates the internal (or variolitic) texture. The same minerals are also detected by X-ray diffraction.

· (94SDPG02H)

Rock: Hypersthene augite Basalt

This rock is collected from the central part of the Erromango Basin. Plagioclase, augite and hypersthene are recognized in its phenocryst, and a moderate amount of plagioclase and glass as well as a small amount of augite and hypersthene are recognized in its matrix. Plagioclase, hypersthene and augite in the phenocryst part assume idiomorphic forms and respective sizes are from 0.3 to 1.7mm, about 0.5mm and from 0.3 to 1.5mm. The matrix part is smaller than 0.1mm and indicates the variolitic or internal texture. The same minerals are also detected by X-ray diffraction.

· (94SDCB02)

Rock: Hypersthene augite Basalt

This rock is collected from the 94S02 Seamount. Plagioclase and augite are recognized in its phenocryst, and a moderate amount of plagioclase and glass as well as a small amount of augite and hypersthene are recognized. Plagioclase, hypersthene and augite in the phenocryst part assume idiomorphic forms and respective sizes are from 0.3 to 1mm, from 0.2 to 0.4mm and from 0.25 to 0.6mm. The matrix part is about 0.1mm except plagioclase of about 0.3mm and indicates the internal texture. The same minerals are also detected by X-ray diffraction.

<Chemical Analysis>

Analytical components and the limit of detection are as follows:

SiO_2, TiO_2, Al_2O_3, Fe_2O_3, FeO, MnO, MgO, CaO, Na_2O, K_2O, P_2O_5, H_2O+, H_2O-, Co_2 (the limit of detection of above 14 components is 0.02%), Ba (1ppm), Rb (0.1ppm), Sr (1ppm), Pb (1ppm), Zr (1ppm), Nb (0.5ppm), Y (1ppm), V (1ppm), Cr (1ppm), Ni (1ppm), Cu (1ppm), Zn (1ppm) Ga (0.5ppm), S (100ppm), Sc (0.1ppm), Cs (0.1ppm), La (0.1ppm) Ce (0.1ppm), Nd (0.1ppm), Sm (0.01ppm), Eu (0.01ppm), Gd (0.1ppm), Tb (0.01ppm), Ho (0.01ppm), Tm (0.01ppm), Yb (0.01ppm), Lu (0.01ppm), Hf (0.1ppm), Ta (0.1ppm) and Th (0.1ppm).

Figures and units in the parentheses of elements other than the 14 whole rock components show the limits of detection.

The determination of samples were made by the following analytical methods:

Analytical Element	Method of Analysis
SiO_2, TiO_2, Al_2O_3, Fe_2O_3, MnO, MgO, CaO, Na_2O, K_2O, P_2O_5, V, Cr, Ni, Cu, Zn, Gd, Ho, Tm	ICP Emmission Analysis
Ba, Rb, Sr, Pb, Zr, Nb, Y, Ga, S	Fluorescence X-ray Analysis (XRF)
Sc, Cs, La, Ce, Nd, Sm, Eu, Tb, Tb, Lu, Hf, Ta, Th	Neutron Activation Analysis (NAA)
Co_2	High Frequency Induction Heat Infrared Absorption Light Intensity Method
FeO	Neutralization Titration Method
LOI	Gravimetric Method

The above-mentioned chemical analyses were conducted on 12 rocks. Analyzed samples were 8 from the 94S01 Seamount, one from the central part of the Vate Trough (94SFDC08-1), one from the Erromango Ridge (94SDPG02H) and 2 from the 94S02 Seamount(94SDCB01 and 94SDCB02).

Results of the analysis are shown in Table 5-4-1. Based on the analytical results, AFM diagram, element relational charts and norm calculations were made (see Fig. 5-4-3 ~ 21).

According to the AFM diagram, rocks from the Erromango Basin and the 94S02

Table 5-4-1 Results of Chemical Analysis for Rocks

Sample No.		94SDLC03 D	94SDLC04 C	94SDLC06 B	94SDCB01 ROCK	94SDCB02 ROCK	94SDPG02 H	94SDPG05 B	94SDPG05 C	94SDPG07 A	94SDPG07 B	94SDLC19	94SFDC081
SiO2	%	49.61	50.45	49.23	53.97	53.16	55.94	50.21	48.72	49.02	49.74	49.55	48.84
TiO2	%	0.88	1.09	1.13	0.71	1.35	0.78	1.09	1.10	1.28	1.31	1.13	1.86
Al2O3	%	13.01	14.80	15.34	18.30	18.00	14.74	14.96	14.97	14.80	14.94	15.39	14.04
Fe2O3	%	11.55	6.90	6.66	6.99	6.68	8.16	7.70	8.06	7.98	7.66	8.10	7.34
FeO	%	1.27	4.85	4.83	0.27	1.45	0.86	3.84	3.11	4.81	5.10	3.41	5.05
MnO	%	0.14	0.22	0.20	0.13	0.14	0.14	0.20	0.19	0.30	0.22	0.19	0.21
MgO	%	4.11	5.69	5.94	5.11	3.27	2.96	5.60	5.67	4.97	4.94	5.90	6.28
CaO	%	7.13	10.35	10.63	10.16	9.97	5.90	10.25	10.42	9.59	9.55	10.77	10.46
Na2O	%	3.35	3.27	3.49	3.12	4.03	3.81	3.32	3.35	3.90	3.91	3.76	3.42
K2O	%	0.92	0.44	0.47	0.44	0.37	2.61	0.53	0.40	0.49	0.49	0.39	0.30
P2O5	%	0.17	0.20	0.18	0.12	0.14	0.37	0.19	0.18	0.22	0.20	0.17	0.21
H2O+	%	0.41	0.29	0.18	0.08	0.22	0.20	0.09	0.08	0.02	0.24	0.16	0.08
H2O-	%	4.40	0.07	0.23	0.37	0.52	2.52	0.57	3.29	0.54	0.13	0.22	0.42
CO2	%	0.04	<0.01	0.16	0.26	<0.01	<0.01	<0.01	0.08	0.26	0.11	<0.01	<0.01
LOI	%	6.97	0.95	0.65	0.89	1.54	3.58	1.15	3.79	1.68	0.45	0.25	0.30
Total	%	99.12	99.20	98.74	100.30	100.12	99.84	99.04	99.95	99.04	98.49	99.01	98.31
Ba	ppm	276	110	82	87	53	537	125	87	101	94	83	36
Rb	ppm	20.3	10.0	8.4	6.2	4.6	30.4	8.2	7.1	8.9	9.7	7.1	3.9
Sr	ppm	249	222	220	301	194	398	228	215	233	221	218	139
Pb	ppm	4	2	1	1	<1	15	<1	3	21	2	<1	<1
Zr	ppm	60	58	61	45	76	89	59	58	67	71	59	106
Nb	ppm	1.7	1.6	1.6	1.1	1.5	2.6	1.6	1.5	1.8	1.7	1.5	2.8
Y	ppm	21	28	29	18	30	25	28	28	33	33	29	44
V	ppm	194	244	248	180	245	231	245	250	285	271	252	283
Cr	ppm	10.5	11.9	11.7	121	25.1	12.7	11.0	11.1	8.2	7.6	10.5	110
Ni	ppm	22	37	38	48	13	14	35	36	26	21	33	43
Cu	ppm	98	128	133	42	74	206	134	115	146	138	122	64
Zn	ppm	64	72	74	57	60	81	75	75	89	83	76	84
Ga	ppm	13.8	16.0	16.0	15.3	17.5	15.6	16.1	16.1	16.9	17.2	16.4	17.2
S	ppm	2000	890	1140	130	395	570	940	1865	1740	1870	1050	2030
Sc	ppm	23.2	29.6	30.6	26.7	29.2	17.8	29.4	29.9	27.6	27.6	31.4	37.4
Cs	ppm	1.0	0.3	0.2	0.3	0.3	1.3	0.2	0.3	0.3	0.3	0.2	0.1
La	ppm	4.8	3.8	3.9	3.3	3.0	14.3	4.4	3.9	5.4	4.6	4.0	4.9
Ce	ppm	11.9	10.6	11.2	8.7	10.5	29.9	11.8	10.4	12.8	13.5	11.3	14.6
Nd	ppm	8.7	9.5	9.5	7.4	11.1	17.2	9.5	9.5	11.3	11.5	9.7	13.8
Sm	ppm	2.76	3.10	2.98	2.15	3.58	4.43	3.20	3.06	3.41	3.55	3.03	4.60
Eu	ppm	0.90	1.01	1.11	0.91	1.39	1.14	1.10	1.06	1.27	1.38	1.18	1.68
Gd	ppm	3.29	3.65	4.07	2.79	4.24	4.46	3.62	3.99	4.79	4.75	4.21	6.36
Tb	ppm	0.61	0.74	0.74	0.50	0.85	0.61	0.71	0.70	0.83	0.84	0.72	1.20
Ho	ppm	0.75	1.13	1.12	0.63	1.24	0.87	1.21	1.07	1.33	1.35	1.10	1.71
Tm	ppm	0.41	0.52	0.52	0.31	0.51	0.41	0.50	0.49	0.60	0.61	0.61	0.71
Yb	ppm	2.18	3.08	3.07	2.05	3.20	2.77	3.04	2.99	3.37	3.77	3.26	4.97
Lu	ppm	0.34	0.42	0.50	0.33	0.36	0.42	0.40	0.40	0.48	0.49	0.41	0.59
Hf	ppm	1.7	1.4	1.5	1.2	1.9	2.4	1.6	1.6	1.7	1.6	1.6	2.9
Ta	ppm	0.2	0.2	0.2	0.1	0.2	0.2	0.2	0.1	0.2	0.2	0.2	0.3
Th	ppm	0.8	0.4	0.4	0.4	0.4	2.9	0.6	0.2	0.4	0.5	0.4	0.3

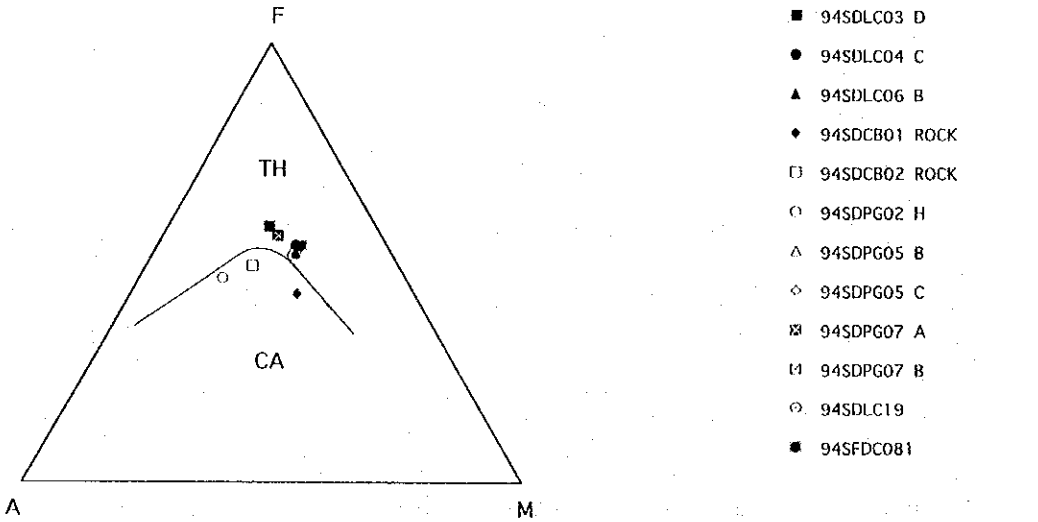

※ A:Na_2O+K_2O, F:$FeO+Fe_2O_3\times0.8998$, M:MgO
境界はIrvine&Baragar(1971)を引用

Figure 5-4-3　AFM diagram for basalts

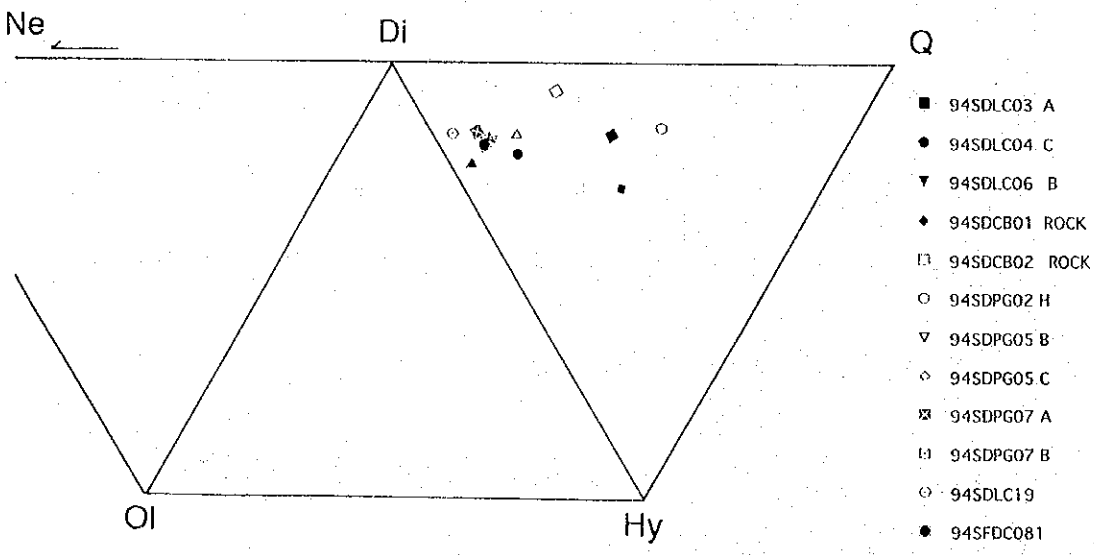

Figure 5-4-4　Diagram using Norm Di-Q-Hy-Ol for basalts

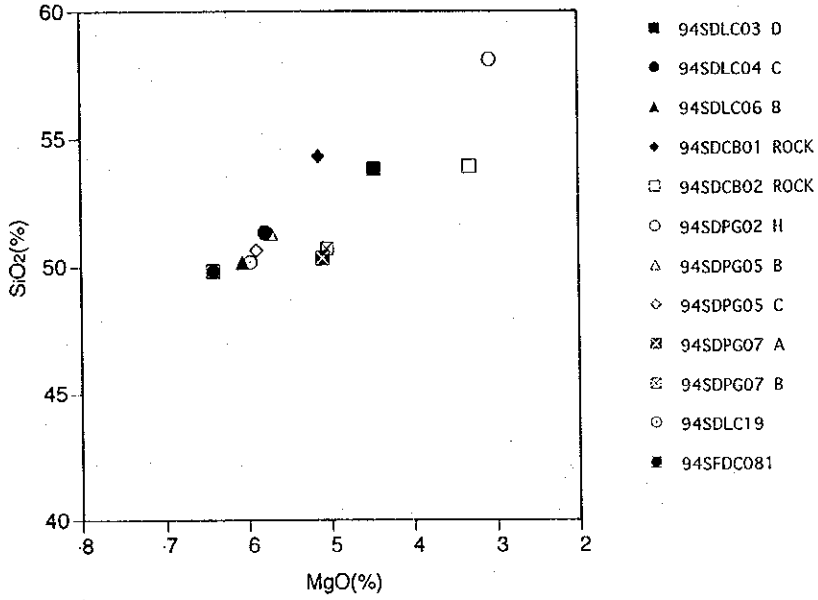

Figure 5-4-5 MgO versus SiO_2 for basalts

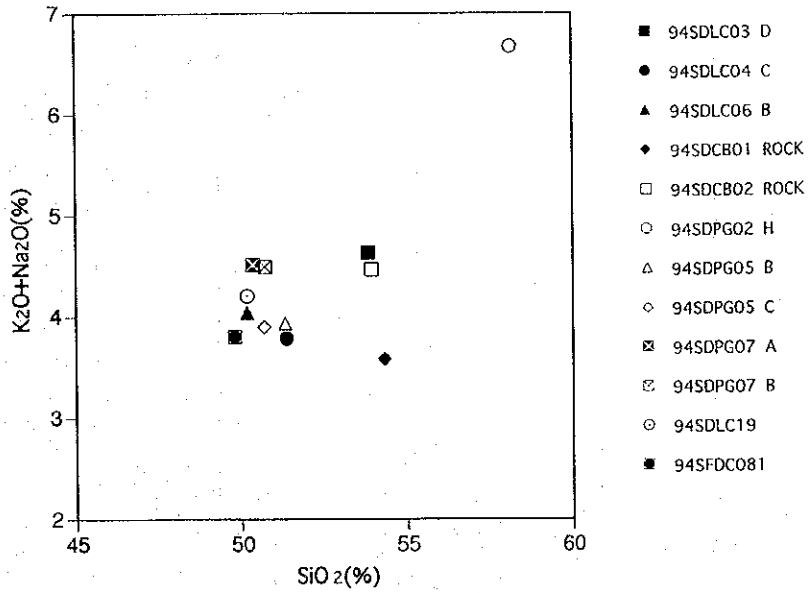

Figure 5-4-6 SiO_2 versus K_2O+Na_2O for basalts

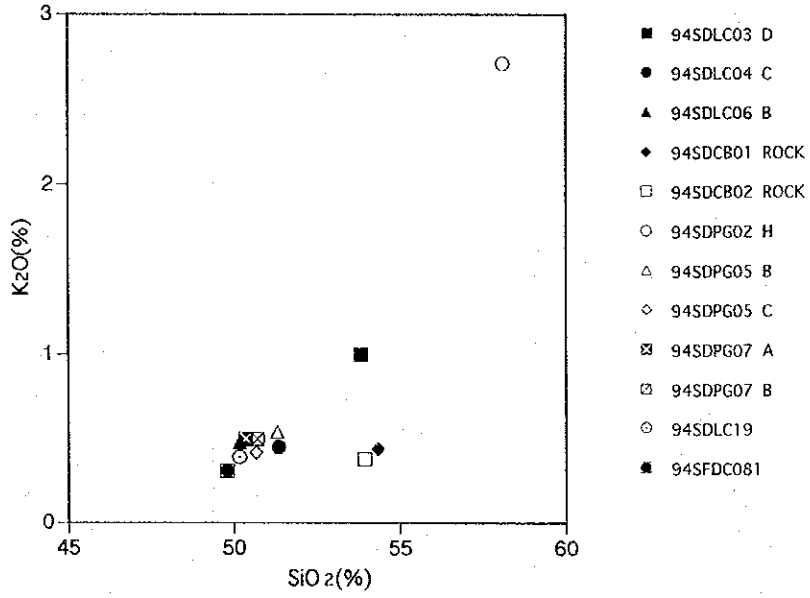

Figure 5-4-7 SiO_2 versus K_2O for basalts

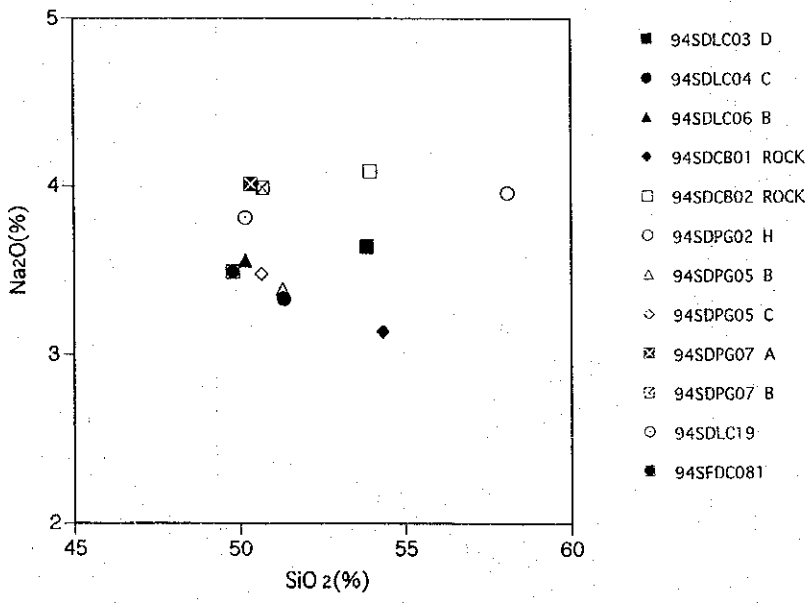

Figure 5-4-8 SiO_2 versus Na_2O for basalts

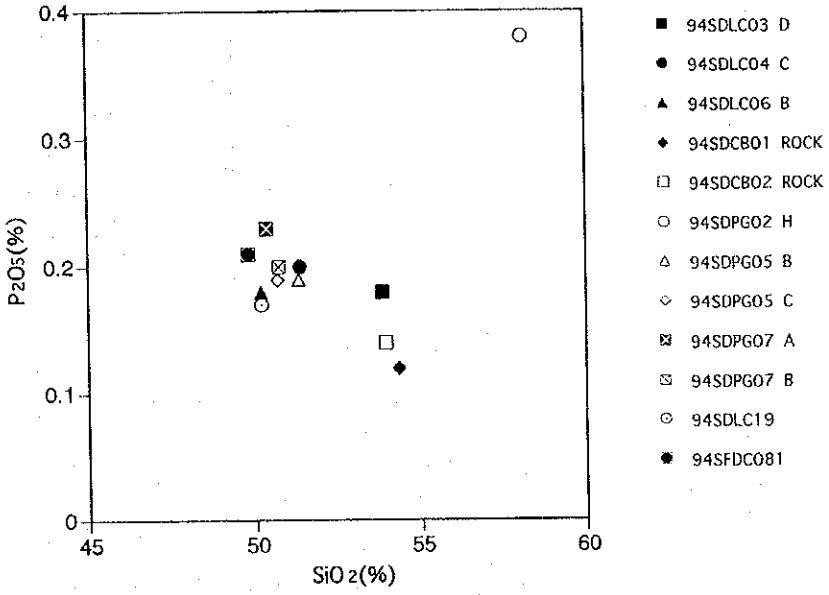

Figure 5-4-9 SiO_2 versus P_2O_5 for basalts

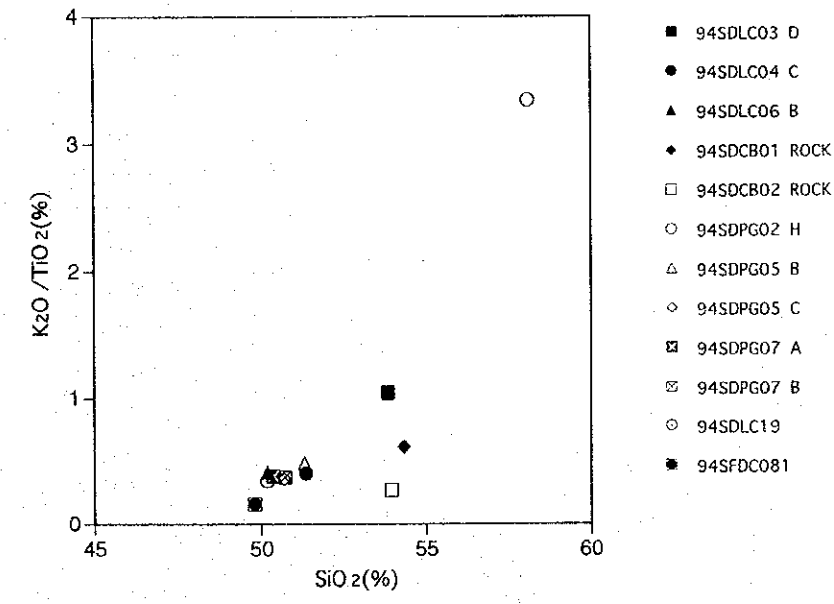

Figure 5-4-10 SiO_2 versus K_2O/TiO_2 for basalts

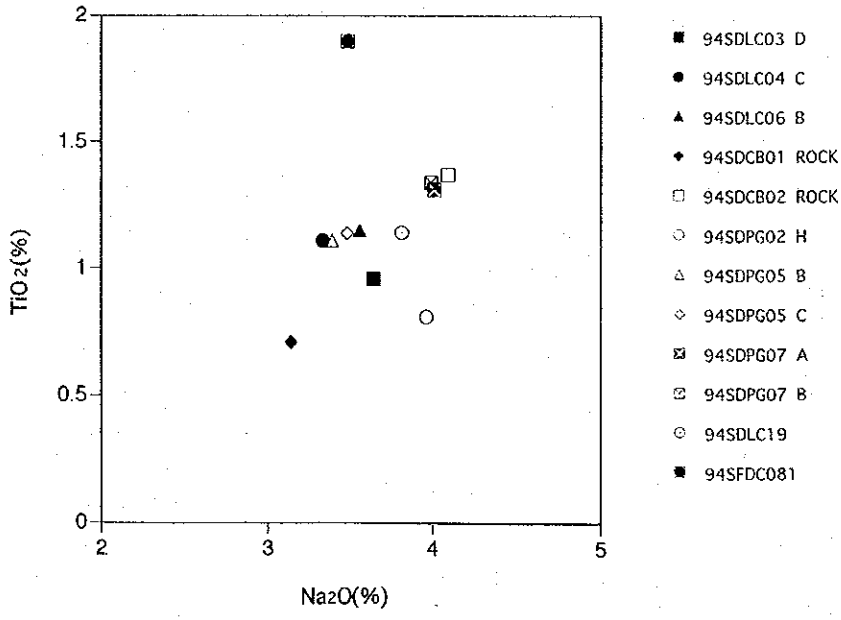

Figure 5-4-11 Na_2O versus TiO_2 for basalts

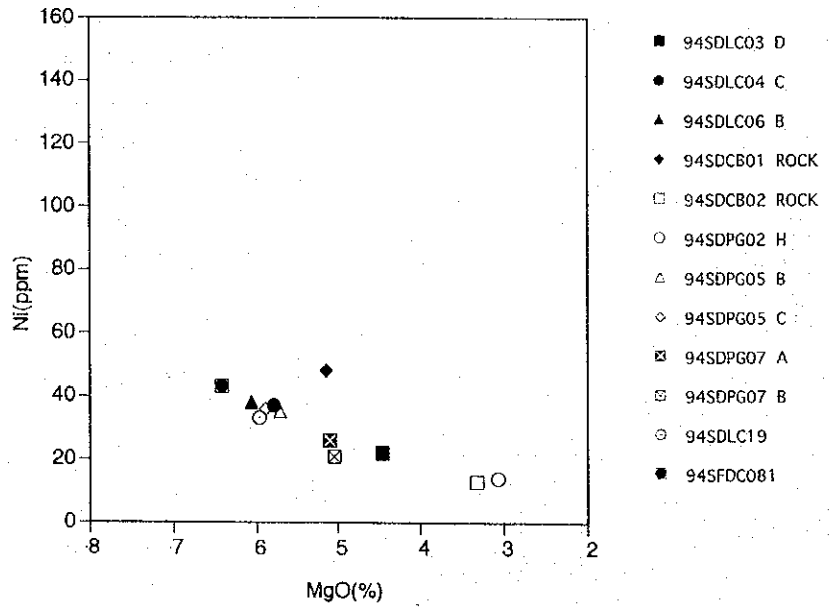

Figure 5-4-12 MgO versus Ni for basalts

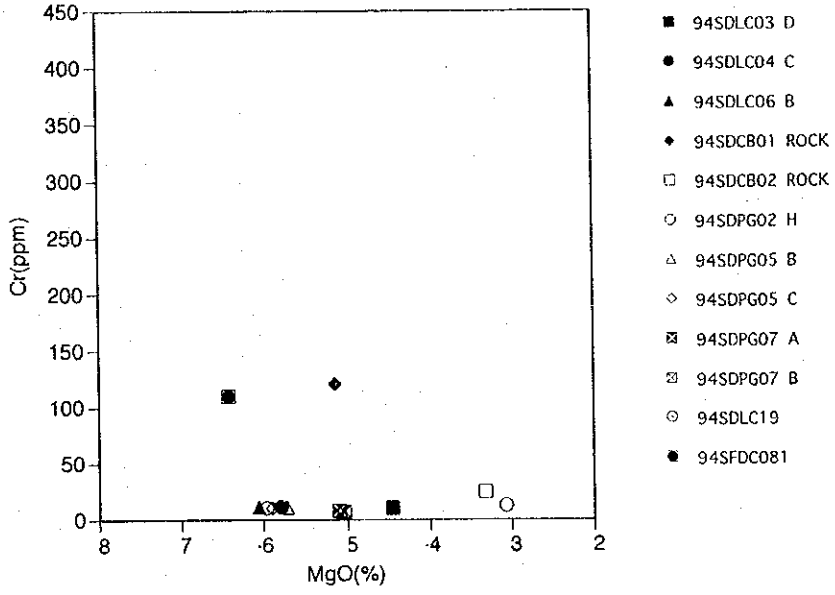

Figure 5-4-13 MgO versus Cr for basalts

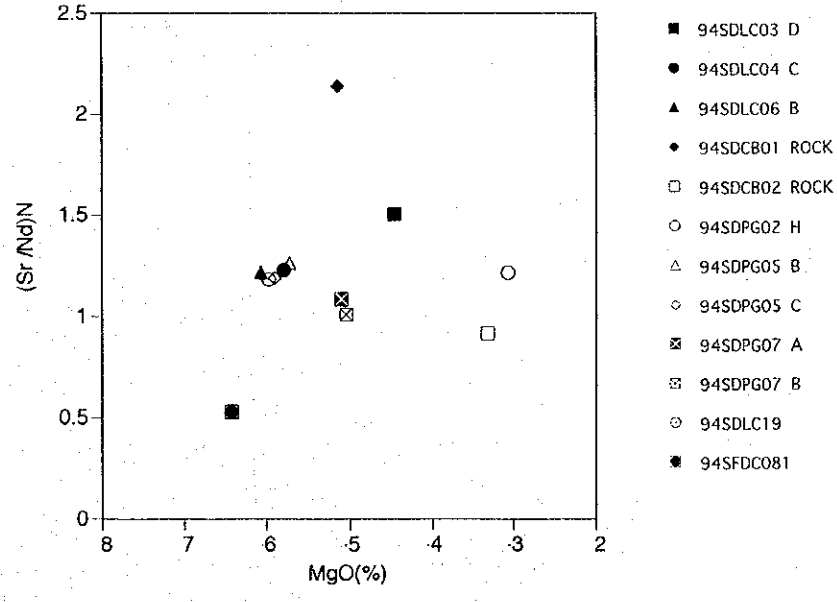

Figure 5-4-14 MgO versus (Sr/Nb)n for basalts

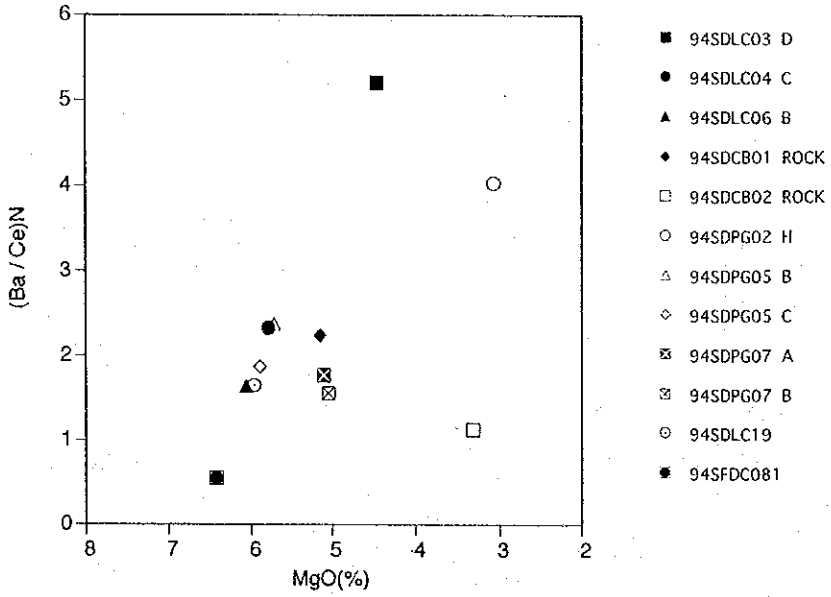

Figure 5-4-15 MgO versus (Ba/Ce)n for basalts

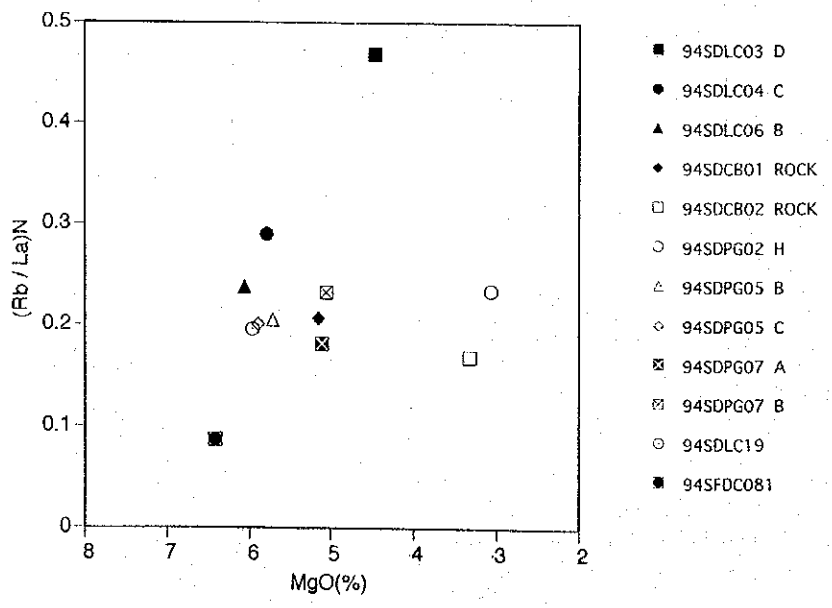

Figure 5-4-16 MgO versus (Rb/La)n for basalts

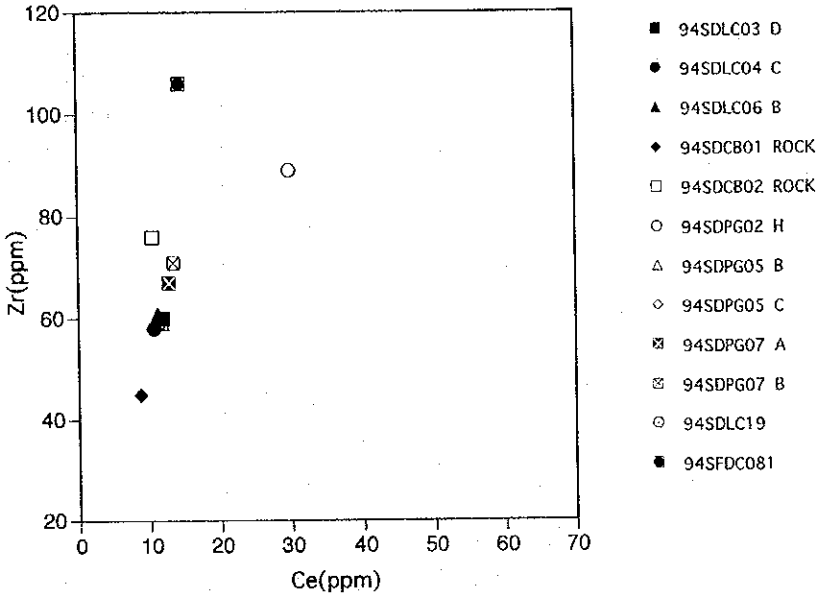

Figure 5-4-17 Ce versus Zr for basalts

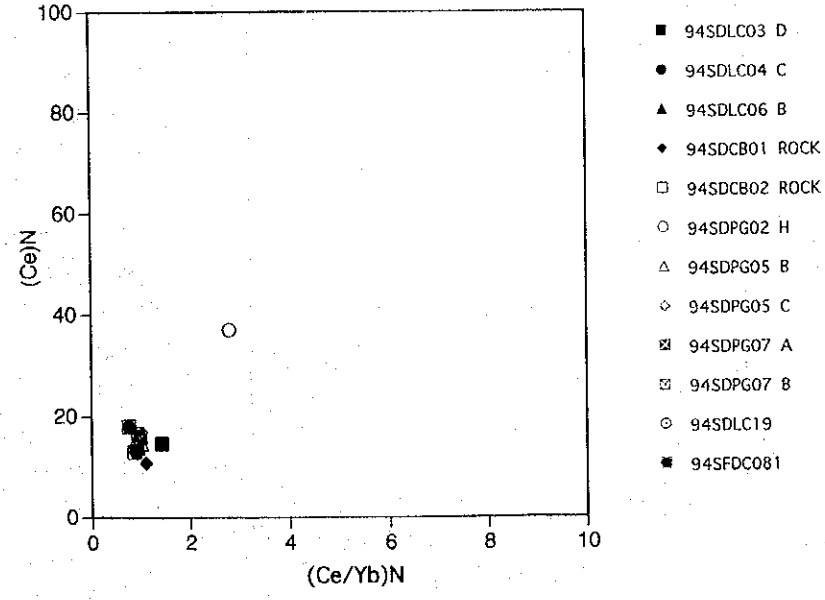

Figure 5-4-18 (Ce/Yb)n versus (Ce)n for basalts

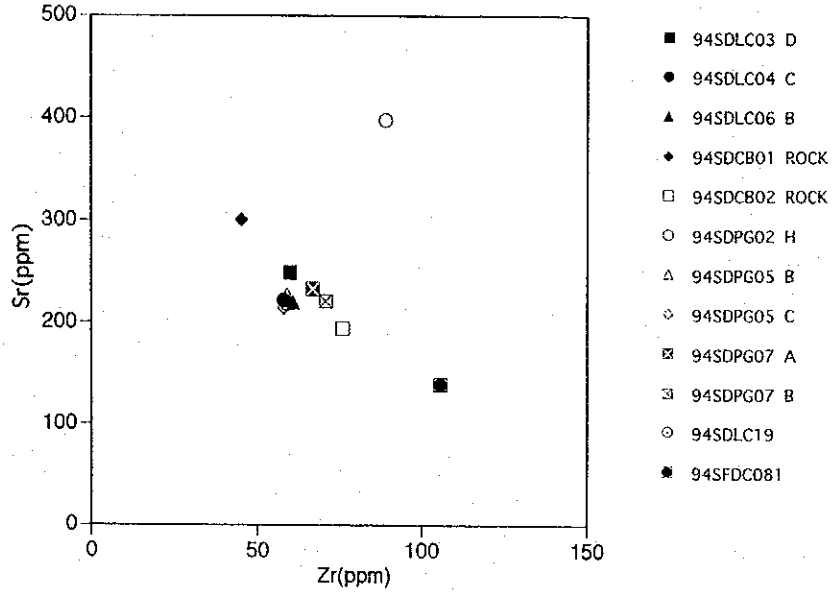

Figure 5-4-19 Zr versus Sr for basalts

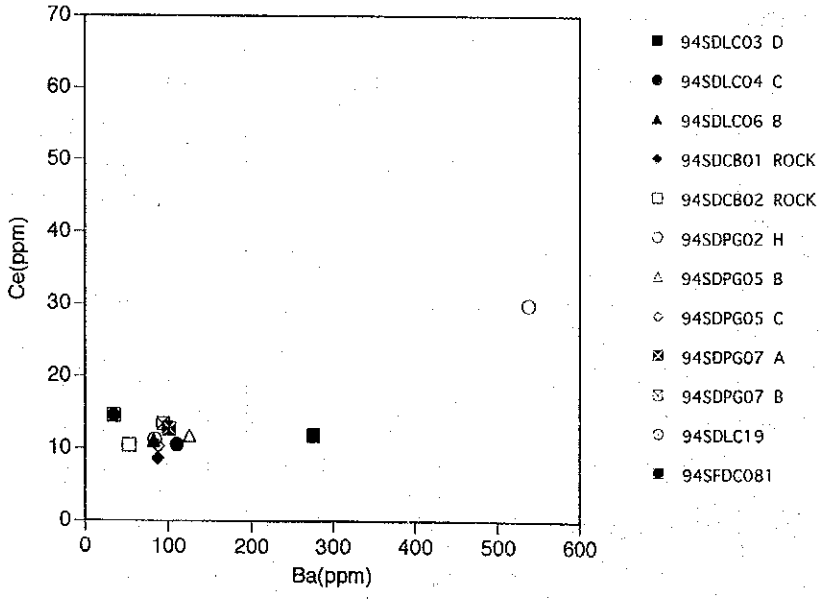

Figure 5-4-20 Ba versus Ce for basalts

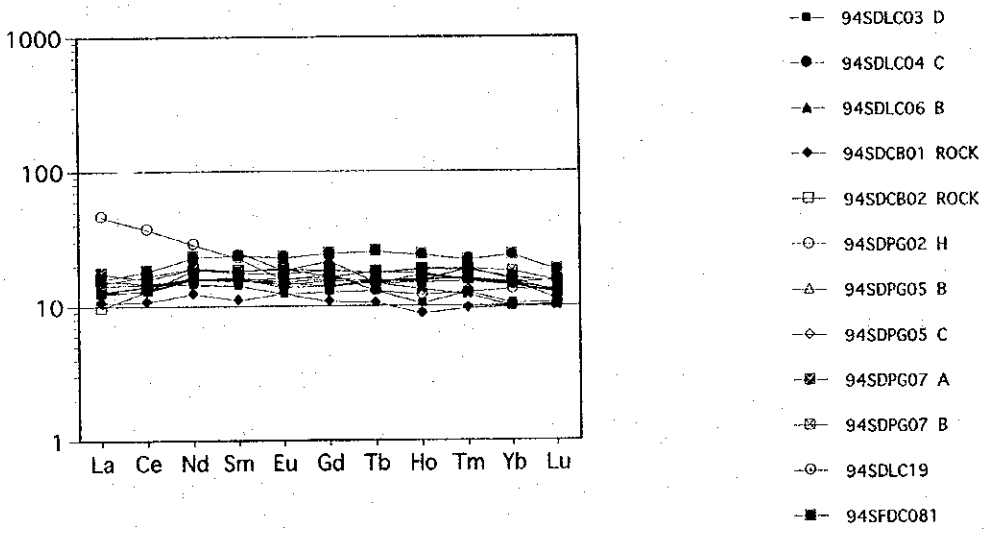

Figure 5-4-21 Chondrite-normalized rare earth element patterns for basalts

Seamount belong to the calc-alkali basalt rock series and rocks from the 94S01 Seamount and the Vate Trough belong to the tholeiite rock series. According to the classification of norm mineral combinations, all of the rocks belong to tholeiite oversaturated with silica. According to rock classification by SiO_2 versus MgO, the rocks from the Erromango Basin belong to High-SiO_2 andesite, onve of the rocks (94SDLC03C) from the 94S02 Seamount and 94S01 Seamount belongs to Low-SiO_2 andesite and the other rocks from the 94S01 Seamount and the Vate Trough belong to basalt.

Furthermore, according to the classification of SiO_2 versus K_2O+Na_2O, the rocks from the Erromango Basin and one of the rocks (94SDLC03C) from the 94S02 Seamount and 94S01 Seamount belong to non-alkali andesite, and the other rocks from the 94S01 Seamount belong to non-alkali basalt. The cassification of SiO_2 versus K_2O, Na_2O or P_2O_5 also show the same tendencies: one of the rocks (94SDLC03C) from the 94S02 Seamount and 94S01 Seamount belong to lower-K_2O, and the other rocks from the 94S01 Seamount and Vate Trough belong to higher-K_2O. From other element relational charts, one of the rocks (94SDLC03C) from the 94S02 Seamount and 94S01 Seamount, and the rock from the Erromango Basin show different behavior from the other rocks of the 94S01 Seamount and Vate Trough. Only the rocks from the Vate Trough are classified into MORB.

5-5 Ore indications

(1) 94S01 Seamount

At this seamount, oxidized alteration was identified throughout all the four FDC track lines on the eastern side and the top of the northwestern side of the seamount with a caldera in its central part. Also, chimneyes and hydrothermal biotic communities are identified on the eastern side of the seamount. Oxidized alteration and hydrothermal biotic communities were identified at one place on track line FDC10, oxidized alteration was identified at three places on track line FDC11, oxidized alteration at four places and hydrothermal communities at one place were identified on track line FDC12 and oxidized alteration was identified at one place on track line FDC13. Horizontal scale on the northwestern side is about 900m but the width in the direction of crossing the range orthogonally is inferred to be short.

The extent of the eastern place, where chimnies and hydrothermal biotic communities were identified, is 500 x 400m and the southern place is 500 x 300m. Oxidized alteration was also recognized at other places but their extents were very

small. The sampling survey was conducted only on the eastern side but the maximum vertical scale of yellowish brown precipitates presumed to contain iron oxides was 40cm.

We tried several times to collect this chimnyes by PG, but we could not even identify the chimnyes. We also tried to collect altered oxides by PG but only rocks were landed. Altered oxides must have been washed away during the landing.

According to the observation results, most of the oxidized alteration was found in cracks of pillow lava so the horizontal scale of oxidized alteration might be narrower than the results of the FDC observation (see Fig. 5-5-1 (1)).

(2) The central part of the Erromango Basin

In this sea area, oxidized alteration or black material was identified at six places in the central ridge on track line FDC01, the same was also identified on sediments on track lines FDC14 and FDC15. From 3 to 20cm thick black manganese oxides were collected by the sampling survey.

Cylindrical, brown consolidated substances, with a diameter of 2cm and length of 5cm, in the foraminiferan ooze under 4cm thick manganese oxides were found on central ridge 94SDLC09. There was a hole with a diameter of 0.5cm in the center of these consolidated substances. Black minerals presumed to be manganese oxides were crystallized (a manganese chimney?).

According to the results of FDC observation and sampling survey, foraminifera ooze often sedimented on manganese oxides, so there is a high potential that the activity has stopped at present. However, the entire 35cm were manganese oxides at 94SDLC10 and fumaroles altered in black were observed in sediments during the FDC survey. So we inferred that some places in the Basin are still in action and that a few centimeters thick manganese oxides are distributed extensively on the Basin (see Fig. 5-5-1 (2)).

(3) 94S02 Seamount

At this Seamount, oxidized alteration of about 800m long was identified on track line FDC04 in the northwestern part of the top of the seamount and oxidized alteration of about 800m long was identified on track line FDC05. Reddish brown precipitates presumed to be Fe-oxides and manganese oxides, found in the manganese survey area were collected by the sampling survey. As for vertical scale, we obtained 65cm

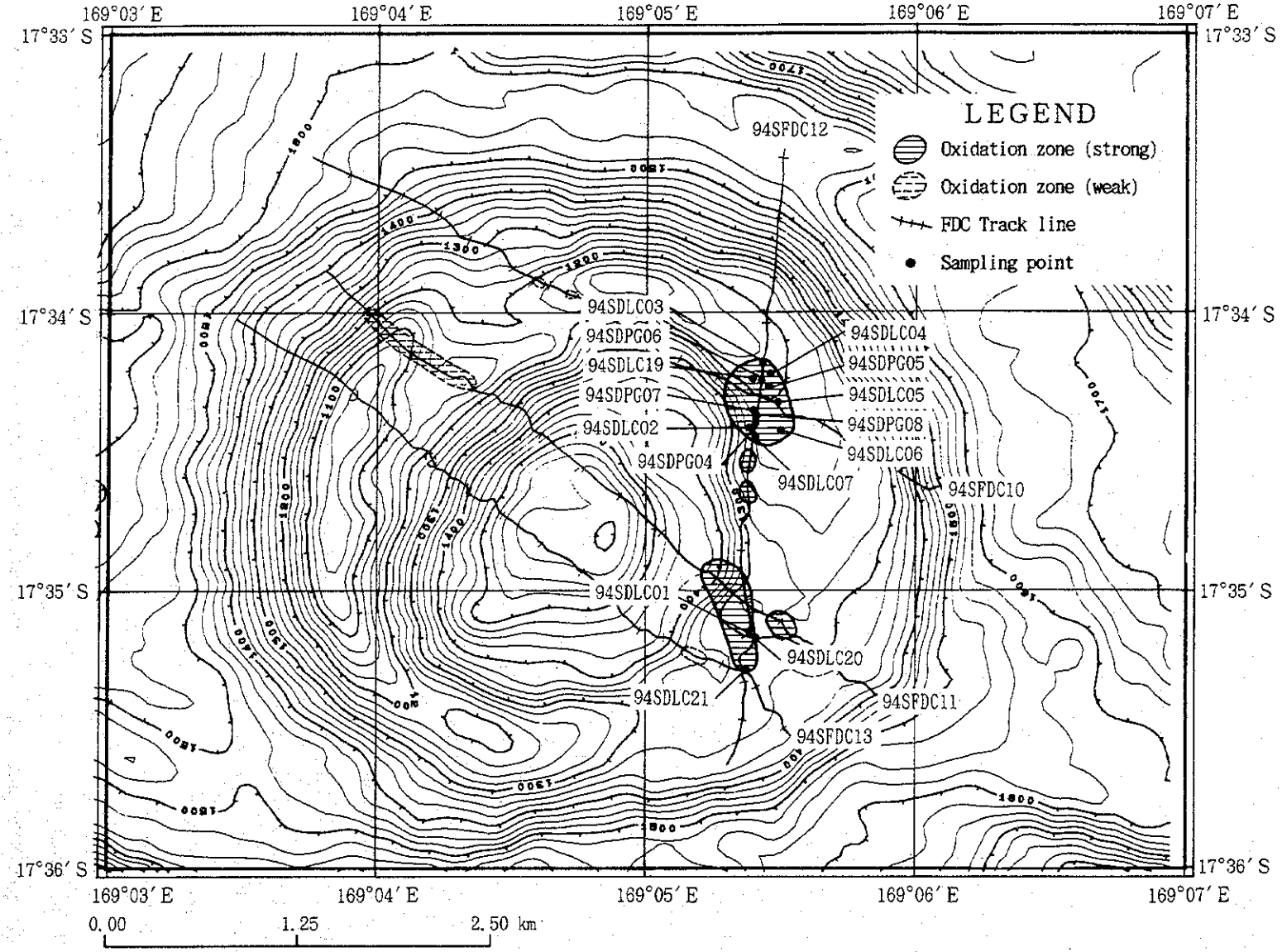

Figure 5-5-1 Ore Indication Map (94S01 Seamount) (1)

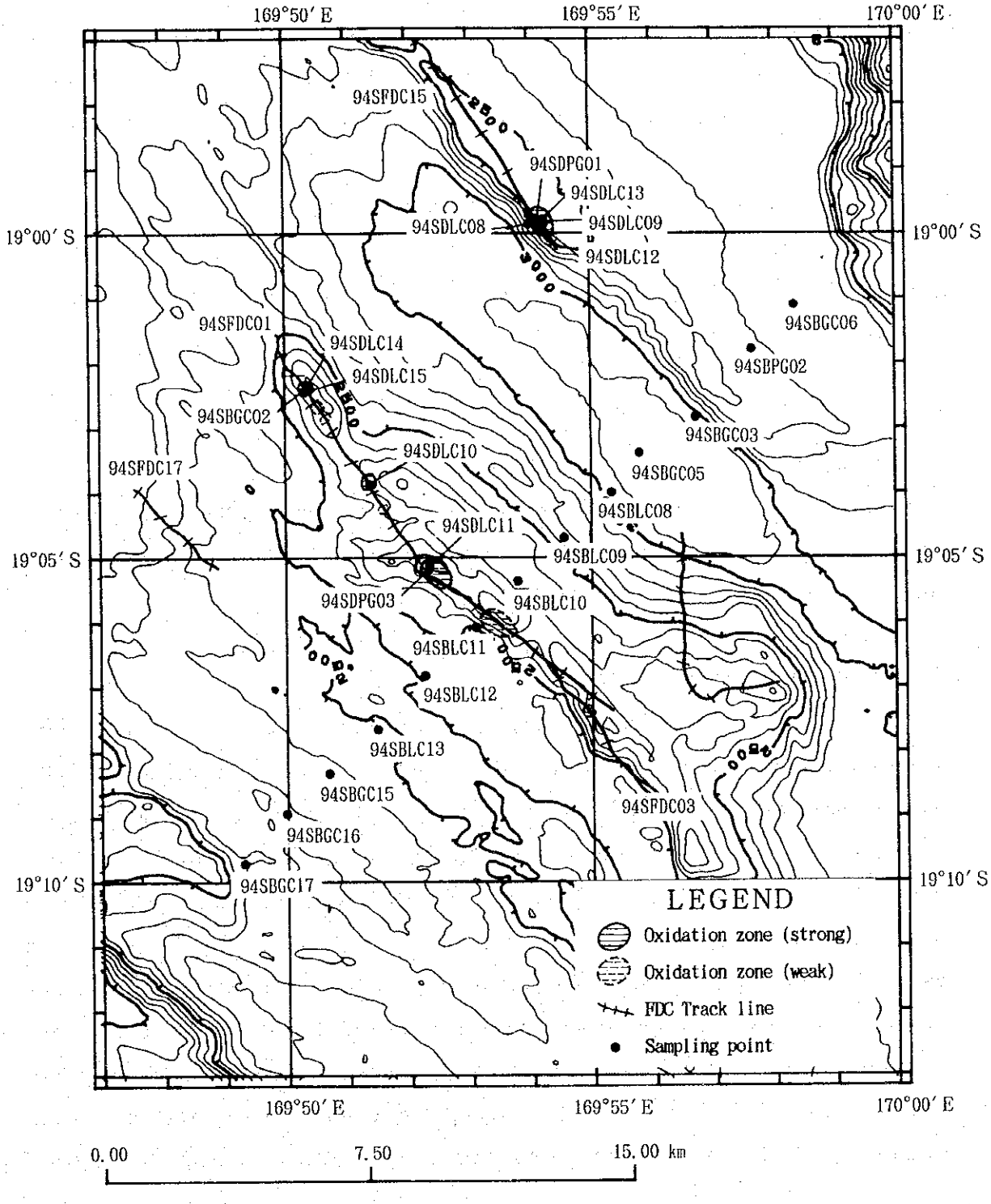

Figure 5-5-1 Ore Indication Map (Central Part of the Erromango Basin) (2)

reddish brown precipitates at 94SDLC18. As for horizontal scale, we estimated that the scope would be narrower than observed by FDC as the surface of rocks are thinly covered with oxides at some places (see Fig. 5-5-1 (3)).

<Polished thin section appraisal and powder X-ray diffraction test>

Polished thin section and X-ray diffraction on typical samples are as follows. Figure 5-5-2 (1), (2) shows microphotographs. Results of polished thin section and X-ray diffraction are shown at the end of this report.

・ (94SDLC01A)

This sample is iron hydroxides collected from the 94S01 Seamount. It is partially mineralized to goethite. It developed in the shape of crust on the both sides of a hollow parts. Some of it grew radially toward the outside. Only a trace amount of clay mineral (smectite) was detected by X-ray diffraction.

・ (94SDLC10A, 94SDPG03C and 94SDPG03D)

These are manganese oxides collected from the central part of the Erromango Basin. Manganese oxides with from mid to low reflective power (todorokite and birnessite?) and manganese oxides with high reflective power (todorokite?) are recognized. The manganese oxides with from mid to low reflective power assume from 1.5 to 0.1mm size nodular textures, from 2.5 to 0.5mm wide colloform crustified textures or from 3.5 to 1mm long columnar colloform textures. The manganese oxides with high reflective power assume from 2.0 to 0.8mm wide colloform crustified textures or from 2.5 to 0.1mm long columnar textures. The highly reflective power part indicates weak anisotropy under reflected light. Clastics and mineral fragments (plagioclase and augite) of basic volcanic rock origin are scattered in the manganese oxides. Birnessite and todorokite are also detected by X-ray diffraction.

・ (94SDLC09)

This sample is a manganese oxide chimney collected from the central part of the Erromango Basin. Manganese oxides with from mid to low reflective power (todorokite and birnessite? 1.5 ～ 0.1mm thick) are generated in its inner wall. Manganese oxides with low reflective power assuming nodular textures (birnessite?) are generated toward the outside hollow parts. Birnessite and todorokite are also

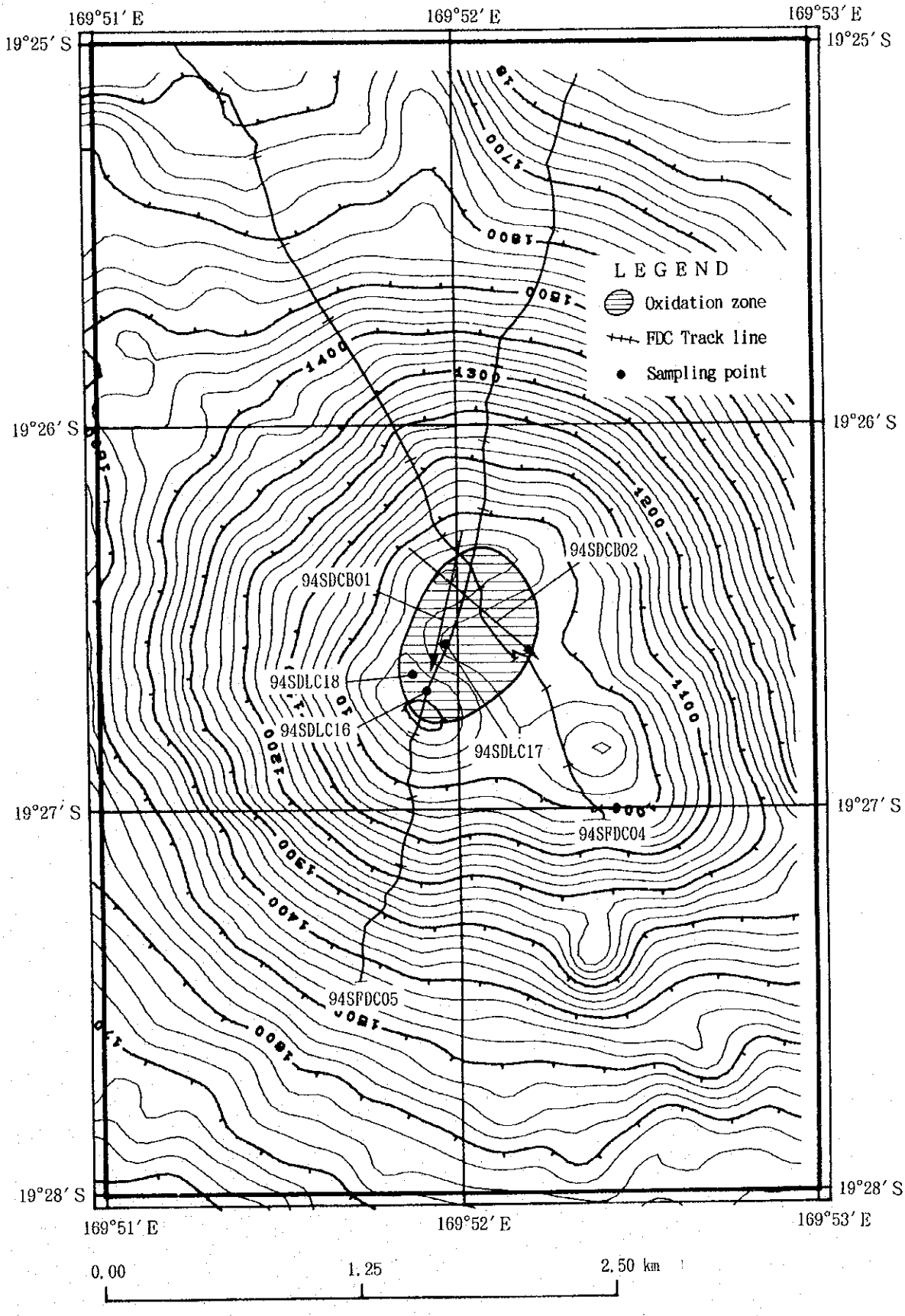

Figure 5-5-1 Ore Indication Map (94S02 Seamount) (3)

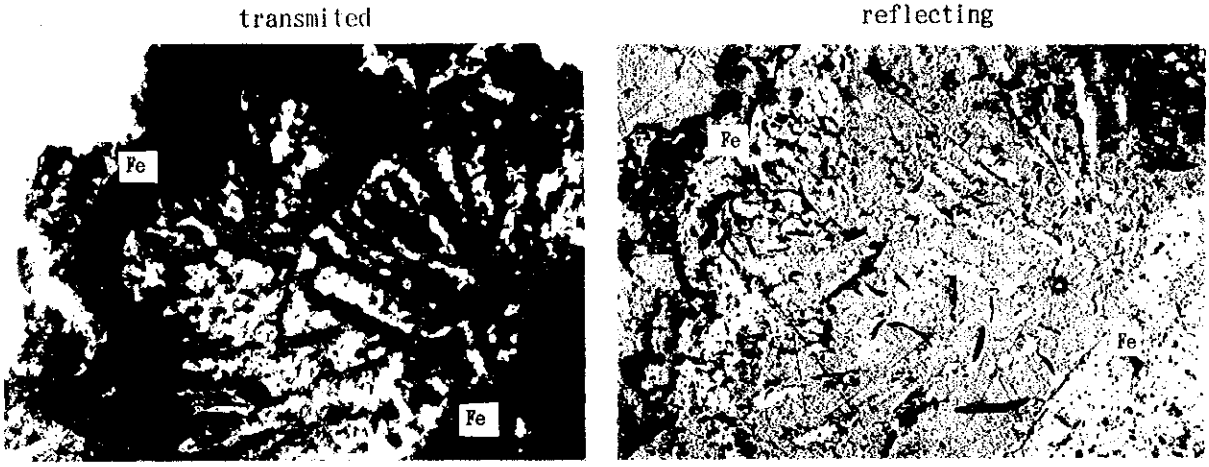

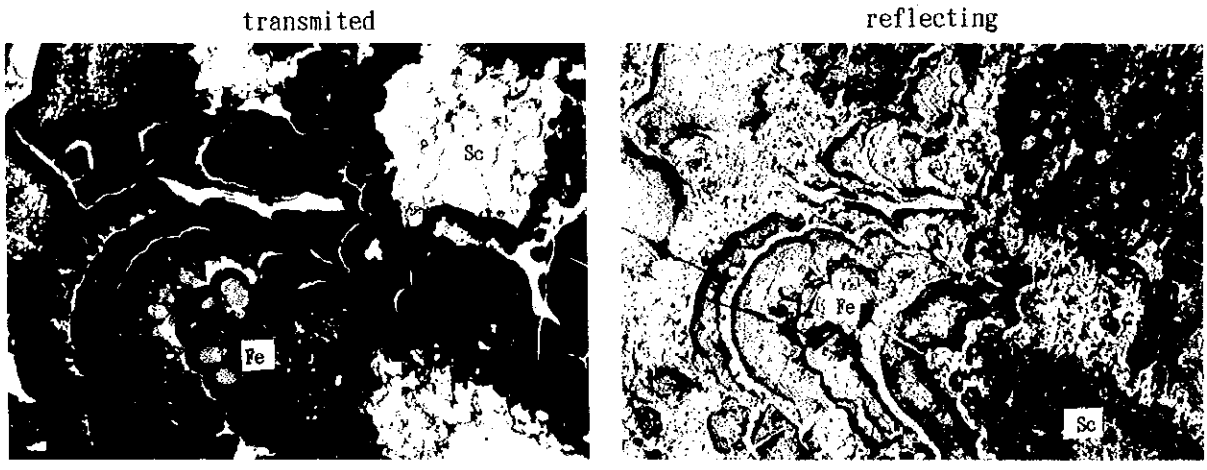

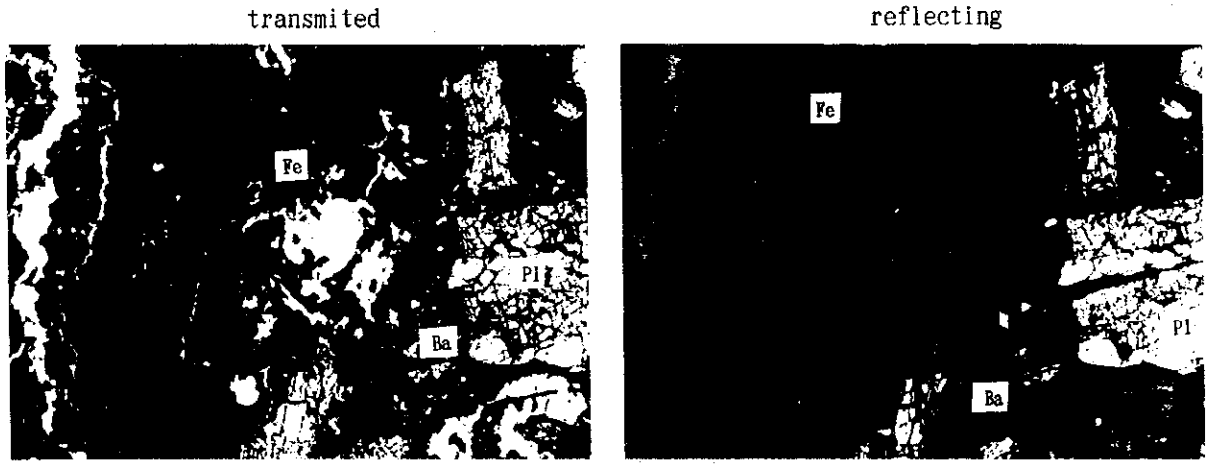

Figure 5-5-2 Microscopic Photos of Polished Thin Section (1)

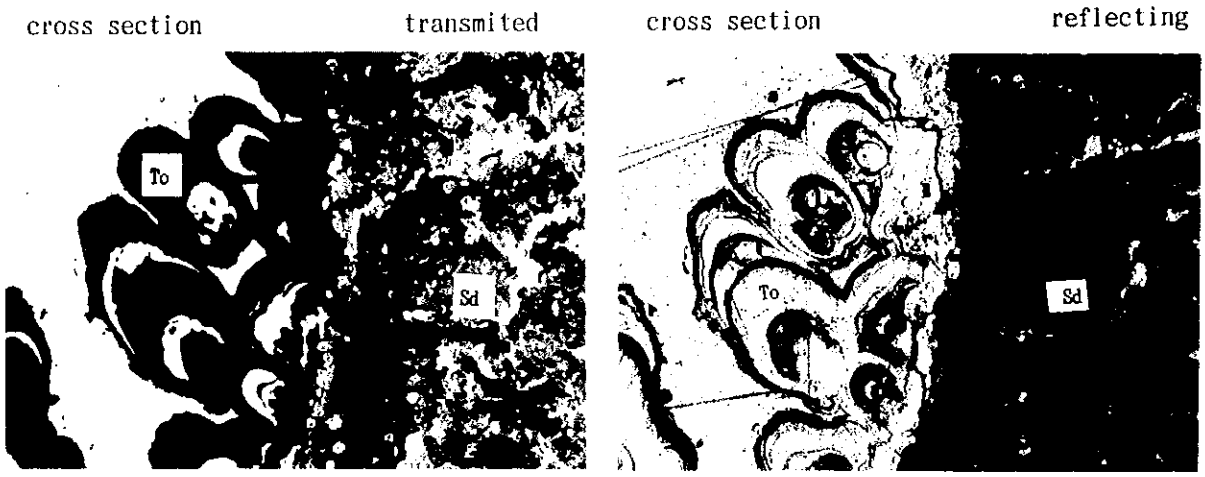

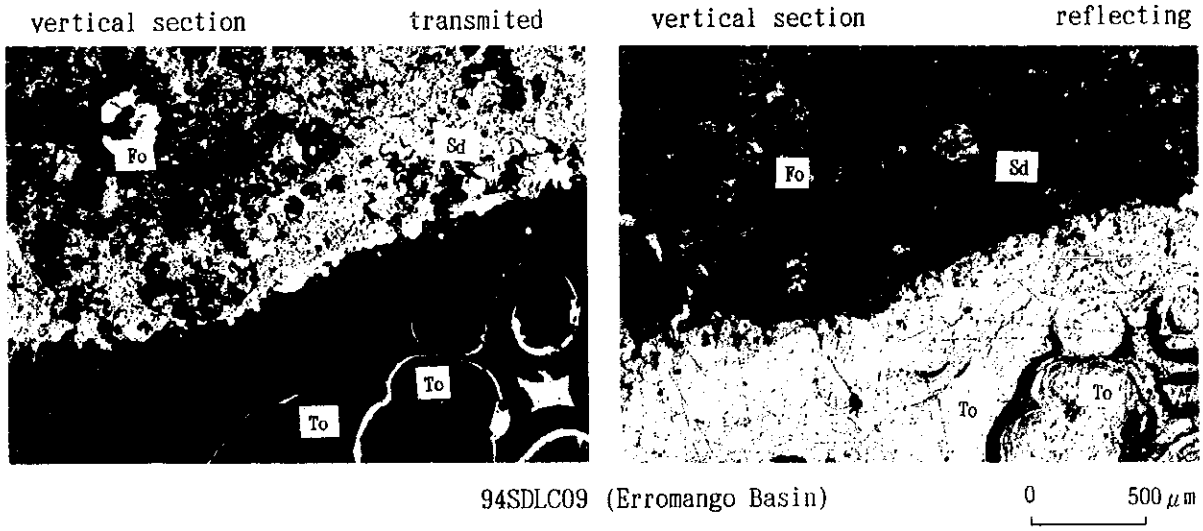

Abbreviation

Ba	:	Basalt
Fe	:	Iron-hydroxides, oxides (including Goethite)
Fo	:	Foraminifera
Mn	:	Birnessite
Pℓ	:	Plagioclase
To	:	Todorokite
Sc	:	Scoria
Sd	:	Sediments
X	:	Unknown minerals

Figure 5-5-2 Microscopic Photos of Polished Thin Section (2)

detected by X-ray diffraction.

· (94SDCB02)

This sample is iron hydroxides collected from the 94S02 Seamount. It shows growth assuming crystified textures by covering scoria and basalt fragments. A trace amount of goethite is detected by X-ray diffraction.

<Chemical Analysis>

Whole rock analysis (13 components) and trace component analysis (20 elements) were conducted on 25 samples of iron and manganese oxides. Table 5-5-1 (1), (2) shows the results of analysis.

Analytical components and the limit of detection are as follows:

SiO_2, TiO_2, Al_2O_3, Fe_2O_3, FeO, MnO, MgO, CaO, BaO, Na_2O, K_2O, P_2O_5, Co_2, LOI (the limit of detection of above 14 whole rock components is 0.01%), Au (2ppm), Ag (0.02ppm), Cu (1ppm), Pb (5ppm), Zn (1ppm), Mn (1ppm), Total-Fe (0.01%), Total-S (0.001%), Cd(0.1ppm), Bi (0.1ppm), Ni (1ppm), Co (1ppm), As (1ppm), Sb (0.2ppm), Hg (10ppb), Ba (5ppm), Sr (1ppm), Mo(1ppm), Sn (1ppm) and W (1ppm).

Figures in the parentheses of above trace components analysis (20 elements) are the limits of detection.

Methods of analysis for each component are listed below:

Analytical Element	Method of Analysis
SiO_2, TiO_2, Al_2O_3, Fe_2O_3, MnO, MgO, CaO, Na_2O, K_2O, P_2O_5, Total- Fe, Ag, Cu, Zn,n, Cd, Ni	ICP Emission Analysis
Bao, Ba, Sr, Sn, Total-S	Fluorescene X-ray Analysis (XRF)
Au, Co, As, Sb, Mo, W	Neutron Activation Analysis (NAA)
CO_2	High Frequency Heat Infrared Absorption Light Intensity Method (LECO)
Hg	Reducing Vaporization Atomic Absorption Method
FeO	Neutralization Titration Method
LOI	Gravimetric Method

Table 5-5-1 Results of Whole Rock Analysis and Trace Level Analysis for Iron-Manganese Oxides (1)

Sample No.		94SDLC01 A	94SDLC01 C	94SDLC03 A	94SDLC03 B	94SDLC03 C	94SDLC04 A	94SDLC04 B	94SDLC18 0-10	94SDLC18 45-50	94SDCB01 U	94SDCB01 L	94SDCB02 MIX	94SDLC09 34-38	94SDLC10 A	94SDLC10 B	94SDLC11	94SDCB01
SiO2	%	29.11	25.00	35.58	44.74	49.96	46.09	40.44	15.40	12.64	12.96	33.94	15.14	22.18	3.03	12.93	17.76	34.03
TiO2	%	0.22	<0.01	<0.01	0.01	0.37	0.63	0.12	0.04	<0.01	<0.01	0.51	0.30	0.34	0.04	0.05	0.15	0.49
Al2O3	%	2.06	0.04	0.14	0.14	5.24	8.63	1.67	0.72	0.70	0.45	9.55	2.19	7.23	0.77	1.11	3.50	8.64
Fe2O3	%	30.82	44.07	37.51	36.13	25.30	20.85	26.30	48.90	53.44	60.50	28.73	53.46	5.45	1.58	11.12	8.79	31.00
FeO	%	<0.01	<0.01	0.50	0.97	0.22	<0.01	4.17	<0.02	<0.02	<0.01	<0.01	0.18	<0.01	<0.01	<0.01	<0.01	0.22
MnO	%	4.28	0.04	0.01	0.12	0.09	0.64	0.58	0.20	0.06	0.84	2.91	1.83	34.15	66.31	47.81	37.87	2.03
MgO	%	1.44	0.87	1.32	2.20	3.10	3.75	1.53	0.76	0.56	0.65	2.79	1.34	2.98	1.44	2.18	3.85	1.54
CaO	%	1.96	0.69	0.55	0.43	2.94	6.33	2.00	1.06	0.68	0.65	4.72	1.97	4.57	1.64	1.16	3.29	3.22
Na2O	%	3.54	2.89	2.77	3.39	3.37	3.91	3.49	3.42	2.84	1.80	3.49	2.18	3.48	4.09	2.10	2.27	2.91
K2O	%	0.45	0.32	0.40	0.58	0.72	0.52	0.39	0.30	0.22	0.26	1.56	0.38	1.02	1.02	1.49	1.15	1.66
P2O5	%	1.03	0.94	0.85	0.11	0.10	0.49	0.81	1.90	1.06	1.12	1.42	1.98	0.19	0.07	0.07	0.12	0.95
CO2	%	1.17	1.42	0.22	0.04	0.04	0.44	0.87	1.90	0.58	1.07	0.92	1.36	1.05	<0.01	<0.01	0.07	0.92
LOI	%	24.79	24.41	18.78	11.24	7.43	8.79	17.64	21.58	19.36	18.22	9.91	17.94	17.98	20.51	20.73	21.28	11.51
TOTAL	%	99.70	99.27	98.41	100.05	98.83	100.62	99.14	94.28	91.58	97.50	99.52	98.70	99.56	100.48	100.75	100.04	98.20
Au	ppb	2	<2	<2	3	5	<2	3	9	2	<2	<2	<2	<2	<2	<2	3	<2
Ag	ppm	0.01	0.01	0.16	0.07	0.05	0.04	0.01	0.51	0.23	<0.01	<0.01	<0.01	<0.01	<0.01	<0.01	<0.01	<0.01
Cu	ppm	41	17	18	9	55	102	41	12	10	114	160	99	115	30	47	290	183
Pb	ppm	<5	<5	<5	<5	6	5	<5	<5	<5	<5	11	6	10	10	7	9	<5
Zn	ppm	27	10	9	7	30	55	33	9	18	34	68	87	82	44	69	57	64
Mn	ppm	33147	310	77	929	697	4957	4492	1549	465	6505	22537	14173	264477	513543	370268	293287	15721
TOTAL-Fe	%	7.43	10.63	9.17	8.95	6.15	5.03	7.35	11.79	12.89	14.59	6.93	12.93	1.31	0.38	2.68	2.12	7.53
TOTAL-S	%	1.127	0.870	0.507	0.647	0.537	0.743	1.033	1.210	1.057	0.733	0.797	0.823	0.653	0.343	0.310	0.103	0.613
Cd	ppm	0.51	<0.01	0.11	<0.01	<0.01	0.16	0.29	<0.10	<0.10	0.08	0.35	0.62	<0.10	3.10	2.34	3.77	0.15
Bi	ppm	0.8	<0.1	0.6	0.2	0.1	0.1	4.5	<0.1	0.2	0.5	1.2	0.3	0.1	<0.1	0.1	<0.1	0.1
Ni	ppm	17	3	3	4	12	25	16	3	4	13	42	51	94	37	54	133	21
Co	ppm	21.4	2.8	2.5	4.8	13.7	33.0	25.8	1.9	1.6	78.6	58.0	71.3	53.5	6.8	18.5	21.7	49.2
As	ppm	75	48	44	13	3	38	77	24000	27000	5780	1480	2960	119	147	128	75	2110
Sb	ppm	1.6	0.8	0.5	1.9	0.8	0.9	1.3	<0.2	<0.3	<0.2	1.2	2.5	6.0	10.2	11.9	4.0	1.1
Hg	ppb	<1	<1	<1	<1	<1	<1	<1	<1	<1	<1	<1	<1	<1	<1	<1	<1	<1
Ba	ppm	175	48	28	65	400	200	100	50	16	46	388	160	2556	661	3117	1017	351
Sr	ppm	254	218	124	52	147	263	288	250	120	205	519	415	743	304	957	436	350
Mo	ppm	110	17	8	9	1	17	21	33	51	261	156	111	261	701	336	497	124
Sn	ppm	<1	<1	<1	<1	<1	<1	<1	<1	<1	<1	<1	<1	<1	<1	<1	<1	1
W	ppm	<1	<1	<1	<1	<1	<1	1	<3	<3	<1	<1	<1	209	<1	<1	5	<1

Table 5-5-1 Results of Whole Rock Analysis and Trace Level Analysis for Iron-Manganese Oxides (2)

Sample No.		94SDCB02	94SDPG01 C	94SDPG02 F	94SDPG02 G	94SDPG03 C	94SDPG03 D
SiO2	%	17.50	12.72	29.28	38.03	1.30	16.75
TiO2	%	0.29	0.20	0.46	0.55	0.02	0.25
Al2O3	%	6.82	4.23	9.24	10.83	0.32	4.48
Fe2O3	%	38.48	4.82	6.22	<0.01	0.28	3.38
FeO	%	<0.01	<0.01	<0.01	6.97	<0.01	<0.01
MnO	%	7.92	46.84	27.06	20.33	64.89	48.96
MgO	%	1.86	2.39	2.82	2.41	1.30	2.01
CaO	%	2.96	3.61	5.53	4.74	2.07	3.05
Na2O	%	2.08	3.64	3.79	4.23	3.59	4.14
K2O	%	0.72	0.80	1.16	2.04	0.75	1.49
P2O5	%	1.84	0.24	0.23	0.36	0.05	0.25
CO2	%	0.99	0.16	0.04	0.14	0.33	0.29
LOI	%	18.54	20.79	14.97	10.27	26.23	15.70
TOTAL	%	98.99	100.28	100.76	99.53	100.79	100.46
Au	ppb	<2	<2	<2	<2	<2	<2
Ag	ppm	<0.01	<0.01	<0.01	<0.01	<0.01	<0.01
Cu	ppm	1012	193	90	139	13	88
Pb	ppm	30	6	5	11	8	<5
Zn	ppm	152	97	64	66	31	70
Mn	ppm	61337	362756	209568	157447	502545	379174
TOTAL-Fe	%	9.28	1.16	1.50	1.68	0.07	0.82
TOTAL-S	%	0.653	0.270	0.153	0.343	0.187	0.397
Cd	ppm	0.71	0.25	0.56	0.16	0.10	0.73
Bi	ppm	<0.1	0.1	0.5	<0.1	<0.1	<0.1
Ni	ppm	174	185	41	27	30	43
Co	ppm	449	77.7	20.7	22.7	7.4	9.0
As	ppm	2610	224	43	21	72	67
Sb	ppm	10.8	5.1	1.6	1.2	6.6	6.2
Hg	ppb	<1	<1	<1	<1	<1	<1
Ba	ppm	411	1363	373	551	1150	1130
Sr	ppm	502	470	510	465	523	463
Mo	ppm	249	454	388	205	659	606
Sn	ppm	<1	<1	<1	<1	<1	<1
W	ppm	<1	197	<1	<1	4	4

Among 25 samples, 7 samples were iron oxides collected from the 94S01 Seamount, 11 samples were manganese oxides collected from the central ridge of the Erromango Basin and the remaining 7 samples were iron oxides collected from the 94S02 Seamount. These samples show characteristic tendencies of each sea area. Fe is about from 15 to 30% and Mn is from 0.01 to 3.37% but mostly less than 1% at the 94S01 Seamount. Fe is from 0.2 to 23.49% but mostly less than 8% and Mn is from 0.79 to 52.20% but mostly more than 20% at the Erromango Basin. Also, Ba is higher than other sea areas. Fe is from 20.09 to 42.32% and Mn is from 0.05 to 6.24% but mostly less than 2% at the 94S02 Seamount. Also, Cu and As are higher than other areas, the maximum of Cu is 0.1% and As is 2.7%.

Grades of Ni, Cu and Co are low in all of the samples, so we can infer that the samples are hydrothermal iron and manganese oxides (see Fig. 5-5-3).

5-6 Temperature Anomalies

Water temperature was measured along all FDC track lines at intervals of five seconds and at cruising speeds of 1 ～ 1.5 knots (sampling intervals: about 3 ～ 4m) by a CTD sensor mounted on FDC.

Considering variations of background values of temperature and depth (topography) along each track lines, values regarded as anomaly were determined.

The details of temperature anomalies are shown in Table 5-6-1, and the temperature and depth profiles are shown in Figures 5-6-1 (1) ～ (3).

The following points can be pointed out from these profiles.

(1) 94S01 Seamount

1) Track line FDC11

① Temperature anomalies were detected at one place. The maximum value of anomalies is 0.191℃.

② According to the comparison with FDC results, these anomalies correspond to signs of hydrothermal activities (hydrothermal precipitates and others).

2) Track line FDC12

① Temperature anomalies were detected at two places. The maximum values of anomalies are 0.097 ℃ and 0.191℃, respectively.

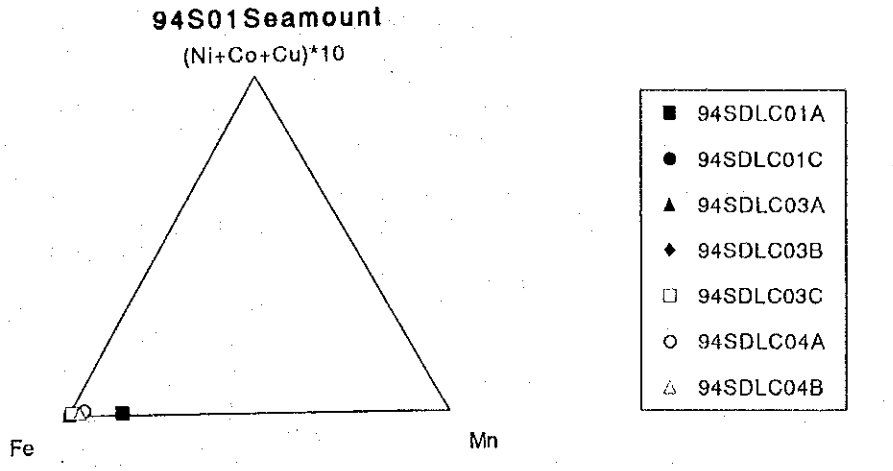

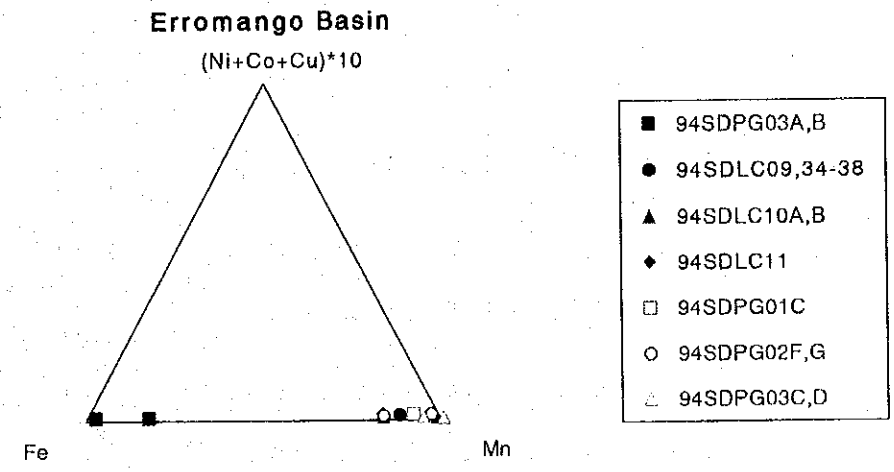

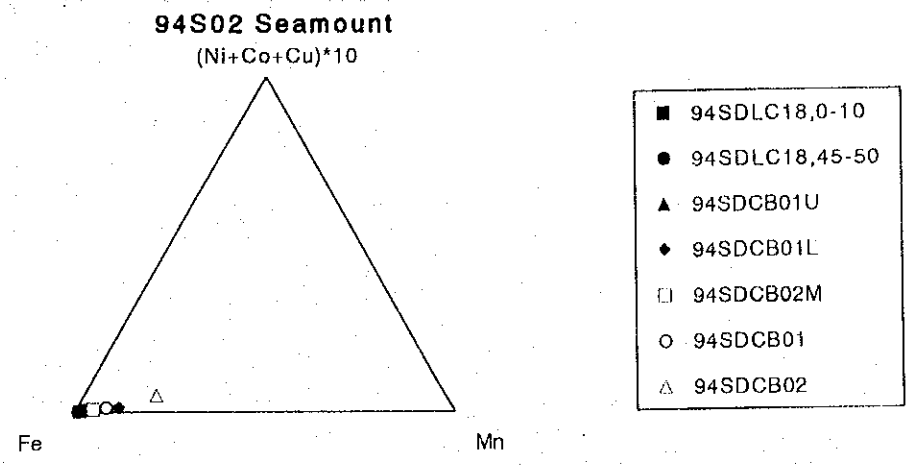

Figure 5-5-3 Mn-Fe-(Ni+Co+Cu)x10 diagram

Table 5-6-1 List of Temperature Anomalies

Line No.	Temperature Anomalies No.	Temperature(℃)	Depth(m)	Date/Time(GMT)	Position	FDC Results of Observation
FDC-01	①	2.101(+0.016)	2,209	09/24 22:37:50	19° 02.300′ S 169° 50.271′ E	
FDC-03	①	2.246(+0.023)	2,132	09/26 05:14:35	19° 07.569′ S 169° 55.076′ E	Oesteichthyes Gorgonian Holothurioidea Crinoidea
	②	2.246(+0.012)	2,456	09/26 06:10:45	19° 08.478′ S 169° 55.822′ E	Gorgonian
FDC-07	①	3.568(+0.023)	1,194	09/28 02:39:30	19° 41.987′ S 169° 48.442′ E	
	②	3.512(+0.102)	1,235	09/28 02:52:15	19° 42.185′ S 169° 48.604′ E	
FDC-09	①	2.744(+0.011)	2,359	09/29 23:04:20	17° 46.324′ S 169° 20.624′ E	Gorgonian Asteroidea
FDC-11	①	3.737(+0.191)	1,128	10/01 02:44:40	17° 34.263′ S 169° 04.356′ E	
FDC-12	①	3.634(+0.097)	1,181	10/02 22:12:35	17° 34.262′ S 169° 05.420′ E	
	②	3.621(+0.191)	1,207	10/02 22:20:15	17° 34.412′ S 169° 05.394′ E	Hydrothermal communities
FDC-13	①	3.854(+0.022)	1,087	10/03 01:43:40	17° 34.271′ S 169° 04.095′ E	Cnidaria
	②	4.117(+0.177)	1,023	10/03 01:49:20	17° 34.314′ S 169° 04.139′ E	Porifera
FDC-14	①	2.218(+0.013)	2,258	10/04 00:18:55	19° 08.478′ S 169° 55.822′ E	Macrura

FDC－01

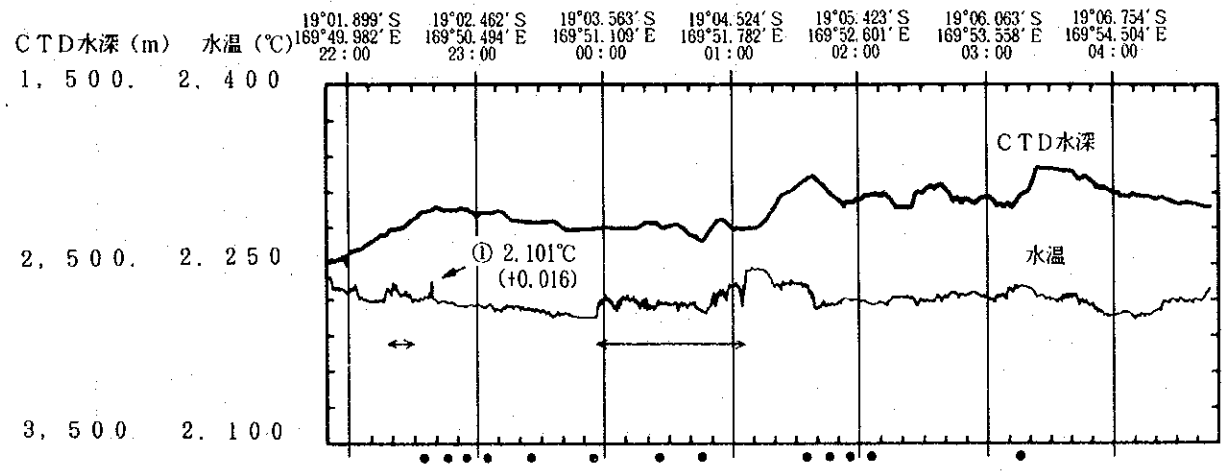

FDC－03

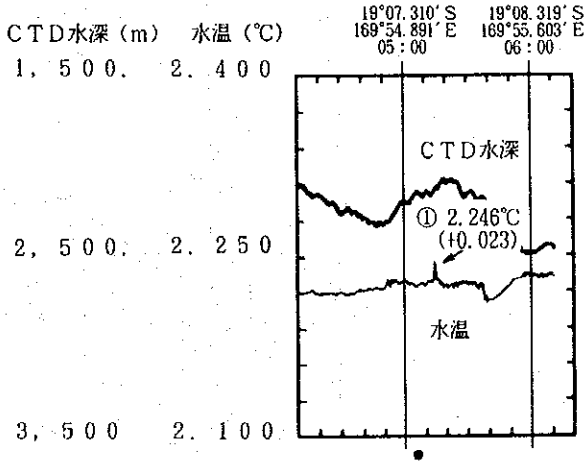

FDC－07

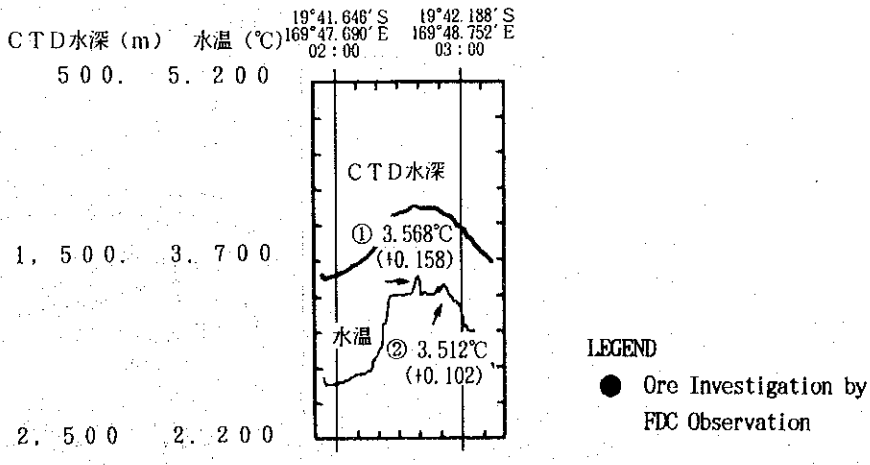

Figure 5-6-1　Temperature・CTD Depth Profiles (1)

FDC－09

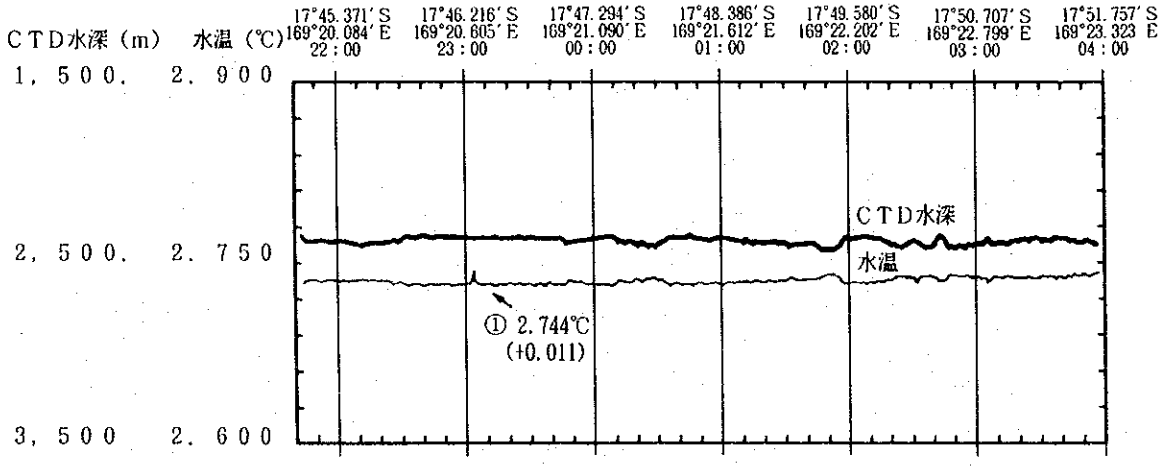

FDC－11

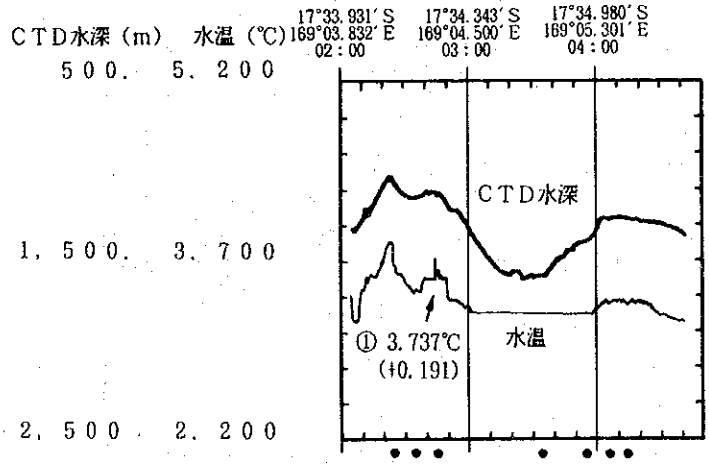

FDC－12

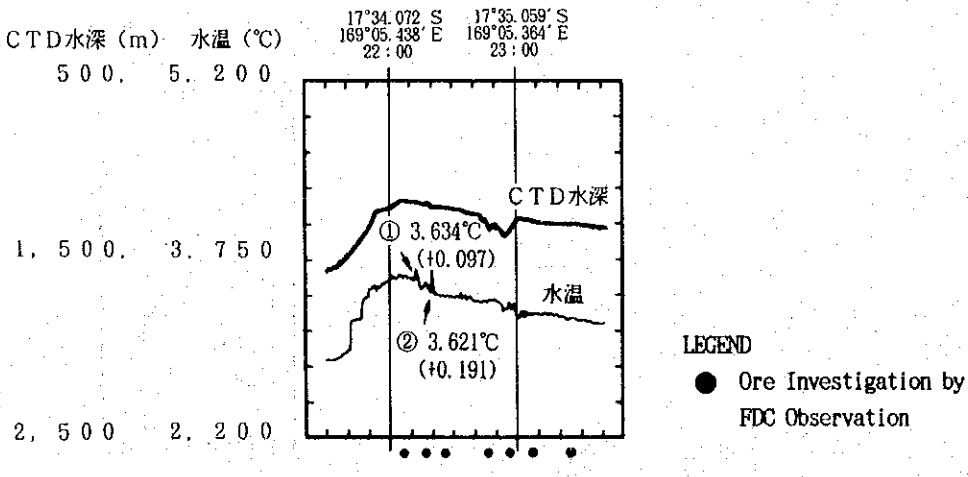

Figure 5-6-1 Temperature・CTD Depth Profiles (2)

FDC－13

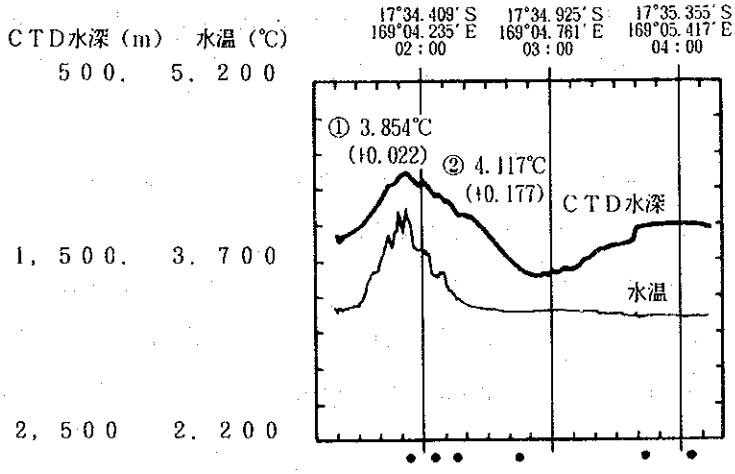

FDC－14

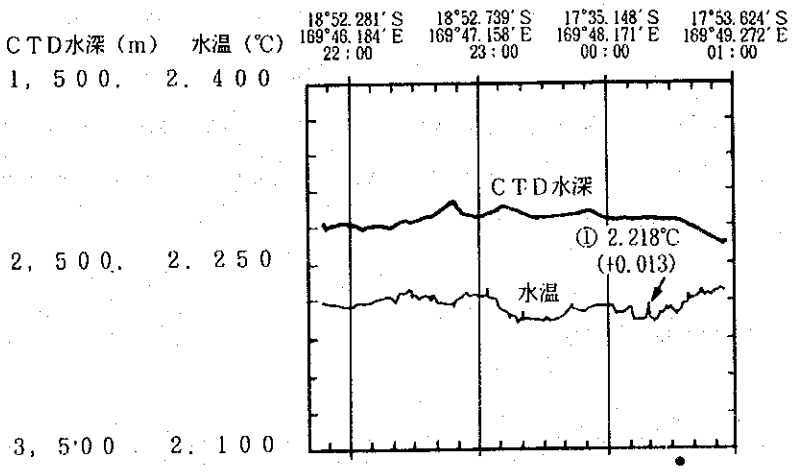

FDC－15

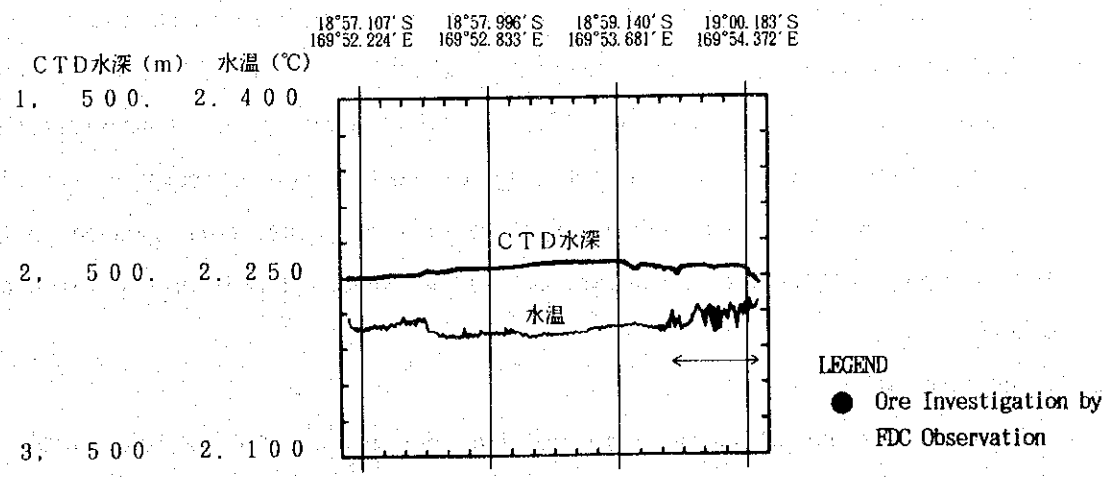

Figure 5-6-1　Temperature・CTD Depth Profiles (3)

② According to the comparison with FDC results, anomalies of water temperature correspond to signs of hydrothermal activities (hydrothermal communities, hydrothermal precipitates and others) at 17° 34.412'S.

3) Track line FDC13

① Temperature anomalies were detected at two places. The maximum values of anomalies are 0.022℃ and 0.177℃, respectively.

② According to the comparison with FDC results, signs of hydrothermal activities (hydrothermal communities, hydrothermal precipitates and others) corresponding to anomalies of water temperature were not observed.

(2) Central part of the Vate Trough

1) Track line FDC09

① Temperature anomalies were detected at one place. The maximum value of anomalies is 0.011℃.

② According to the comparison with FDC results, signs of hydrothermal activities (hydrothermal communities, hydrothermal precipitates and others) corresponding to anomalies were not obeserved.

(3) Central part of the Erromango Basin

1) Track line FDC01

① Temperature anomalies were anomalies detected at one place. The maximum value of anomalies of water temperature is 0.016℃.

② According to the comparison with FDC results, temperature anomalies correspond to signs of hydrothermal activities (hydrothermal precipitates and others).

③ High temperature zones were observed in the vicinity of 19° 02.13'N, 169° 50.20'E and 19° 04.05'N, 169° 51.47'E. Such broad anomalies of temperature have not been observed in EPR and other area up to now but when we compared them with FDC results, we found that anomalies of water temperature corresponded to the location with signs of hydrothermal activities (hydrothermal precipitates and others).

2) Track line FDC03

① Temperature anomalies were detected at one place. The maximum value of anomalies of water temperature is 0.023℃.

② According to the comparison with FDC results, signs of hydrothermal activities (hydrothermal communities, hydrothermal precipitates and others) corresponding to anomalies of water temperature were not observed.

3) Track line FDC14

① Temperature anomalies were detected at one place. The maximum value of anomalies of water temperature is 0.011℃.

② According to the comparison with FDC results, signs of hydrothermal activities (biotic communities, hydrothermal precipitates and others) corresponding to anomalies of water temperature were not observed.

4) Track line FDC15

① Variation of temperature was observed broadly, as in the case of the track line FDC01. According to the comparison with FDC results, anomalies of water temperature correspond to locations with signs of hydrothermal activities (hydrothermal precipitates and others).

(4) Track line FDC07

① Temperature anomalies were detected at two places. The maximum value of anomalies are 0.158℃ and 0.102℃, respectively.

② According to the comparison with FDC results, signs of hydrothermal activities (biotic communities, hydrothermal precipitates and others) corresponding to anomalies of water temperature were not observed.

Chapter 6. Discussions

<Survey Method and Procedures>

The volcanic central chain of the New Hebrides Trench exists on the western side of the survey area and the existence of submarine volcanoes around this sea area is well-known.

The possibility of generation of hydrothermal deposits at submarine volcanoes have been suggested. But up to now, neither systematic surveys nor reports of signs of hydrothermal deposits has been made in this sea area. This survey, therefore, is significant for determining the ideal method of submarine hydrothermal deposit exploration, procedures of exploration and methods of approaching an entirely new sea area.

In implementing our actual survey, we reviewed precedent methods for exploring hydrothermal deposits in other sea areas and bore in mind what sort of methods and procedures could be effective in vast sea areas.

The possibility of submarine hydrothermal deposits at ridge topography and sea knolls within back basins, seamounts concomitant with tectonic lines in the vicinity of volcanic fronts, seamounts and sea knolls with craters, regions of outcropping rocks or magnetic anomalies associated with new activities are known. We therefore covered the entire target area with a submarine topography survey and magnetic survey first. Based on the results of these surveys, we selected structures and other elements mentioned above, and established the locations for FDC submarine observation.

In ore deposit exploration, it is important to tow the vehicle as much as possible over areas with outcropping rocks to conduct the FDC survey. But it is difficult to determine such areas merely by topography maps and magnetic anomaly maps. For this year's survey, we drew up acoustic reflection image processed from MBES data. We found that the coverage of sea-floor sediments can be prospected by strength of sound pressure reflection. These maps, therefore, played an important role in identifying outcropping rocks that are important in establishing the locations for FDC track lines.

As the result of the FDC survey, we were able to discover and observe relatively extensive ore indications and altered zones at 7 track lines out of 17. For a survey in such a vast area, an area poor in existing data, we could say that this survey produced excellent results. Furthermore, in establishing sampling locations, we

conducted a comprehensive study by implementing the SSS survey at some part of the target area so as to obtain more detailed submarine topography. Results of the SSS survey also played an important role in determining sampling points by identifying the shape of mounds.

We conducted minute samplings in the center of ore indications, mounds, water temperature anomaly zones and places with signs of hydrothermal living things. As a result, we obtained samples of manganese oxides and others but we did not collect rocks concomitant with sulphide minerals and ores. We could not reach the mounds observed by FDC even by FPG. We inferred that this was because mounds concomitant with ore indications were distributed in limited narrow ranges. Although ore indications observed by FDC elongated in the direction of a major axis for a few hundred meters, such outcropping parts as mounds were lacking in continuity. Therefore, location assessment is an important issue if we wish to conduct our sampling operations at correct locations. If we take into consideration the precision of the GPS we are using now and a tendency of towed vehicles (such as FDC) to become unstable in bad oceanographic conditions, the precision of location might be about 100m. We, therefore, think that it is very difficult to reach the above-mentioned mounds precisely.

The methods and procedures of exploration we adopted during this year's survey might indicate a direction for efficient application of hydrothermal deposit exploration but the issues of towed vehicles at the final sampling stage and precise location assessment of sampling sites remain to be resolved.

Although we could not obtain data suggesting the existence of hydrothermal deposits with sulphide minerals in the survey area, we could presume a significant level of hydrothermal activity in this area.

<Topographic Survey>

The entire aspect of the Coriolis Troughs is revealed by the topographic survey using MBES and several topographic shapes suggesting tectonic movement were identified. According to a topographic map, the inner part of the Coriolis Troughs is divided in three, a small-scaled trough, a basin and so on.

A topographic shape suggesting several tectonic movements was identified at each trough or in the neighborhood of their boundaries. As the result of detailed studies of topography and a magnetic survey at the Yate Trough, we were able to detect sea

areas presumed to be currently most active regarding tectonic movement. Furthermore, areas starting to open as troughs or forms indicating the direction of spreading were identified at other troughs and provided effective data for selecting the location for submarine observations.

We spent most of the first half of the schedule for our topographic survey but it played an important role in the development of subsequent surveys, i.e. in applying methods of submarine observation and sampling. Ridge topography in troughs or seamounts concomitant with tectonic lines is assumed to be favorable environments for generation of hydrothermal deposits. It is therefore indispensable for effective exploration to identify in early stages the complicated topographic structure of sea areas lacking existing data.

<Acoustic Reflection Image>

To assist in determining sampling points, we drew up acoustic reflection image (sound pressure maps) utilizing the sound pressure of each beam received by MBES (see Fig. 3-2-3). High sound pressure reflected from the sea-floor is represented in black and low sound pressure is represented in white on the charts. Qualitatively, hard substances like rock masses are considered to exist in the high sound pressure part and soft substances like sediments in the low part. When we compared acoustic reflection image with the results of FDC observations, we found that the high reflection areas correspond to regions with outcropping rock masses and the low areas, correspond to regions where sediments are distributed, which shows that this method is effective for identifying the state of sea-floor, especially the coverage of sediments. The advantage of sound pressure image is that we can cover the same range in parallel with topographic maps. We believe, therefore, that acoustic reflection image can be effectively used in determining locations for FDC submarine observation and sampling.

<Magnetic Anomalies>

According to the Total Magnetic Force Map, the total magnetic force is within the range from 42,000 to 48,000nT and its value is generally low at the north and high at the south.

According to the Reduction to the Pole Map, the distribution of magnetic anomalies trending NNW-SSE and NW-SE are stressed on the whole, and high magnetic

anomalies are prominent in the northern part of the sea area and low magnetic anomalies are prominent in the southern part. The high magnetic anomalies zone in the northern part corresponds to the distribution of oceanic basalt (tholeiite) which indicates that the high magnetic anomalies zone reflects this distribution situation.

The distribution map of magnetization shows most of the seamounts in this sea area are normally magnetized but, on the whole, values of magnetic anomalies in this sea area are low. The reason for this may be because the deep part under the sea-floor is inversely magnetized.

Furthermore, magnetic lineation related to seafloor spreading and running parallel with axes of troughs is not clearly recognized in this sea area. This may be because the spreading rate was very small or it suggests that the spreading movement stopped at a certain period. Evidence showing that the troughs in this area are currently spreading is not apparent from the data of magnetic anomalies.

<Baseline Geochemical Survey>

Characteristics of sediments distributed on the Coriolis Troughs show volcanic clastics mingled very conspicuously in muddy substances. This is harmonious with this sea area's characteristics, specifically that volcanic activities are active in this sea area. It is inferred that the origin of these volcanic activities is around the ridges distributed in this sea area.

Although signs of hydrothermal activities were not confirmed by this survey, manganese oxides presumed to be hydrothermal were collected by deposit survey sampling.

As for reasons why we could not identify any ore indications by the baseline geochemical exploration, we can enumerate the facts that samples were not collectable around the ridges, that the intervals of sampling points were too long (1 mile) and that the scale of ore indications in the track line direction was too small (about 100m), so that the geochemical halos did not affect the sampling points. If we conduct future surveys by the same methods, we should take some measures to narrow the intervals of sampling points.

<FDC Survey>

Most of the ore indications observed by the FDC survey are mainly composed of oxidized altered zones. Even at the 94S01 Seamount where the scale is relatively extensive (about 500m in the direction of its major axis), the main mineralization is

less than 100m. Generally, the occurrence of rocks has the tendency for rocks to transit to pillow lava, underwater autobrecciated lava, slaggy lava (or lobate lava, sheet lava) toward the center of the main mineralization. The main mineralization generally indicate mound-shaped topography but the scope is not discernible by FDC observation. From this, there are possibilities that the slaggy, lobate or sheet forms are not lava but the forms of precipitates themselves.

Although, biotic communities presumed to indicate the existence of hydrothermal activities were observed on lobate lava in the central area of the ore indications and around the pillow lava zones, relevance to the form of lava in the neighborhood was not confirmed as the number of places observed was too few.

<Rocks>

Rocks were collected only from some parts of the survey area at the 94S01 Seamount and the Vate Trough on the north side of the survey area, in the central part of the Erromango Basin and the 94S02 Seamount on the south. Olivine, the typical feature of oceanic rocks, was not detected by macroscopical observation nor X-ray diffration. These rocks do not belong to olivine tholeiite.

According to the results of chemical analysis, rocks from the 94S01 Seamount and the Vate Trough, located on the north side, belong to tholeiite series, rocks from the south side of these rocks (Erromango Basin and 94S02 Seamount) belong to calc-alkali series and only rocks from further north (Vate Trough) are classified as MORB. From this, we can infer that the rocks from the 94S01 Seamount and Vate Trough are oceanic rocks but not concomitant with olivine, and that the rocks from the south (Erromango Basin and 94S02 Seamount) are rocks of island arcs or back arcs. There are possibilities that the geological structure of the Vate Trough (on the north side) differs from that of the Erromango Basin and southward.

<Ore Indications>

Although sampling surveys are conducted only 3 sites, which are a parts of the survey area, iron oxides on the 94S01 Seamount, manganese oxides at the central part of the Erromango Basin and iron oxides on the 94S01 Seamount are collected. The results of these specimens' chemical analysis plotted on a triangular diagram of Mn/Fe/(Cu+Ni+Co) x 10 is shown in Figure 6-1. The feature described above suggests that hydrothermal origin. We, therefore, infer that these suggest the possibility of

the existence of something in the survey area more than what we found.

Iron oxides were collected from the 94S01 Seamount and 94S02 Seamount in this year's survey. Properties of these iron oxides are somewhat different. Iron oxides collected from the 94S02 Seamount contained higher grade of Fe, maximum 0.1% of Cu and maximum 2.7% of As. Their native rock is island arc rocks or back arc rocks resembling precipitates of Epi submarine volcanoes in the north outside part of the survey area.

Most of the manganese oxides collected from the Erromango Basin are thin (only a few centimeters thick) but distributed extensively. Some of them are thicker than 35cm. Such manganese minerals as todorokite and birnessite are detected. These manganese minerals are inferred to be resembling Efate Island's manganese mine.

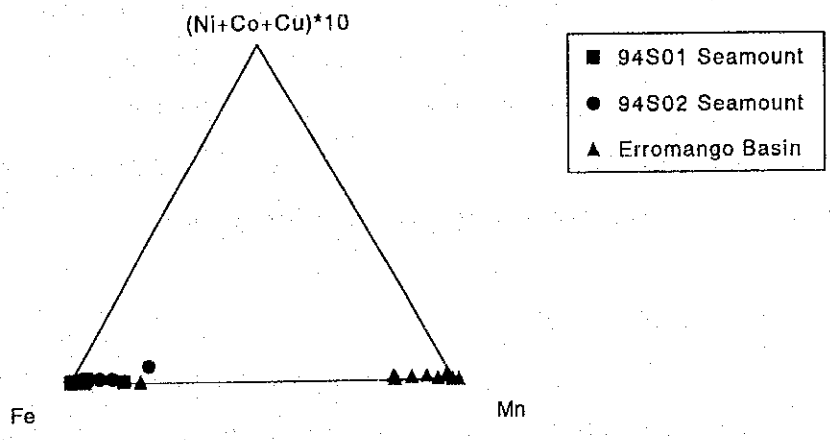

Figure 6-1 Fe-Mn-(Ni+Co+Cu)×10 Diagram

Chapter 7. Summary

In 1994, the last fiscal year of the second phase of the five year SOPAC Program, a topographical survey and a survey related to submarine hydrothermal deposits were carried out within the exclusive economic zone of the Republic of Vanuatu on the eastern side of Efate, Erromango, Tanna and Anatom Islands, in the southern part of the New Hebrides Arc. The duration of the survey was 45 days.

The survey area is located to the west of the North Fiji Basin and the Coriolis Troughs, trending NNW ~ SSE, and is distributed nearly in the central part of this area.

The survey was composed of the topographical survey for drawing up bathymetric maps using MBES, submarine observation by FDC for a mineral deposit survey, the SSS survey and sampling using LC, GC and FPG. With the objective of estimating the geological structure, magnetic surveys were carried out in conjunction with the topographical survey and a CTD survey on water temperature anomalies caused by hydrothermal activities was carried out by a CTD mounted on FDC.

Also, with the objective of determining geological properties of sediments, base-line geochemical exploration was carried out as a background.

(Results of Topographical Survey)

In principle, track lines for the topographical survey were established at intervals of 2 miles and additional interpolation lines at intervals of 1 mile were established in the areas where water depths were shallow. The total cruising distance was 6,690.3 miles.

According to the bathymetric map obtained, detailed topographic structure of the entire survey area and the whole aspect of the Coriolis Troughs were made clear. Several topographic forms suggesting tectonic movement were also identified. The Coriolis Troughs has a major axis of about 320km and a minor axis of about 100km. The strike trends N25° W. The inner part of the Coriolis Troughs is divided by small-scaled troughs and basins. Cliffs on the both sides of the Coriolis Troughs are steep, especially the cliffs on the eastern side incline steeply. The average water depth within the Coriolis Troughs is about 2,600m, depths of which increase gradually from north toward south.

(Acoustic Reflection Image)

Acoustic reflection image were drawn using the sound pressure of each beam received by MBES.

By studing the acoustic reflection image and the results of FDC observation, we found that the coverage of seafloor sediments can be estimated to a certain extent by the strength of reflection sound pressure. We verified the general principles of rocks outcropping in high reflection sound pressure areas and seafloors thickly covered with sediments in low pressure parts. This became effective data for identifying the state of submarine conditions and determining locations for FDC observation and samplings.

(Results of Magnetic Survey)

According to the Total Magnetic Force Map, the total magnetic force is within the range from 42,000nT to 48,000nT, and, on the whole, the degree of total magnetic force gently varies (increases) from north toward south.

From the IGRF residual anomaly distribution, this sea area can be seen, on the whole, as a magnetic tranquility region.

Except for prominent, positive magnetic anomalies found in the northwestern part of the sea area, others are small-scaled anomalies.

According to the distribution of reduction to the pole, the northern part of the sea area shows high magnetic anomalies and the southern part shows low magnetic anomalies.

From the point of magnetization distribution, this sea area can be classified into a high magnetized zone distributed in the western tip corresponding to the east slopes of the Vanuatu island arc and the southeastern part, and a low magnetized zone distribued in the central part ~ southern part.

This is inferred to reflect the different geological structures between the Vate Trough and the Erromango Basin/Futuna Trough.

Also, magnetic lineation is not clearly recognized. The PGM sensor was towed a distance of 5,258.9 miles.

(Baseline Geochemical Survey)

Sampling by GC and or LC was conducted with the objective of identifying the general situation of sediments in the Coriolis Troughs.

As a result of sampling, the most conspicuous vertical variation recognized in sediments is found to be color tones.

General rules that the brown series sediments relatively distribute on the upper layer of olive series sediments are found to be true at every point. Furthermore, volcanic sediments are mingled in the above-mentioned sediments, which shows this is an area with active volcanic activities.

We could not detect signs of hydrothermal activities by this sampling.

(Ore Deposit Investigation)

In selecting target areas, we paid attention to ridge topography within the back basin, sea knolls, seamounts concomitant with tectonic lines in the neighborhood of volcanic fronts, seamounts and sea knolls with caldera and outcropping rocks or magnetic anomalies appearing to be new activities from the bathymetric map, acoustic refelction image and magnetic anomaly maps, and selected five sea areas (see Fig. 5-1-1).

During the mineral deposit survey, we extracted ore indications and altered zones during the FDC survey, then carried out sampling using FPG, CB and LC. The SSS survey was carried out on the ore indications detected by the FDC survey to identify their extent.

(FDC Survey)

As a result of submarine observation at the five sea areas selected during the mineral deposit survey, relatively extensive ore indications and altered zones were recognized at three sea areas (94S01 Seamount, the central part of the Erromango Basin and 94S02 Seamount) and temperature anomalies were recognized at two sea areas (94S01 Seamount and the central part of the Erromango Basin). Also, hydrothermal biotic communities were observed at the 94S01 Seamount. The location observed roughly coincides with the place showing temperature anomalies.

Especially, black holes appearing to be blow holes of Mn oxides are abundantly observed in the central part of the ore indications and altered zones.

Track lines were established at places with high potentials of outcropping rocks by utilizing the acoustic reflection image.

(SSS Survey)

Among three sea areas in which ore indications and altered zones were observed by the FDC survey, the SSS survey was carried out to identify detailed topography and the distribution of rocks and sediments at two sea areas (94S01 Seamount and the central part of the Erromango Basin) where alteration was prominent or temperature anomalies were observed. As a result, mound-shaped rises, from where the generation of hydrothermal deposit could be expected, were extracted, which gave us important information for determining sampling points.

(Sampling)

Total 31 rounds of sampling, using FPG, LC and CB, were carried out at the sea areas of the 94S01 Seamount, the central part of the Erromango Basin and the 94S02 Seamount where relatively extensive ore indications and altered zones had been observed by the FDC and SSS surveys.

As a result, reddish brown precipitates appearing to contain iron oxides and a layer of manganese oxides, a few centimeters thick, appearing to be hydrothermal substances were collected from the central part of the Erromango Basin and the 94S02 Seamount. Similar precipitates and Mn oxides were recognized by FPG observation but we were not able to collect sulphide minerals.

From the above, we found that the hydrothermal altered zones and ore indications occurring in this sea area existed around ridges and on seamounts with structural control. We were not able to identify sulphide mineral deposits in this year's survey. Even if sulphide mineral deposits existed, they must be oxidized or occurring at lower levels.

(Temperature Anomalies)

Measurement of water temperature was carried out on a line at 17 FDC track lines by CTD sensor mounted on FDC. If variation of background was considered, distinct anomalies of water temperature were detected at several places, at water depths of 2,000m. These anomaly zones roughly correspond to the locations where signs of hydrothermal activities (biotic communities, hydrothermal precipitates and others) were recognized.

(Discussions)

As for this year's survey area, hydrothermal deposits have never been reported except in the neighborhood of Epi Volcano and the area is poor in existing data. The survey, therefore, is significant for considering methods of hydrothermal deposit exploration in an entirely new area. In conducting the actual survey, we made a bathymetric map (in parallel with magnetic survey) and selected promising regions by taking into consideration the places of origin of mineral deposits already known, then decided the sampling points based on the FDC and SSS survey results. We found, from the MBES acoustic reflection image, that the situation of sediment coverage can be estimated to a certain extent. It became clear that this method will be effective in the future surveys.

The methods and procedures of exploration we adopted during this year's survey may indicate a direction as an efficient application for hydrothermal deposit exploration but the issue of the precise location of samplings remains to be resolved.

Putting all survey results together, it became clear that the ore indications occurring in this sea area exist around ridges and seamounts with structural control.

Although sulphide minerals were not collected by sampling, we can presume a significant level of hydrothermal activity in this area.

[Reference]

Akimoto, K., Hasegawa, S., 1989:
Bathymetric Distribution of the Recnt Benthic Foraminifers around Japan - As a Contribution to the New Paleobathymetric Scale -.
The Memories of the Geological Society of Japan, 32, 229-240.

Alpha, T.R., 1988:
Perspective Physiographic Diagram of Vanuatu.
Geology and Offshore Resources of Pacific Island Arcs-Vanuatu Region, Circum-Pacific Council for Energy and Mineral Resources Earth Science Series, 8, 29-34.

B, A. W.H., 1977:
An Ecological Zoogeograhic and Taxonomic Review of Recent Planktonic Foraminifera.
In Ramsay, A.T.S.(ed.), Oceanic Micropaleontology. London, Academic Press, 1, 1-100.

Berggen, W.A., Kent, D.V., Flynn, J.J. and Van Couvering, J.A., 1985:
Cenozoic Geochoronology.
Geol. Soc. Am. Bull., 96, 1407-1418.

Blow, W.H., 1969:
Late Middle Eocene to Recent Planktonic Foraminiferal Biostratigraphy.
Proceedings of the First International Conference on Planktonic Microfossils, 1, 199-422.

Brocher, T.M., 1985:
On the Age Progression of the Seamounts West of the Samoan Islands, SW Pacific.
Investegations of the Northern Melanesian Borderland, Circum-Pacific Council for Energy and Mineral Resources Earth Science Series, 3, 173-186.

Brocher, T.M., 1985:
On the Formation of the Vitiaz Trench Lineament and North Fiji Basin.
Investegations of the Northern Melanesian Borderland, Circum-Pacific Council for Energy and Mineral Resources Earth Science Series, 3, 13-34.

Brocher, T.M., and Holmes, R., 1985:
Tectonic and Geochemical Framework of the Northern Melanesian Borderland:
An Overview of the KK820316 Leg 2 Objectives and Results.
Investegations of the Northern Melanesian Borderland, Circum-Pacific Council for Energy and Mineral Resources Earth Science Series, 3, 1-12.

Brocher, T.M., and Holmas, R., 1985:
The Marine Geology of Sedimentary Basins South of Viti Levu, Fuji.
Investegations of the Northern Melanesian Borderland, Circum-Pacific Council for Energy and Mineral Resources Earth Science Series, 3, 123-138.

Brocher, T.M., and Wirasantosa, S., 1985:
Regional Sedimentation Patterns along the Northern Melanesian Borderland.
Investegations of the Northern Melanesian Borderland, Circum-Pacific Council for Energy and Mineral Resources Earth Science Series, 3, 77-102.

Buchbinder, B., and Halley, R.B., 1988:
Source-Rock Evaluation of Outcrop Sample from Vanuatu (Malakula, Espiritu Santo, Maewo, and Pentecost).
Geology and Offshore Resources of Pacific Island Arcs-Vanuatu Region, Circum-Pacific Council for Energy and Mineral Resources Earth Science Series, 8, 255-266.

Burne, R.V., Collot, J.Y., and Deniel, J., 1988:
Superficial Structures and Stress Regimes of the Downgoing Plate Accociated with Subduction-collision in the Central New Hebrides Arc (Vanuatu).
Geology and Offshore Resources of Pacific Island Arcs-Vanuatu Region, Circum-Pacific Council for Energy and Mineral Resources Earth Science Series, 8, 357-376.

Chaproniere, G.C.H., 1983:
Late Tertiary and Quaternary Foraminiferal Biostratigraphy and Paleobathymetry of Cores and Dredge Samples from Cruise KK820316 Leg 2.
Investegations of the Northern Melanesian Borderland, Circum-Pacific Council for Energy and Mineral Resources Earth Science Series, 3, 103-122.

Chaproniere, G.C.H., 1991:
Pleistocene to Holocene Planktic Foraminiferal Biostratigraphy of the Coral Sea, Offshore Queensland, Australia.
BMR J. Aus. Geol. Geophys, 12, 3, 195-221.

Chase, T.E., and Seekins, B.A., 1988:
Submarine Topography of the Vanuatu and Southeastern Solomon Islands Region.
Geology and Offshore Resources of Pacific Island Arcs-Vanuatu Region, Circum-Pacific Council for Energy and Mineral Resources Earth Science Series, 8, 35-36.

Collot, J.Y., and Fisher, M.A., 1988:
Crustal Structure, from Gravity Data, of a Collision Zone in the Central New Hebrides Island Arc.
Geology and Offshore Resources of Pacific Island Arcs-Vanuatu Region, Circum-Pacific Council for Energy and Mineral Resources Earth Science Series, 8, 125-140.

Crawford, A.J., Greene, H.G., and Exon, N.F., 1988:
Geology, Petrology and Geochemistory of Submarine Volcanoes around Epi Island, New Hebrides Island Arc.
Geology and Offshore Resources of Pacific Island Arcs-Vanuatu Region, Circum-Pacific Council for Energy and Mineral Resources Earth Science Series, 8, 301-328.

Duncan, R.A., 1985:
Radiometric Ages form Volcanic Rocks along the New Hebrides-Samoa Lineament.
Investegations of the Northern Melanesian Borderland, Circum-Pacific Council for Energy and Mineral Resources Earth Science Series, 3, 67-76.

Falvey, D.A., and Greene, H.G., 1988:
Origin and Evolution of the Sedimentary Basins of the New Hebrides Arc.
Geology and Offshore Resources of Pacific Island Arcs-Vanuatu Region, Circum-Pacific Council for Energy and Mineral Resources Earth Science Series, 8, 413-442.

Fisher, M.A., 1988:
Petroleum Geology of the Central New Hebrides Arc.
Geology and Offshore Resources of Pacific Island Arcs-Vanuatu Region, Circum-Pacific Council for Energy and Mineral Resources Earth Science Series, 8, 279-286.

Fisher, M.A., Falvey, D.A., and Smith, G.A., 1988:
Seismic Stratigraphy of the Summit Basins of the New Hebrides Island Arc.
Geology and Offshore Resources of Pacific Island Arcs-Vanuatu Region, Circum-Pacific Council for Energy and Mineral Resources Earth Science Series, 8, 201-224.

Glikson, M., 1988:
Miocene Algal Reef-Derived Deposits in Vanuatu-Possible Petroleum Source Rocks.
Geology and Offshore Resources of Pacific Island Arcs-Vanuatu Region, Circum-Pacific Council for Energy and Mineral Resources Earth Science Series, 8, 267-274.

Golan-bac, M., and Kvenvolden, K.A., 1988:
Hydrocarbon Gases in Surface Sediments of the South Aoba Basin, Vanuatu.
Geology and Offshore Resources of Pacific Island Arcs-Vanuatu Region, Circum-Pacific Council for Energy and Mineral Resources Earth Science Series, 8, 275-278.

Greene, H.G., and Johnson, D.P., 1988:
Geology of the Central Basin Region of the New Hebrides Arc Inferred from Single-channel Seismic-reflection Data.
Geology and Offshore Resources of Pacific Island Arcs-Vanuatu Region, Circum-Pacific Council for Energy and Mineral Resources Earth Science Series, 8, 177-200.

Greene, H.G., Macfarlane, A., Johnson, D.P., and Crawford, A.J., 1988:
Structure and Tectonics of the Central New Hebrides Arc.
Geology and Offshore Resources of Pacific Island Arcs-Vanuatu Region, Circum-Pacific Council for Energy and Mineral Resources Earth Science Series, 8, 377-412.

Greene, H.G., Macfarlane, A., and Wong, F.L., 1988:
Geology and Offshore Resources of Vanuatu-Introduction and Summary.
Geology and Offshore Resources of Pacific Island Arcs-Vanuatu Region, Circum-Pacific

Council for Energy and Mineral Resources Earth Science Series, 8, 1-28.

Holmes, M.L., 1988:
Seismic Refraction Measurements in the Summit Basin of the New Hebeides Arc.
Geology and Offshore Resources of Pacific Island Arcs-Vanuatu Region, Circum-Pacific Council for Energy and Mineral Resources Earth Science Series, 8, 163-176.

Ingle, J.C.Jr., 1980:
Cenozoic Paleobathymetry and Depositional History of Selected Sequences within the Southern California Continental Borderland.
Cushman Foundation Special Publication, 19, 163-195.

Johonson, D.P., Belford, D.J., Cater, A.N., Crawford, A.J., 1988:
Petrology and Age of Dredge Sample Collected in the Central Basin, Vanuatu.
Geology and Offshore Resources of Pacific Island Arcs-Vanuatu Region, Circum-Pacific Council for Energy and Mineral Resources Earth Science Series, 8, 141-162.

Johnson, D.P., and Greene, H.G., 1988:
Modern Depositional Regimes, Offshore Vanuatu.
Geology and Offshore Resources of Pacific Island Arcs-Vanuatu Region, Circum-Pacific Council for Energy and Mineral Resources Earth Science Series, 8, 287-300.

Katz, H.R., 1988:
Offshore Geology of Vanuatu-Previous Work.
Geology and Offshore Resources of Pacific Island Arcs-Vanuatu Region, Circum-Pacific Council for Energy and Mineral Resources Earth Science Series, 8, 93-124.

Keating, B., 1983:
Paleomagnetic Studies of the Samoan Island: Results from the Islands of Tutuila and Savaii.
Investegations of the Northern Melanesian Borderland, Circum-Pacific Council for Energy and Mineral Resources Earth Science Series, 3, 187-199.

Louat, R., Hamburger, M., and Monzier, M., 1988:
Shallow and Intermediate-depth Seismicity in the New Hebrides Arc: Constraints on the Subduction Process.
Geology and Offshore Resources of Pacific Island Arcs-Vanuatu Region, Circum-Pacific Council for Energy and Mineral Resources Earth Science Series, 8, 329-356.

Macfarlane, A., Carney, J.N., Crawford, A.J., and Greene, H.G., 1988:
Vanuatu-A Review of the Onshore Geology.
Geology and Offshore Resources of Pacific Island Arcs-Vanuatu Region, Circum-Pacific Council for Energy and Mineral Resources Earth Science Series, 8, 45-92.

Natland, J.H., and Turner, D.L., 1983:
Age Progression and Petrological Development of Samoan Shield Volcanoes: Evidence from K-Ar Ages, Lava Compositions, and Mineral Studies.
Investegations of the Northern Melanesian Borderland, Circum-Pacific Council for Energy and Mineral Resources Earth Science Series, 3, 139-172.

Okuma, S., Makino, M., and Nakatuka, T., 1989:
Two-Layer Model Inversion of Magnetic Anomalies Using Pseudogravity and Reduction to the Pole: An Application to the Analysis of Aeromagnetic Anomalies over Izu-Oshima.
Butsuri-Tansa (Geophysical Exploration), 42, 2, 82-96.

Person, L., Hawkins, J., et al, 1992:
Proc.ODP, Init. Repts., 135
College Station, TX (Ocean Drilling Program).

Price, R.C., Maillet, P., and Johonson, D.P., 1993:
Interpretation of GLORIA Side-Scan Sonar Imagery for the Coriolis Troughs of the New Hebrides Backarc.
Geo-Marine Letters, 13, 71-81.

Sinton, J.M., Johonson, Kevin T.M., and Price, R.C., 1985:
Petrology and Geochemistry of Volcanic Rocks form Northen Melanesian Borderland.
Investegations of the Northern Melanesian Borderland, Circum-Pacific Council for

Energy and Mineral Resources Earth Science Series, 3, 35-66.

Smith, G.L., Falvey, D.A., and Shaw, R., 1988:
Multichannel Data Acquisition and Processing.
Geology and Offshore Resources of Pacific Island Arcs-Vanuatu Region, Circum-Pacific Council for Energy and Mineral Resources Earth Science Series, 8, 39-44.

Steele, W.C., and Kinoshita, K.L., 1988:
Navigational Data Collection, Processing, and Display.
Geology and Offshore Resources of Pacific Island Arcs-Vanuatu Region, Circum-Pacific Council for Energy and Mineral Resources Earth Science Series, 8, 37-38.

Tiffin, D.L., 1993:
Tectonic and Structural Features of the Pacific/Indo-Australian Plate Boundary in the North Fiji-Lau Basin Regions, Southwest Pacific.
Geo-Marine Letters, 13, 126-131.

Wong, F.L., and Greene, H.G., 1988:
Geologic Hazards Identified in the Central Basin Region, Vanuatu.
Geology and Offshore Resources of Pacific Island Arcs-Vanuatu Region, Circum-Pacific Council for Energy and Mineral Resources Earth Science Series, 8, 225-254.

[Appendix]

1. Sampling Results of the BaseLine Geochemical Survey
2. Results of the FDC Observation
3. List of the Ore Indications
4. Sampling Results of the Ore Deposit Investigation (1), (2)
5. List of Samples (1) ~ (4)
6. Results of Chemical Analysis for Sampling Sediments (1) ~ (4)
7. Results of Microscopic Observation (1), (2)
8. Results of X-ray Diffraction Analysis (1), (2)
9. Sea-water Sound Velocity for MBES
10. Weather and Sea-state Data

Appendix Table 1 Sampling Results of the Baseline Geochemical Survey

Sample No.	Date	Time	Latitude	Longitude	Depth	Core length	Remarks
94SBGC01	09/09	20:37105	19°01.293' S	169°58.146' E	2,710m	5cm	
94SBGC02	09/09	23:02:50	19°01.856' S	169°57.623' E	2,685m	107cm	
94SBGC03	09/10	01:20:40	19°02.915' S	169°56.743' E	3,080m	0cm	No Sample
94SBGC04	09/10	03:46:55	19°03.336' S	169°56.047' E	3,128m	0cm	No Sample
94SBGC05	09/10	06:12:15	19°03.485' S	169°55.832' E	3,119m	153cm	Same point GC04
94SBGC06	09/10	20:29:05	19°01.184' S	169°58.285' E	2,727m	93cm	Same point GC01
94SBGC07	09/11	22:00:35	19°03.920' S	169°55.279' E	3,050m	0cm	Fail
94SBLC08	09/11	01:46:55	19°04.073' S	169°55.315' E	3,055m	44cm	Same point GC07
94SBLC09	09/11	04:09:30	19°04.776' S	169°54.580' E	2,594m	73cm	
94SBLC10	09/11	20:19:20	19°05.372' S	169°53.840' E	2,339m	0cm	No Sample
94SBLC11	09/11	22:24:35	19°06.081' S	169°53.063' E	2,511m	0cm	Bit damage
94SBLC12	09/12	00:32:20	19°06.805' S	169°52.280' E	2,540m	82cm	
94SBLC13	09/12	02:40:10	19°07.592' S	169°51.509' E	2,510m	110cm	
94SBLC14	09/12	04:47:25	19°08.260' S	169°50.771' E	2,618m	0cm	No Sample
94SBGC15	09/22	21:24:00	19°08.245' S	169°50.713' E	2,633m	70cm	Same point GC14
94SBGC16	09/22	23:36:40	19°08.889' S	169°50.062' E	2,715m	61cm	
94SBGC17	09/23	01:51:40	19°09.671' S	169°49.294' E	2,673m	27cm	

Note:Data and Time represent the GMT,Time is Sampler on bottom.
(94SBGC07 is plunging data)

Appendix Table 2 Results of the FDC Observation (1)

Date	Track Line No.	Plumbing Time (a) / Landing Time (b) / Taking-off Time (c) / Hauling-up Time (d) Time	Location Latitude	Location Longitude	Depth (m)	Duration of Operation (a)～(d)	Duration of Observation (b)～(c)	Length Observed (mile)	Number of Photos Taken	Details of the Observation
9/24 9/25	94SFDC01	Plumbing Time (a) 21:00 Landing Time (b) 21:52 Veering 1:06 Taking-off Time (c) 4:45 Hauling-up Time (d) 5:30	19° 1.826'S 19° 4.621'S 19° 7.302'S	169° 49.930' E 169° 51.867' E 169° 55.251' E	2,504 2,318 2,193	8:30	6:53	7.5	353	Observed along a ridge in the central part of Erromango Basin for 7.5 miles in the NW→SE direction. Outcrops of rocks were prominent. Rock types mainy observed were sheet lava, slaggy lava and underwater autobrecciated lava. Typical pillow lava was not observed. Ore indication were recognized at six places.
9/25 9/26	94SFDC02	Plumbing Time (a) 20:59 Landing Time (b) 22:02 Veering 0:12 Taking-off Time (c) 1:59 Hauling-up Time (d) 2:45	19° 4.664'S 19° 7.010'S 19° 6.982'S	169° 56.460' E 169° 56.066' E 169° 58.072' E	3,057 2,339 2,241	5:46	3:57	4.3	92	Observed along a ridge in the central part of the Erromango Basin for 4.3 miles in the N→S, W→E directions. Sediments were prominent. Rock types observed were underwater autobrecciated lava and sheet lava. Ore indications were not recognized.
9/26	94SFDC03	Plumbing Time (a) 3:26 Landing Time (b) 4:11 Taking-off Time (c) 6:11 Hauling-up Time (d) 7:07	19° 6.607'S 19° 8.486'S	169° 54.302' E 169° 55.826' E	2,082 2,451	3:41	2:00	2.4	71	Observed along a ridge in the central part of the Erromango Basin (Southeastern part of track line 02) for 2.4 miles in the NW→SE direction. Outcrops of rocks were relatively prominent. Rock types mainly observed were slaggy lava and underwater autobrecciated lava. Ore indications were not recognized.
9/26 9/27	94SFDC04	Plumbing Time (a) 20:56 Landing Time (b) 21:38 Taking-off Time (c) 0:52 Hauling-up Time (d) 1:18	19° 23.845'S 19° 27.032'S	169° 50.680' E 169° 52.419' E	1,841 1,001	4:22	3:14	3.6	159	Observed at a seamount on the boundary between Futuna Trough and Erromango Basin for 3.6 miles in the NW→SE direction. Outcrops of rocks were prominent. Rock types mainly observed were pillow lava, sheet lava, slaggy lava and talus. Ore indications were recognized on the top pf the seamount.
9/27	94SFDC05	Plumbing Time (a) 1:52 Landing Time (b) 2:31 Taking-off Time (c) 4:40 Hauling-up Time (d) 5:11	19° 25.113'S 19° 27.445'S	169° 52.359' E 169° 51.735' E	1,803 1,416	3:19	2:09	2.4	154	Observed at a same seamout as the track line 04 for 2.4 miles in the NNE→SSW direction. Outcrops of rocks were prominent. Rock types mainly observed were pillow lava, sheet lava, slaggy lava and talus (same as track line 04). Ore indications were recognized on the top of the seamount.
9/27 9/28	94SFDC06	Plumbing Time (a) 21:12 Landing Time (b) 21:45 Taking-off Time (c) 0:49 Hauling-up Time (d) 1:25	19° 41.699'S 19° 41.787'S	169° 42.773' E 169° 46.579' E	1,409 1,621	4:23	3:04	3.6	114	Observed two seamounts, where magnetic anomalies were found, on the boundary between the Futuna Trough and the Erromango Basin for 3.6 miles in the W→E direction. Sediments were prominent. Black and white sediments on lutaceous substances were observed. Ore indications were not recognized.
9/28	94SFDC07	Plumbing Time (a) 1:48 Landing Time (b) 1:53 Taking-off Time (c) 3:14 Hauling-up Time (d) 3:48	19° 41.559'S 19° 42.327'S	169° 47.523' E 169° 48.958' E	1,567 1,508	2:00	1:21	1.6	45	Observed at a seamount (different from track line 06) on the boundary between the Futuna Trough and Erromango Basin for 1.6 miles in the NW→SE direction. Sediments were prominent. Black and White sediments on lutaceous substances were observed. Ore indications were not recognized.
9/28 9/29	94SFDC08-0	Plumbing Time (a) 20:57 Landing Time (b) 21:50 Taking-off Time (c) 1:07 Hauling-up Time (d) 2:03	17° 55.597'S 17° 59.306'S	169° 25.000' E 169° 24.965' E	2,630 2,692	5:06	3:17	3.7	106	Observed at the central part of the Vate Trough, on the north side of the survey aera, for 7.4 miles in the N→S direction. Outcrops of rocks were observed for approximately 70% of entire track line. Rock types mainly observed were pillow lava, lobate lava and talus. Ore indications were not observed.
9/29	94SFDC08-1	Plumbing Time (a) 2:34 Landing Time (b) 3:28 Taking-off Time (c) 7:26 Hauling-up Time (d) 8:17	17° 59.002'S 18° 2.679'S	169° 24.986' E 169° 24.965' E	2,666 2,621	5:43	4:00	3.7	80	

Appendix Table 2 Results of the FDC Observation (2)

Date	Track Line No.	Time: Plumbing Time (a), Landing Time (b), Taking-off Time (c), Hauling-up Time (d)	Location: Latitude	Location: Longitude	Depth (m)	Duration of Operation (a)~(d)	Duration of Observation (b)~(c)	Length Observed (mile)	Number of Photos Taken	Details of the Observation
9/29 9/30	94SFDC09	Plumbing Time (a) 20:56 Landing Time (b) 21:44 Taking-off Time (c) 3:56 Hauling-up Time (d) 4:49	17° 45.099'S 17° 51.679'S	169° 19.956' E 169° 23.272' E	2,354 2,389	7:53	6:12	7.3	171	Observed the central part of the Vate Trough, on the north side of the survey area, for 7.3 miles in the NW→SE direction. Outcrops of rocks were prominent. Rock types mainly observed were pillow lava, lobate lava and talus. Ore indications were not recognized.
9/30 10/1	94SFDC10	Plumbing Time (a) 20:57 Landing Time (b) 21:32 Taking-off Time (c) 0:24 Hauling-up Time (d) 0:57	17° 33.452'S 17° 34.667'S	169° 3.754' E 169° 6.072' E	1,520 1,439	4:00	2:56	2.5	176	Observed at a seamount with a caldera on its top, located at the norhern part of Vate Trongh, for 2.5 miles in the NW→SE direction. Outcrops of rocks were prominent. Rock types mainly observed were pillow lava and partially slaggy lava and lobate lava. Ore indications and hydrothermal communities were recognized at one place.
10/1	94SFDC11	Plumbing Time (a) 1:34 Landing Time (b) 2:05 Taking-off Time (c) 4:40 Hauling-up Time (d) 5:12	17° 33.894'S 17° 35.412'S	169° 3.843' E 169° 5.856' E	1,324 1,364	3:38	2:35	2.5	220	Observed at the same seamount as the track line 10 for 2.5 miles in the NW→SE direction. Outcrops of rocks were prominent. Rock types mainly observed were pillow lava and partially slaggy lava and lobate lava. Ore indications were recognized at three places.
10/2 10/3	94SFDC12	Plumbing Time (a) 20:55 Landing Time (b) 21:29 Taking-off Time (c) 23:40 Hauling-up Time (d) 0:12	17° 33.449'S 17° 35.658'S	169° 5.503' E 169° 5.303' E	1,532 1,331	3:17	2:11	2.2	235	Observed at the same seamount as the track line 10 for 2.2 miles in the N→S direction (the direction intersecting with track lines 10, 11and13). Outcrops of rocks were prominent. Same rock types as track line 10 were observed. Ore indications were recognized at four places and hydrothermal communities were recognized at one place.
10/3	94SFDC13	Plumbing Time (a) 0:46 Landing Time (b) 1:19 Taking-off Time (c) 4:12 Hauling-up Time (d) 4:43	17° 34.041'S 17° 35.524'S	169° 3.485' E 169° 5.532' E	1,356 1,316	3:57	2:53	2.5	167	Observed at the same seamount as track line 10 the south side of the track line 10 for 2.5 miles in the NW →SE direction. Outcrops of rocks were prominent. Same rock types as track line 10 were observed. Ore indications were recognized at one place.
10/3 10/4	94SFDC14	Plumbing Time (a) 20:57 Landing Time (b) 21:45 Taking-off Time (c) 0:52 Hauling-up Time (d) 1:44	18° 52.225'S 18° 53.580'S	169° 45.909' E 169° 49.128' E	2,281 2,400	4:47	3:07	3.4	120	Observed along the ridge in the northern part of the Erromango Basin for 3.4 miles in the NNW→SEE direction. Sediment were prominent. Rock types observed were sheet lava, Slaggy lava and talus. Ore indications were recognized at one place.
10/4	94SFDC15	Plumbing Time (a) 2:04 Landing Time (b) 2:53 Taking-off Time (c) 6:02 Hauling-up Time (d) 6:56	18° 56.976'S 19° 0.256'S	169° 52.111' E 169° 54.433' E	2,472 2,524	4:52	3:09	4.0	172	Observed along the same ridge as track line 14, the southeastern side of the track line 14, for 4.0 miles in the NW→SE direction. Sediments were prominent. Rock types observed were slaggy lava. Ore indication were recognized at one place.
10/4 10/5	94SFDC16	Plumbing Time (a) 20:57 Landing Time (b) 21:56 Taking-off Time (c) 0:45 Hauling-up Time (d) 1:41	19° 15.757'S 19° 18.449'S	169° 58.106' E 169° 59.719' E	2,222 2,250	4:44	2:49	3.1	84	Observed the southern part of the Erromango Basin for 3.1 miles in the NNW→SSE direction. Outcrops of rocks were approximately 80% of entire track line. Rock types observed were pillow lava and talus. Ore indications were not observed.
10/5	94SFDC17	Plumbing Time (a) 3:25 Landing Time (b) 4:28 Taking-off Time (c) 6:02 Hauling-up Time (d) 6:59	19° 3.974'S 19° 5.123'S	169° 47.612' E 169° 48.831' E	2,792 2,508	3.34	1:34	1.6	41	Observed the western part of the Erromango Basin for 1.6 miles in the NW→SE direction. Sediments were prominent throughout the track line. Talus were outcropping extremely rarely. Ore indications were not recognized.

Appendix Table 3 List of Ore Indications

Track Line No.	Ore Indsecation No.		Location	Depth (m)	Duration of Observation (m:s)	Length of Observation (m:s)	Ore Indication	Living Things	Temperature Anomalies	Photo No.	Time (GMT)
94SFDC01	1-1	from	19° 2.378′ S 169° 50.324′ E	2,214			Hydrothermal Sediments	—	—	35~46 (12)	22:42:55
		to	19° 2.427′ S 169° 50.328′ E	2,214	02:30	91					22:42:25
	1-2	from	19° 2.703′ S 169° 50.535′ E	2,228			Hydrothermal Sediments	—	—	62~73 (12)	23:04:55
		to	19° 2.863′ S 169° 50.694′ E	2,270	11:50	418					23:16:45
	1-3	from	19° 3.860′ S 169° 51.346′ E	2,277			Hydrothermal Sediments	Macrura (red) Cnidaria	—	102~114 (13)	0:19:10
		to	19° 3.981′ S 169° 51.385′ E	2,301	05:05	235					0:25:15
	1-4	from	19° 4.267′ S 169° 51.629′ E	2,374			Hydrothermal Sediments	—	—	124~128 (5)	0:45:30
		to	19° 4.278′ S 169° 51.644′ E	2,362	00:45	34					0:46:15
	1-5	from	19° 5.240′ S 169° 52.119′ E	2,032			Hydrothermal Sediments	Holothurioidea Anthozoa Gorgonian Macrura (red)	—	156~242 (87)	1:37:55
		to	19° 5.559′ S 169° 52.798′ E	2,111	32:50	1389					2:10:45
	1-6	from	19° 5.928′ S 169° 53.281′ E	2,151			Hydrothermal Sediments	Porifera Gorgonian Brachyura	—	266~316 (51)	2:42:40
		to	19° 6.526′ S 169° 54.218′ E	1,986	57:40	2059					3:40:20
94SFDC03	3-1	from	19° 7.413′ S 169° 54.983′ E	2,153			Hydrothermal Sediments	—	—	3-34 (1)	5:05:20
		to	° ′ S ° ′ E	—	—	—					
94SFDC04	4-1	from	19° 26.376′ S 169° 52.056′ E	931			Hydrothermal Sediments	Gorgonian Anthozoa	—	91~146 (56)	0:04:50
		to	19° 26.768′ S 169° 52.293′ E	1,039	29:00	848					0:33:50
94SFDC05	5-1	from	19° 26.405′ S 169° 52.044′ E	926			Hydrothermal Sediments	Gorgonian Anthozoa Osteichthyes	—	50~120 (71)	3:37:10
		to	19° 26.847′ S 169° 51.885′ E	898	20:30	870					3:57:40
94SFDC10	10-1	from	17° 34.223′ S 169° 5.191′ E	1,285			Chimney Hydrothermal Sediments	Munidopsis sp. Gastropod Gorgonian Macrura (red)	—	68~141 (84)	23:15:40
		to	17° 34.399′ S 169° 5.534′ E	1,208	26:00	714					23:41:40
94SFDC11	11-1	from	17° 33.987′ S 169° 3.958′ E	1,196			Hydrothermal Sediments	Brachyura Gorgonian	0.19↑	8~58 (51)	2:15:15
		to	17° 34.290′ S 169° 4.358′ E	1,188	34:35	929					2:49:50
	11-2	from	17° 34.947′ S 169° 5.228′ E	1,421			Hydrothermal Sediments	Gorgonian	—	107~164 (58)	3:51:45
		to	17° 35.045′ S 169° 5.372′ E	1,301	09:40	323					4:01:25
	11-3	from	17° 35.098′ S 169° 5.453′ E	1,276			Hydrothermal Sediments	Anthozoa Holothurioidea	—	169~206 (38)	4:06:35
		to	17° 35.182′ S 169° 5.532′ E	1,283	09:10	214					4:15:45
94SFDC12	12-1	from	17° 34.166′ S 169° 5.442′ E	1,176			Chimney Hydrothermal Sediments	Bythograea thermydron Gorgonian	+0.09↑	25~64 (40)	22:06:00
		to	17° 34.284′ S 169° 5.414′ E	1,185	07:50	225					22:13:50
	12-2	from	17° 34.293′ S 169° 5.402′ E	1,182			Hydrothermal Sediments	Munidopsis sp. Bythograea thermydron Gastropod Anthozoa	+0.19↑	70~128 (59)	22:17:30
		to	17° 34.552′ S 169° 5.376′ E	1,217	11:35	482					22:29:05
	12-3	from	17° 34.933′ S 169° 5.330′ E	1,332			Chimney Hydrothermal Sediments	Gorgonian	—	154~202 (49)	22:47:15
		to	17° 35.205′ S 169° 5.389′ E	1,297	22:25	515					23:09:40
	12-4	from	17° 35.262′ S 169° 5.336′ E	1,308			Hydrothermal Sediments (weak)	—	—	210~219 (10)	23:14:25
		to	17° 35.381′ S 169° 5.360′ E	1,306	08:00	225					23:22:25
94SFDC13	13-1	from	17° 34.549′ S 169° 4.237′ E	1,243			Hydrothermal Sediments	—	—	61~65 (5)	2:15:50
		to	17° 34.583′ S 169° 4.252′ E	1,245	01:05	69					2:16:55
94SFDC14	14-1	from	18° 53.462′ S 169° 48.808′ E	2,286			Hydrothermal Sediments	Macrura (red)	—	79~85 (7)	0:35:00
		to	18° 53.473′ S 169° 48.823′ E	2,296	00:50	34					0:35:50
	14-2	from	18° 53.489′ S 169° 48.913′ E	2,325			Hydrothermal Sediments	—	—	95~102 (8)	0:39:20
		to	18° 53.500′ S 169° 48.934′ E	2,333	01:30	44					0:40:50
94SFDC15	15-1	from	18° 59.715′ S 169° 54.077′ E	2,489			Hydrothermal Sediments	Asteroidea Gorgonian Holothurioidea Macrura (red)	—	75~164 (90)	5:28:00
		to	18° 59.992′ S 169° 54.266′ E	2,467	16:50	621					5:44:50

Appendix Table 4 Sampling Results of Ore Deposit Investigation (1)

Sample No.	Date	Time	Latitude	Longitude	Depth	Core length	Remarks
94SDLC01	10/07	01:21:30	17°35.154' S	169°05.378' E	1,287m	50cm	※
94SDLC02	10/07	03:00:05	17°34.423' S	169°05.370' E	1,212m	0cm	No Sample, ※
94SDLC03	10/07	21:34:20	17°34.197' S	169°05.427' E	1,160m	86cm	
94SDLC04	10/07	23:05:55	17°34.239' S	169°05.457' E	1,180m	30cm	
94SDLC05	10/08	00:43:25	17°34.338' S	169°05.481' E	1,192m	0cm	Recovery Rock 97g, ※
94SDLC06	10/08	02:25:20	17°34.429' S	169°05.506' E	1,193m	20cm	
94SDLC07	10/08	03:47:15	17°34.453' S	169°05.396' E	1,200m	0cm	Recovery Rock 13g, ※
94SDLC08	10/08	21:50:40	18°59.898' S	169°54.068' E	2,417m	5cm	
94SDLC09	10/08	23:56:20	18°59.775' S	169°54.147' E	2,419m	146cm	
94SDLC10	10/09	02:46:45	19°04.928' S	169°51.382' E	2,303m	40cm	
94SDLC11	10/09	04:22:55	19°05.128' S	169°52.359' E	2,056m	35cm	
94SDLC12	10/09	22:33:15	18°59.816' S	169°54.191' E	2,417m	70cm	
94SDLC13	10/10	00:51:10	18°59.863' S	169°54.203' E	2,432m	93cm	
94SDLC14	10/10	03:16:35	19°02.408' S	169°50.340' E	2,153m	0cm	No Sample, ※
94SDLC15	10/10	05:17:15	19°02.404' S	169°50.377' E	2,141m	69cm	
94SDLC16	10/10	21:28:55	19°26.671' S	169°51.948' E	938m	0cm	No Sample, ※
94SDLC17	10/10	22:45:05	19°26.557' S	169°51.979' E	980m	0cm	No Sample
94SDLC18	10/11	00:03:25	19°26.636' S	169°51.906' E	938m	65cm	※
94SDLC19	10/14	00:17:30	17°34.262' S	169°05.395' E	1,189m	0cm	Recovery Rock 720g, ※
94SDLC20	10/14	01:43:30	17°35.172' S	169°05.415' E	1,291m	0cm	No Sample, ※
94SDLC21	10/14	03:11:45	17°35.298' S	169°05.371' E	1,304m	0cm	No Sample, ※

Note: Data and Time represent the GMT, Time is Sampler on bottom.
Legend ※: Bit Damage

Appendix Table 4 Sampling Results of Ore Deposit Investigation (2)

Sample No.		Date	Time	Latitude	Longitude	Depth	Recovery (kg)
94SDCB01	On Bottom Off Bottom	10/11	01:36:55 02:14:55	19°26.426' S 19°26.818' S	169°52.010' E 169°51.818' E	946m 892m	59
94SDCB02	On Bottom Off Bottom	10/11	03:39:55 04:29:25	19°26.375' S 19°26.639' S	169°51.975' E 169°52.281' E	903m 983m	100
94SDPG01	On Bottom Off Bottom	10/11	22:22:25 22:27:35	18°59.786' S 18°59.788' S	169°54.144' E 169°54.137' E	2,427m 2,435m	1,300
94SDPG02	On Bottom Off Bottom	10/12	01:40:40 01:43:15	19°02.414' S 19°02.437' S	169°50.362' E 169°50.366' E	2,147m 2,167m	150
94SDPG03	On Bottom Off Bottom	10/12	04:07:10 04:09:45	19°05.191' S 19°05.210' S	169°52.358' E 169°52.371' E	2,067m 2,066m	315
94SDPG04	On Bottom Off Bottom	10/12	22:02:15 22:16:10	17°34.402' S 17°34.471' S	169°05.398' E 169°05.397' E	1,237m 1,250m	-
94SDPG05	On Bottom Off Bottom	10/13	00:26:10 00:28:40	17°34.280' S 17°34.253' S	169°05.441' E 169°05.435' E	1,184m 1,181m	10.5
94SDPG06	On Bottom Off Bottom	10/13	02:08:30 02:11:10	17°34.266' S 17°34.258' S	169°05.428' E 169°05.427' E	1,180m 1,181m	-
94SDPG07	On Bottom Off Bottom	10/13	04:58:10 05:00:55	17°34.366' S 17°34.348' S	169°05.391' E 169°05.365' E	1,190m 1,194m	400
94SDPG08	On Bottom Off Bottom	10/13	22:12:40 22:22:25	17°34.388' S 17°34.457' S	169°05.399' E 169°05.344' E	1,219m 1,214m	-
94SFDC081	On Bottom	09/29	06:32:15	18°02.698' S	169°24.977' E	2,646m	15

Note:Data and Time the represent GMT
Latitude and Longitude are GPS Vessel position and Depth by NBS
Location of towing vehicle were calculated from the winch length and depth by CTD.(94SFDC081)

Appendix Table 5 List of Samples (Baseline Geochemical Survey) (1)

Sample No.	S.Lat. (°)	(′)	E.Lon. (°)	(′)	Dp. (m)	Sampling Depth TOP	BTM	MED	Sediment Munsell No. & Color	Size	Under microscopic observation Cm	Dm	Am	Gl	Fo	Ra	Di	Sp	Description	Analysis Xr	Ca	Fo	Sp	Ts	Description
94SBGC02-0~10	19	1.856	169	57.62	2,685	0	10	5	10YR3/3 dark brown	clay	◎	·		△	·	·	△			○	○	×	×	×	
94SBGC02-10~20						10	20	15	10YR3/3 dark brown	clay	◎			○	△		△	·		×	×	○	×	×	
94SBGC02-21~23						21	23	22	10YR2/1 black	sand	○	·		○				△		○	×	×	×	×	
94SBGC02-25~35						25	35	30	10YR3/3 dark brown	clay	◎			△		△	△			○	○	×	×	×	
94SBGC02-35~45						35	45	40	10YR3/3 dark brown	clay	◎		△	○						×	×	○	×	×	
94SBGC02-60~70						60	70	65	10YR5/2 grayish brown	clay	◎			△	·					○	○	×	×	×	
94SBGC02-70~79						70	79	75	10YR5/2 grayish brown	clay	○			○	·			·		×	×	○	×	×	
94SBGC02-80~87						80	87	84	5Y3/2 dark olive gray	clay	△			◎	·		·	·		○	○	×	×	×	
94SBGC02-88~91						88	91	90	5Y2.5/1 black	clay	-	-	-	-	-	-	-	-		○	×	×	×	×	
94SBGC02-91~100						91	100	96	5Y4/2 olive gray	clay	○		·	◎	·	·		·		○	○	○	×	×	
94SBGC02-100~107						100	107	104	5Y2.5/1 black	clay		·		◎						○	○	×	×	×	
94SBGC05-0~10	19	3.485	169	55.83	3,119	0	10	5	5Y3/2 dark olive gray	clay	○			◎		·	·			○	○	×	×	×	
94SBGC05-10~20						10	20	15	5Y3/2 dark olive gray	clay	-	-	-	-	-	-	-	-		×	×	○	×	×	
94SBGC05-20~30						20	30	25	5Y3/2 dark olive gray	clay	-	-	-	-	-	-	-	-		×	×	×	○	×	
94SBGC05-40~50						40	50	45	5Y3/2 dark olive gray	clay	-	-	-	-	-	-	-	-		○	○	×	×	×	
94SBGC05-70~80						70	80	75	5Y3/2 dark olive gray	clay	◎			○	·	·	·			×	×	○	×	×	
94SBGC05-80~81						80	81	81	5Y2.5/1 black	sand	-	-	-	-	-	-	-	-		○	×	×	×	×	
94SBGC05-90~100						90	100	95	5Y3/2 dark olive gray	clay	·	-	-	-	·	-	-	-		○	○	×	×	×	
94SBGC05-100~110						100	110	105	5Y3/2 dark olive gray	clay	·	-	-	-	-	-	-	-		×	×	○	×	×	
94SBGC05-110~120						110	120	115	5Y3/2 dark olive gray	clay	-	-	-	·	-	-	-	-		×	×	×	○	×	
94SBGC05-146~148						146	148	147	5Y2.5/1 black	sand	-	-	-	-	-	-	-	-		○	×	×	×	×	
94SBGC05-148~153						148	153	151	2.5Y3/2 very dark grayish brown	clay	○			◎	·	·	·			○	○	×	×	×	
94SBGC06-0~20	19	1.184	169	58.29	2,727	0	20	10	10YR3/3 dark brown	clay	◎			·	·	·	·			○	○	○	○	×	
94SBGC06-22~23						22	23	23	5Y2.5/2 black	sand	·	-	-	-	-	-	-	-		○	×	×	×	×	
94SBGC06-27~28						27	28	28	5Y2.5/2 black	sand	·	-	-	-	·	-	-	-		○	×	×	×	×	
94SBGC06-30~36						30	36	33	5Y2.5/2 black	clay	-	-	-	-	-	-	-	-		×	○	×	×	×	
94SBGC06-36~44						36	44	40	2.5Y4/4 olive brown	clay	◎	△		○	△	·				○	○	×	×	×	
94SBGC06-49~50						49	50	50	5Y2.5/1 black	sand	-	-	-	-	-	-	-	-		○	×	×	×	×	
94SBGC06-53~53.5						53	54	53	5Y4/2 olive gray	clay	-	-	-	-	-	-	-	-		○	×	×	×	×	
94SBGC06-54~60						54	60	57	5Y4/2 olive gray	clay	◎			○	·	·				○	○	×	×	×	
94SBGC06-64~72						64	72	68	5Y4/1 dark gray	clay	△			◎	·					○	○	×	×	×	
94SBGC06-72~75						72	75	74	5Y4/1 dark gray	clay	-	-	-	-	-	-	-	-		×	×	○	×	×	
94SBGC06-75~93						75	93	84	5Y4/1 dark gray	clay	-	-	-	-	-	-	-	-		×	×	×	○	×	
94SBLC08-0~4	19	4.073	169	55.32	3,055	0	4	2	5Y3/2 dark olive gray	clay	◎			○	·					○	○	×	×	×	
94SBLC08-4~14						4	14	9	5Y3/2 dark olive gray	clay	-	-	-	-	-	-	-	-		×	×	○	○	×	
94SBLC08-14~20						14	20	17	2.5Y3/2 very dark grayish brown	clay	·	-	-	-	-	-	-	-		×	×	×	○	×	
94SBLC08-20~30						20	30	25	2.5Y2/0 black	sand				◎	·		·			○	○	○	×	×	
94SBLC09-0~13	19	4.776	169	54.580	2,594	0	13	7	2.5Y4/4 olive brown	clay	◎	△	·	·	△					○	○	○	○	×	
94SBLC09-14~15						14	15	15	5Y2.5/1 black	sand	-	-	·	-	-	-	-	-		○	×	×	×	×	
94SBLC09-18~28						18	28	23	2.5Y4/4 olive brown	clay	◎			△	○	·				○	○	○	○	×	
94SBLC09-38~40						38	40	39	5Y2.5/1 black	clay	○		·	○						○	×	×	×	×	
94SBLC09-45~67						45	67	56	2.5Y4/2 dark grayish brown	clay	◎	○		○			△			○	○	○	○	×	

Appendix Table 5 List of Samples (Baseline Geochemical Survey) (2)

Sample No.	S.Lat. (°)	(′)	E.Lon. (°)	(′)	Dp. (m)	Sampling Depth TOP	BTM	MED	Sediment Munsell No. & Color	Size	Under microscopic observation Cm	Dm	Am	Gl	Fo	Ra	Di	Sp	Description	Analysis Xr	Ca	Fo	Sp	Ts	Description
94SBLC09-67~68						67	68	68	5Y3/2 dark olive gray	sand	-	-	-	-	-	-	-	-		○	×	×	×	×	
94SBLC12-0~10	19	6.805	169	52.280	2,540	0	10	5	2.5Y3/2 very dark grayish brown	clay	◎				△	·	○	·		○	○	○	○	×	
94SBLC12-25~35						25	35	30	2.5Y3/2 very dark grayish brown	clay	◎		○		△	·				○	○	○	○	×	
94SBLC12-62~72						62	72	67	5Y2.5/2 black	clay				◎			·			○	○	○	○	×	
94SBLC12-72~74						72	74	73	5Y2.5/2 black	clay	-	-	-	-	-	-	-	-		×	×	×	×	○	
94SBLC12-74~75						74	75	75	2.5Y3/2 very dark grayish brown	clay	-	-	-	-	-	-	-	-		○	×	×	×	×	
94SBLC12-75~82						75	82	79	2.5Y3/2 very dark grayish brown	clay	◎				△		△			○	○	○	×	×	
94SBLC13-0-10	19	7.592	169	51.51	2,510	0	10	5	10YR3/3 dark brown	clay	◎				△	△		·		○	○	○	○	×	
94SBLC13-23-25						23	25	24	5Y2.5/1 black	sand	-	-	-	-	-	-	-	-		○	×	×	×	×	
94SBLC13-25~31						25	31	28	5Y2.5/2 black	clay	-	-	-	-	-	-	-	-		○	○	×	×	×	
94SBLC13-31~40						31	40	36	5Y2.5/2 black	clay	-	-	-	-	-	-	-	-		○	○	○	×	×	
94SBLC13-43~50						43	50	47	2.5Y4/2 dark grayish brown	clay	◎		·	△				·		○	○	○	×	×	
94SBLC13-65~75						65	75	70	5Y3/2 dark olive gray	clay	◎	○	·	△	△		·			○	○	○	○	×	
94SBLC13-100~110						100	110	105	5Y3/2 dark olive gray	clay	◎	△	△	○	·		·	·		○	○	○	○	×	
94SBGC15-0-10	19	8.245	169	50.71	2,633	0	10	5	10YR3/3 dark brown	clay	○	·	·	○	△	△				○	○	×	×	×	
94SBGC15-10~20						10	20	15	10YR3/3 dark brown	clay	○	△	△	○			·			×	×	○	○	×	
94SBGC15-28~29						28	29	29	2.5Y3/2 very dark grayish brown	sand	-	-	-	-	-	-	-	-		○	×	×	×	×	
94SBGC15-30~31						30	31	31	2.5Y3/2 very dark grayish brown	clay	-	-	-	-	-	-	-	-		○	×	×	×	×	
94SBGC15-33~35						33	35	34	2.5Y2/0 black	sand	-	-	-	-	-	-	-	-		○	×	×	×	×	
94SBGC15-38~39						38	39	39	2.5Y2/0 black	sand	-	-	-	-	-	-	-	-		○	×	×	×	×	
94SBGC15-39~44						39	44	42	5Y2.5/1 black	sand	-	-	-	-	-	-	-	-		○	×	×	×	×	
94SBGC15-38~44						38	44	41	5Y2.5/1 black	sand	-	-	-	-	-	-	-	-		×	○	○	×	×	
94SBGC15-44~48						44	48	46	2.5Y4/2 dark grayish brown	clay	○	△	·	△	○					×	×	○	×	×	
94SBGC15-50~57						50	57	54	5Y3/2 dark olive gray	clay	-	-	-	-	-	-	-	-		○	○	×	×	×	
94SBGC15-57~70						57	70	64	5Y3/2 dark olive gray	clay	-	·		◎	·					×	×	○	○	×	
94SBGC16-0~10	19	8.889	169	50.03	2,715	0	10	5	10YR3/3 dark brown	clay	◎	·	·		○		·	△		○	○	×	×	×	
94SBGC16-10~19						10	19	15	2.5Y3/2 very dark grayish brown	clay	-	-	-	-	-	-	-	-		×	×	○	○	×	
94SBGC16-32~33						32	33	33	5Y2.5/1 black	sand	-	-	-	-	-	-	-	-		○	×	×	×	×	
94SBGC16-36~49						36	49	43	5Y2.5/1 black	sand	-	-	-	-	-	-	-	-		○	○	○	×	×	
94SBGC16-49~55						49	55	52	5Y3/2 dark olive gray	clay	○	·		◎	·					×	×	○	×	×	
94SBGC16-55~61						55	61	58	5Y2.5/1 black	clay	-	-	-	-	-	-	-	-		○	○	×	×	×	
94SBGC17-0~11	19	9.671	169	49.29	2,673	0	11	6	10YR3/3 dark brown	clay	◎	·	·	△		△		·		○	○	×	×	×	
94SBGC17-11~19						11	19	15	2.5Y3/2 very dark grayish brown	clay	△	·	·	◎	·	·		·		×	×	○	○	×	
94SBGC17-19~24						19	24	22	5Y3/2 dark olive gray	clay	△	·	·	◎						○	○	×	×	×	
94SBGC17-24~27						24	27	26	2.5Y3/2 very dark grayish brown	clay	-	-	-	-	-	-	-	-		○	×	×	×	×	

TOP(cm):Upper plane from sea floor
BTM(cm):Lower plane from sea floor
MED(cm):Medium plane of TOP and BTM

Cm:Clay minerals
Dm:Detrital minerals
Am:Autigenic minerals
Fo:Foraminifera test
Ra:Radiolaria test
Di:Diatom test
Sp:Sponge spicule

◎ :much
○ :medium
△ :little
· :rare

Xr:X-ray diffraction for whole sedime
Ca:Chemical analysis
Fo:Fossil analysis
Sp:Mechanical analysis
○:operated, ×:un-operated

Appendix Table 5 List of Samples (Ore Drposit Investigation) (3)

Sample No.	S.Lat. (°)	(')	E.Lon. (°)	(')	Dp. (m)	Sampling Depth TOP	BTM	MED	Sediment Munsell No. & Color	Size	Under microscopic observation Cm	Dm	Am	Gl	Fo	Ra	Di	Sp	Description	Analysis Xr	Ca	Fe	Sp	Ts	Pts	Description
94SDLC01-A	17	35.154	169	2.378	1,287	0	40	20	2.5YR4/6	clay,rock	△	◎								○	○	×	×	×	○	
94SDLC01-B						40	50	45	black	sand	-	-	-	-	-	-	-	-		○	○	×	×	○	×	
94SDLC01-C						0	50	25	5Y3/2	clay	-	-	-	-	-	-	-	-		○	○	×	×	×	×	
94SDLC03-A	17	34.197	169	5.427	1,160	0	10	5	2.5YR4/8	clay	-	-	-	-	-	-	-	-		○	○	×	×	×	×	
94SDLC03-B						10	56	33	5Y3/1	clay	△	◎		-	-	-	-	-		○	○	×	×	×	×	
94SDLC03-C						56	70	63	5Y2.5/1	clay	-	-	-	-	-	-	-	-		○	○	×	×	×	×	
94SDLC03-D						73	86	80	black	rock	-	-	-	-	-	-	-	-		○	○	×	×	×	×	
94SDLC04-A	17	34.239	169	5.457	1,180	0	15	8	2.5YR5/8	clay	△	◎		-	-	-	-	-		○	○	×	×	×	×	
94SDLC04-B						15	30	23	5Y3/2	clay	-	-	-	-	-	-	-	-		○	○	×	×	×	×	
94SDLC04-C						25	30	28	black	rock	-	-	-	-	-	-	-	-		○	○	×	×	○	×	
94SDLC05	17	34.338	169	5.481	1,192	-	-	-	black	rock	-	-	-	-	-	-	-	-		○	×	×	×	○	×	
94SDLC06-A	17	34.429	169	5.506	1,193	0	5	3	2.5YR4/4	clay+sand			△	◎	•					○	○	×	×	×	×	
94SDLC06-B						5	20	13	black	rock	-	-	-	-	-	-	-	-		○	○	×	×	○	×	
94SDLC07	17	34.453	169	5.398	1,200	-	-	-	black	rock	-	-	-	-	-	-	-	-		○	×	×	×	×	×	
94SDLC08-A	18	59.898	169	54.068	2,417	0	5	3	2.5Y3/2	clay	◎	•	○	•	△					○	×	×	×	×	×	
94SDLC08-B						5	15	10	10YR3/2	clay	◎		△	△	•		•			○	×	×	×	×	×	
94SDLC08(A+B)						0	15	8	2.5Y3/2+10YR3/2	clay	-	-	-	-	-	-	-	-		×	○	×	×	×	×	
94SDLC09-0~10	18	59.775	169	54.147	2,419	0	10	5	10YR3/3	clay	◎	•	•	△	△	△	•	△		○	○	×	×	×	×	
94SDLC09-10~20						10	20	15	10YR3/3	clay	◎	•	○	△	○					○	○	○	×	×	×	
94SDLC09-22~27						22	27	25	black	rock	-	-	-	-	-	-	-	-		×	×	×	×	×	○	
94SDLC09-34~38						34	38	36	2.5Y4/2	clay	-	•	-	-	-	-	-	-		○	○	×	×	×	×	
94SDLC09-41~47						41	47	44	5Y3/2	clay	◎	○	△	△	△					○	○	×	×	×	×	
94SDLC09-49~57						49	57	53	5Y4/2	clay	◎	○	△	△	•					○	○	○	×	×	×	
94SDLC09-64~74						64	74	69	5Y4/2	clay	○	◎		○						○	○	×	×	×	×	
94SDLC09-91~101						91	101	96	2.5YR5/2	clay	◎		○		○		•			○	○	○	×	×	×	
94SDLC09-113~123						113	123	118	5Y5/2	clay	◎	△	○	△	○					○	○	×	×	×	×	
94SDLC09-123~133						123	133	128	5Y4/2	clay	◎	△	△	△	○					○	○	×	×	×	×	
94SDLC09-136~146						136	146	141	5Y4/3	clay	◎	•	•	○	△					○	○	○	×	×	×	
94SDLC10-A	19	4.928	169	51.382	2,303	0	18	9	black	rock	-	-	-	-	-	-	-	-		○	○	×	×	×	○	
94SDLC10-B						18	35	27	10YR3/2+black	rock+clay	◎	△	◎	△						○	○	×	×	×	×	
94SDLC11	19	5.128	169	52.359	2,056	0	35	18	black	rock	△	◎	○	-	-	-	-	-		○	○	×	×	×	×	
94SDLC12-0~0.5	18	59.816	169	54.191	2,417	0	0.5	0	black	sand+clay	•	◎	•	-	-	-	-	-		○	×	×	×	×	×	
94SDLC12-10~20						10	20	15	2.5Y4/2	clay	○	◎	△	-	-	-	-	-		○	○	○	×	×	×	
94SDLC12-20~30						20	30	25	2.5Y4/2	clay	-	-	-	-	-	-	-	-		×	×	×	○	×	×	
94SDLC12-35~45						35	45	40	2.5Y4/2	clay	-	-	-	-	-	-	-	-		○	○	○	×	×	×	
94SDLC12-60~70						60	70	65	5Y4/2	clay	-	-	-	-	-	-	-	-		○	○	○	×	×	×	
94SDLC13-0~0.5	18	59.863	169	54.203	2,432	0	0.5	0	black	clay	-	-	-	-	-	-	-	-		○	×	×	×	×	×	
94SDLC13-10~20						10	20	15	2.5Y4/2	clay	•	◎	△	-	-	-	-	-		○	○	×	×	×	×	
94SDLC13-25~30						25	30	28	2.5Y3/2	clay	○	○		△	○		△			○	○	○	×	×	×	
94SDLC13-35~40						35	40	38	5Y4/2	clay	○	◎	△	-	-	-	-	-		○	○	×	×	×	×	
94SDLC13-45~48						45	48	47	dark graen	clay	-	-	-	-	-	-	-	-		○	○	×	×	×	×	
94SDLC13-60~70						60	70	65	5Y4/1	clay	○	◎	•	-	-	-	-	-		○	○	○	×	×	×	
94SDLC13-70~80						70	80	75	5Y4/1	clay	-	-	-	-	-	-	-	-		×	×	×	○	×	×	
94SDLC15-0~8	19	2.404	169	50.377	2,141	0	8	4	10YR3/3	clay	◎	○	○		△					○	○	×	×	×	×	
94SDLC15-8~10						8	10	9	5Y2.5/1	sand	-	-	-	-	-	-	-	-		○	×	×	×	×	×	
94SDLC15-10~17						10	17	14		clay	-	-	-	-	-	-	-	-		○	○	○	×	×	×	
94SDLC15-22~30						22	30	26		clay	◎	○	○		△					○	○	○	×	×	×	
94SDLC15-39~41						39	41	40		sand	-	-	-	-	-	-	-	-		○	×	×	×	○	×	
94SDLC15-41~50						41	50	46		clay	-	-	-	-	-	-	-	-		○	○	×	×	×	×	
94SDLC15-52~62						52	62	57		clay	-	-	-	-	-	-	-	-		×	×	○	×	×	×	

Appendix Table 5 List of Samples (Ore Drposit Investigation) (4)

Sample No.	S.Lat. (°)	(′)	E.Lon. (°)	(′)	Dp. (m)	Sampling Depth TOP	BTM	MED	Sediment Munsell No. & Color	Size	Under microscopic observation Cm	Dm	Am	Gl	Fo	Ra	Di	Sp	Description	Analysis Xr	Ca	Fo	Sp	Ts	Pts	Description
94SDLC15-62~69						62	69	66		clay	◎	△	・	○	△					○	○	○	×	×	×	
94SDLC18-0~10	19	26.636	169	51.906	938	0	10	5		clay		◎	・	-	-	-	-	-		○	○	×	×	×	×	
94SDLC18-45~50						45	50	48		clay	-	-	-	-	-	-	-	-		○	○	×	×	×	×	block
94SDLC18-50~60						50	60	55		clay		◎		-	-	-	-	-		○	○	×	×	×	×	grean
94SDLC18-50~60						50	60	55		clay		◎		-	-	-	-	-		○	○	×	×	×	×	mix
94SDCB01-MIX						-	-	-		clay		◎		-	-	-	-	-		○	○	×	×	×	×	
94SDCB01-Mn oxide						-	-	-		Mn-oxide	-	-	-	-	-	-	-	-		○	○	×	×	×	×	
94SDCB01-上面						-	-	-		Fe-oxide	-	-	-	-	-	-	-	-		○	○	×	×	×	×	
94SDCB01-下面						-	-	-		Fe-oxide	-	-	-	-	-	-	-	-		○	○	×	×	×	×	
94SDCB01-ROCK						-	-	-		rock	-	-	-	-	-	-	-	-		○	○	×	×	○	×	
94SDCB01-ROCK2						-	-	-		rock	-	-	-	-	-	-	-	-		○	×	×	×	×	×	
94SDCB02-MIX						-	-	-		Fe-oxide	-	-	-	-	-	-	-	-		○	○	×	×	×	×	
94SDCB02-Mn						-	-	-		Mn-oxide	-	-	-	-	-	-	-	-		○	○	×	×	×	○	
94SDCB02-ROCK						-	-	-		rock	-	-	-	-	-	-	-	-		○	○	×	×	○	×	
94SDPG01-A	18	59.786	169	54.144	2,427	-	-	-		clay	-	-	-	-	-	-	-	-		○	○	×	×	×	×	
94SDPG01-B						-	-	-		clay	-	-	-	-	-	-	-	-		○	○	×	×	×	×	
94SDPG01-C						-	-	-		Mn-oxide	-	-	-	-	-	-	-	-		○	○	×	×	×	×	
94SDPG01-D						-	-	-		clay	-	-	-	-	-	-	-	-		○	○	×	×	×	×	
94SDPG01-E						-	-	-		clay	-	-	・	-	-	-	-	-		○	○	×	×	×	×	
94SDPG01-F						-	-	-		clay	-	-	-	-	-	-	-	-		○	○	×	×	×	×	
94SDPG01-G						-	-	-		clay	-	-	-	-	-	-	-	-		○	○	×	×	×	×	
94SDPG01-H						-	-	-		Mn-oxide	-	-	-	-	-	-	-	-		×	×	×	×	×	○	
94SDPG02-A	19	2.414	169	50.362	2,147	-	-	-		clay	-	-	-	-	-	-	-	-		○	○	×	×	×	×	
94SDPG02-B						-	-	-		clay	-	-	-	-	-	-	-	-		○	○	×	×	×	×	
94SDPG02-C						-	-	-		clay	-	-	-	-	-	-	-	-		○	○	×	×	×	×	
94SDPG02-D						-	-	-		clay	-	・	-	-	-	-	-	-		○	○	×	×	×	×	
94SDPG02-E						-	-	-		clay	-	-	-	-	-	-	-	-		○	○	×	×	×	×	
94SDPG02-F						-	-	-		Mn-oxide	-	-	-	-	-	-	-	-		○	○	×	×	×	○	
94SDPG02-G						-	-	-		Mn-oxide	-	-	-	-	-	-	-	-		○	○	×	×	×	×	
94SDPG02-H						-	-	-		rock	-	-	-	-	-	-	-	-		○	○	×	×	○	×	
94SDPG03-A	19	5.191	169	52.358	2,067	-	-	-		Fe-oxide	-	-	-	-	-	-	-	-		○	○	×	×	×	×	
94SDPG03-B						-	-	-		Fe-oxide	-	-	-	-	-	-	-	-		○	○	×	×	×	×	
94SDPG03-C						-	-	-		Mn-oxide	-	-	-	-	-	-	-	-		○	○	×	×	×	○	
94SDPG03-D						-	-	-		Mn-oxide	-	-	-	-	-	-	-	-		○	○	×	×	×	○	
94SDPG03-E						-	-	-		rock	-	-	-	-	-	-	-	-		×	×	×	×	○	×	
94SDPG05-A	17	34.280	169	5.441	1,184	-	-	-		clay	-	-	-	-	-	-	-	-		○	○	×	×	×	×	
94SDPG05-B						-	-	-		rock	-	-	-	-	-	-	-	-		○	○	×	×	○	×	
94SDPG05-C						-	-	-		rock	-	-	-	-	-	-	-	-		○	○	×	×	○	×	
94SDPG07-A	17	34.366	169	5.391	1,190	-	-	-		rock	-	-	-	-	-	-	-	-		○	○	×	×	×	×	
94SDPG07-B						-	-	-		rock	-	-	-	-	-	-	-	-		○	○	×	×	○	×	
94SDLC19	17	34.252	169	5.395	1,189	-	-	-		rock	-	-	-	-	-	-	-	-		○	○	×	×	×	×	
94SDFDC081	18	2.698	169	24.977	2,646	-	-	-	BLACK	ROCK	-	-	-	-	-	-	-	-		○	○	×	×	○	×	

TOP(cm):Upper plane from sea floor
BTM(cm):Lower plane from sea floor
MED(cm):Medium plane of TOP and BTM

Cm:Clay minerals
Dm:Detrital minerals
Am:Autigenic minerals
Fo:Foraminifera test
Ra:Radiolaria test
Di:Diatom test
Sp:Sponge spicule

◎ :much
○ :medium
△ :little
・ :rare

Xr:X-ray diffraction for whole sediment
Ca:Chemical analysis
Fo:Fossil analysis
Sp:Mechanical analysis
○:operated, ×:un-operated

Appendix Table 6 Results of Chemical Analysis for Sampling Sediments (1)

Sample No.		94SBGC02	94SBGC02	94SBGC02	94SBGC02	94SBGC02	94SBGC02	94SBGC05	94SBGC05	94SBGC05	94SBGC05	94SBGC06	94SBGC06	94SBGC06	94SBGC06	94SBGC06	94SBLC08	94SBLC08	94SBLC09	94SBLC09	94SBLC09
		0-10	25-35	60-70	80-87	91-100	100-107	0-10	40-50	90-100	148-153	0-20	30-36	36-44	54-60	64-72	0-4	20-30	0-13	18-28	45-67
SiO2	%	39.56	39.61	41.06	50.33	44.96	53.70	52.94	52.59	52.53	51.32	38.58	53.40	36.68	43.82	53.47	46.43	54.38	39.31	31.51	35.10
TiO2	%	0.58	0.62	0.61	0.72	0.64	0.74	0.70	0.71	0.71	0.70	0.61	0.80	0.60	0.63	0.74	0.68	0.82	0.60	0.48	0.50
Al2O3	%	11.87	12.76	12.67	14.33	13.37	15.94	14.70	14.70	14.71	14.48	11.75	15.81	12.16	12.89	15.30	13.48	15.25	12.33	9.74	11.79
Fe2O3	%	7.60	7.78	8.18	10.21	7.74	8.79	9.47	9.44	9.26	9.11	7.43	8.28	7.62	7.44	8.65	8.75	8.63	7.76	6.22	7.37
FeO	%	2.36	2.65	2.66	4.97	3.73	4.93	5.56	5.32	5.15	4.97	2.02	4.01	2.79	3.53	4.81	3.95	4.65	2.58	2.03	1.63
MnO	%	0.46	0.52	0.45	0.20	0.22	0.17	0.22	0.20	0.22	0.22	0.52	0.53	0.20	0.18	0.17	0.32	0.18	0.37	0.26	0.26
MgO	%	2.41	2.62	2.71	3.26	2.82	3.31	3.07	3.07	3.07	3.12	2.41	2.74	2.67	2.74	3.13	2.90	2.63	2.57	2.25	3.41
CaO	%	15.51	16.34	15.34	7.80	13.56	7.79	7.63	8.01	8.29	8.99	17.02	7.82	18.34	13.60	7.00	11.92	6.96	17.40	24.42	20.42
BaO	%	0.07	0.05	0.06	0.05	0.06	0.06	0.04	0.04	0.05	0.04	0.07	0.06	0.06	0.06	0.06	0.05	0.07	0.06	0.05	0.05
Na2O	%	3.46	3.19	3.27	4.14	3.61	4.41	4.15	4.12	4.05	4.02	2.93	4.35	2.64	3.46	4.52	3.54	4.43	2.85	2.08	2.19
K2O	%	1.33	1.02	1.19	2.22	1.59	2.34	1.77	1.80	1.79	1.51	1.22	2.63	0.73	1.81	2.62	1.48	3.02	1.09	0.66	0.59
P2O5	%	0.32	0.26	0.27	0.42	0.29	0.37	0.25	0.26	0.27	0.26	0.35	0.44	0.23	0.29	0.36	0.29	0.50	0.29	0.19	0.21
CO2	%	9.64	9.39	8.73	1.61	7.08	0.88	1.32	1.61	2.02	2.60	11.00	1.76	11.33	7.55	1.17	5.61	1.21	10.27	16.54	12.17
LOI	%	16.54	15.32	14.16	5.14	11.74	2.44	3.95	4.42	5.02	5.90	17.90	4.14	17.68	12.63	3.62	9.85	3.26	15.50	21.64	18.08
Total	%	99.71	100.09	99.97	98.82	100.60	100.06	98.89	99.36	99.97	99.67	100.79	101.00	99.61	99.55	99.64	99.69	100.13	100.13	99.50	99.97
Ag	ppm	0.02	0.02	<0.02	0.08	0.04	0.02	0.02	<0.02	<0.02	0.02	<0.02	0.02	0.08	0.02	0.04	0.02	0.02	<0.02	<0.02	<0.02
As	ppm	11.2	10.4	10.0	15.6	3.4	0.4	2.2	2.6	3.6	4.2	12.2	2.4	10.8	3.4	1.8	6.6	1.8	9.4	6.6	6.2
Cu	ppm	93.4	96.2	89.6	71.6	84.8	61.0	54.2	58.4	60.2	63.8	110.0	97.2	105.5	142.0	116.5	71.0	76.8	91.4	67.2	85.0
Hg	ppm	70	40	90	20	4550	30	30	50	30	20	80	20	70	50	30	50	20	30	20	20
Pb	ppm	12.5	15.0	12.0	6.0	14.0	8.5	4.0	4.0	6.0	6.0	13.5	6.0	20.5	8.5	5.0	8.5	8.5	14.0	11.5	14.0
Sb	ppm	<0.2	0.2	<0.2	<0.2	0.6	<0.2	<0.2	<0.2	<0.2	<0.2	0.4	0.2	<0.2	0.2	<0.2	0.2	0.4	0.2	0.4	0.4
Zn	ppm	49	57	47	45	49	32	27	34	34	35	56	38	67	46	34	39	23	46	38	52
Ba	ppm	600	490	520	480	580	520	400	390	420	370	610	540	500	540	530	480	600	540	480	420
Cd	ppm	0.5	<0.5	<0.5	0.5	0.5	0.5	<0.5	0.5	0.5	0.5	<0.5	<0.5	<0.5	0.5	0.5	0.5	0.5	<0.5	<0.5	0.5
Co	ppm	22	24	24	26	21	23	24	23	22	23	23	22	20	20	20	23	17	22	21	23
Cr	ppm	44	40	37	22	27	44	28	30	24	38	34	34	32	18	6	28	21	24	25	70
Mn	ppm	3140	3660	3260	1510	1560	1215	1700	1500	1620	1600	3630	3670	1415	1260	1185	2220	1210	2540	1805	1815
Ni	ppm	20	24	18	11	12	11	9	9	11	13	27	12	23	12	9	13	7	17	17	30
P	ppm	1370	1220	1270	1960	1340	1640	1160	1130	1190	1130	1560	1850	1090	1280	1640	1240	2230	1270	930	990
Sr	ppm	655	660	816	574	657	570	456	458	464	490	734	507	696	639	538	541	496	692	764	842
Tl	ppm	0.2	0.1	<0.1	<0.1	<0.1	<0.1	0.1	0.1	0.1	0.1	0.1	0.3	0.2	0.1	0.7	0.1	0.1	0.1	0.1	0.1
V	ppm	172	187	204	267	207	234	212	211	209	197	176	187	196	204	225	197	200	191	159	166
Li	ppm	10	10	9	9	11	9	8	8	9	9	11	13	10	12	11	9	11	9	7	10
Cl	ppm	>10000	>10000	>10000	9100	>10000	7900	7100	8000	9000	8400	>10000	8000	>10000	>10000	7700	>10000	>10000	>10000	>10000	>10000
B	ppm	40	35	35	45	30	30	35	30	30	35	35	30	35	25	30	35	45	45	40	40
Rb	ppm	11	15	14	23	17	31	21	18	19	22	17	39	7	20	31	12	40	16	11	14
U	ppm	0.6	0.8	0.6	2.4	0.8	1.0	0.6	0.4	0.6	0.6	0.8	1.2	0.6	2.2	1.0	0.6	1.2	0.8	0.8	0.6
Total-S	%	0.105	0.091	0.079	0.041	0.065	0.046	0.056	0.059	0.059	0.064	0.102	0.054	0.087	0.072	0.049	0.074	0.052	0.063	0.066	0.067
SO4	%	0.13	0.10	0.10	0.04	0.07	0.04	0.04	0.04	0.04	0.04	0.13	0.04	0.10	0.08	0.06	0.06	0.04	0.08	0.07	0.07
CO2	%	9.64	9.39	8.73	1.61	7.08	0.88	1.32	1.61	2.02	2.60	11.00	1.76	11.33	7.55	1.17	5.61	1.21	10.27	16.54	12.17

Appendix Table 6 Results of Chemical Analysis for Sampling Sediments (2)

Sample No.		94SBLC12	94SBLC12	94SBLC12	94SBLC12	94SBLC13	94SBLC13	94SBLC13	94SBLC13	94SBLC13	94SBLC13	94SBGC15	94SBGC15	94SBGC15	94SBGC16	94SBGC16	94SBGC16	94SBGC17	94SBGC17
		0-10	25-35	62-72	75-82	0-10	25-31	31-40	43-50	65-75	100-110	0-10	38-44	50-57	0-10	36-49	55-61	0-11	19-24
SiO2	%	38.47	34.20	44.93	45.61	37.40	54.23	48.64	38.58	35.44	44.57	37.57	53.41	52.75	39.14	52.22	50.10	40.79	52.96
TiO2	%	0.60	0.57	0.67	0.65	0.59	0.83	0.72	0.64	0.57	0.67	0.58	0.80	0.77	0.61	0.80	0.69	0.63	0.79
Al2O3	%	11.76	11.78	13.66	13.57	11.57	15.42	14.30	12.98	11.87	13.57	11.72	15.26	15.41	12.43	15.59	15.30	12.69	15.13
Fe2O3	%	6.91	7.91	8.12	7.50	6.92	8.02	7.78	7.62	8.27	8.55	7.30	8.56	9.75	7.60	8.73	8.79	7.66	8.20
FeO	%	1.84	1.35	3.61	3.15	1.77	4.41	3.56	2.88	1.67	3.59	1.73	4.47	5.15	2.02	4.20	4.71	2.51	4.08
MnO	%	0.50	0.53	0.34	0.34	0.50	0.22	0.36	0.23	0.62	0.30	0.49	0.19	0.18	0.44	0.25	0.20	0.40	0.37
MgO	%	2.23	2.50	2.93	2.85	2.23	2.56	2.63	2.65	2.52	2.91	2.40	2.66	3.51	2.61	3.01	3.33	2.63	2.46
CaO	%	17.36	19.51	12.78	13.18	17.77	6.70	12.23	17.85	18.35	13.24	17.12	7.63	7.32	15.77	8.16	9.51	15.04	6.88
BaO	%	0.07	0.06	0.05	0.07	0.07	0.07	0.06	0.05	0.06	0.06	0.07	0.07	0.06	0.06	0.06	0.05	0.06	0.07
Na2O	%	3.03	2.36	3.69	3.54	2.83	4.37	3.80	2.65	2.59	3.44	2.94	4.33	4.26	2.92	4.16	3.95	3.14	4.38
K2O	%	1.27	0.59	1.67	1.80	1.16	3.04	2.10	0.64	0.71	1.51	1.01	2.88	2.32	1.00	2.53	2.01	1.24	3.03
P2O5	%	0.34	0.26	0.28	0.31	0.32	0.48	0.39	0.24	0.29	0.28	0.34	0.47	0.31	0.33	0.42	0.29	0.34	0.46
CO2	%	11.40	12.61	5.94	6.42	11.88	1.25	5.24	10.45	11.66	6.49	11.29	1.87	0.81	9.79	1.72	2.79	8.91	1.98
LOI	%	17.72	19.96	10.24	10.24	18.51	3.48	7.80	16.43	18.86	10.82	18.90	3.86	3.47	17.40	3.76	5.38	15.93	5.28
Total	%	100.26	100.23	99.36	99.66	99.87	99.42	100.81	100.56	100.15	99.92	100.44	100.12	100.11	100.31	99.69	99.60	100.55	100.01
Ag	ppm	0.02	<0.02	<0.02	0.02	0.04	<0.02	<0.02	0.02	0.02	0.02	0.02	0.04	0.04	0.02	0.04	0.02	0.02	0.02
As	ppm	14.2	14.8	5.8	6.0	13.4	3.0	2.2	11.8	15.0	7.2	13.0	2.2	2.6	12.0	2.8	4.0	10.6	4.2
Cu	ppm	99.4	125.0	79.8	82.2	100.5	89.0	78.6	92.4	126.5	88.8	103.0	121.0	67.4	99.8	95.2	98.8	102.0	101.0
Hg	ppm	70	30	100	50	80	30	20	100	70	40	110	30	20	90	30	20	60	30
Pb	ppm	18.0	24.5	9.0	8.5	15.0	6.0	6.5	14.0	31.0	9.0	25.5	13.5	7.5	20.0	13.5	12.5	12.5	8.0
Sb	ppm	0.2	<0.2	0.2	0.6	1.4	<0.2	<0.2	<0.2	0.6	<0.2	2.8	<0.2	<0.2	1	2.4	0.2	0.2	<0.2
Zn	ppm	53	67	37	35	54	27	31	56	64	39	58	64	39	54	43	53	55	33
Ba	ppm	660	500	490	590	620	600	540	490	530	520	640	600	500	580	540	430	550	600
Cd	ppm	<0.5	0.5	0.5	0.5	<0.5	<0.5	<0.5	0.5	<0.5	<0.5	0.5	0.5	0.5	0.5	0.5	<0.5	<0.5	0.5
Co	ppm	22	24	23	22	22	21	21	20	25	24	22	20	25	24	22	22	22	20
Cr	ppm	23	29	16	25	25	18	21	43	26	16	25	33	7	27	23	34	29	18
Mn	ppm	3300	3500	2380	2350	3420	1645	2520	1585	4140	2060	3310	1390	1330	3020	1775	1365	2720	2560
Ni	ppm	22	27	11	14	27	6	10	18	27	12	22	9	6	22	9	11	20	7
P	ppm	1540	1150	1260	1350	1530	2160	1750	1080	1240	1260	1480	2110	1400	1450	1850	1270	1490	2030
Sr	ppm	696	818	684	639	725	497	542	655	885	707	712	528	522	676	550	561	663	497
Tl	ppm	0.3	0.5	0.1	<0.1	0.3	0.2	0.5	0.1	0.2	0.2	0.3	0.3	0.1	0.3	0.2	<0.1	0.1	0.1
V	ppm	169	179	219	198	173	193	178	193	189	214	175	195	258	186	220	221	182	166
Li	ppm	11	11	9	8	10	11	10	9	10	9	11	11	9	11	10	9	11	12
Cl	ppm	>10000	>10000	>10000	9900	>10000	7600	>10000	>10000	>10000	>10000	>10000	7900	8500	>10000	8300	9300	>10000	8600
B	ppm	35	40	25	35	50	50	30	35	40	40	40	40	30	45	45	40	40	45
Rb	ppm	20	11	19	23	17	40	31	9	13	21	16	40	28	11	35	24	19	39
U	ppm	0.6	0.6	0.6	1.0	1.0	1.4	1.0	0.6	0.6	0.6	1.0	1.2	1.0	0.8	1.2	1.0	1.0	1.6
Total-S	%	0.108	0.083	0.060	0.060	0.089	0.050	0.059	0.089	0.084	0.065	0.104	0.058	0.043	0.105	0.067	0.061	0.099	0.064
SO4	%	0.11	0.11	0.06	0.04	0.11	0.02	0.04	0.08	0.10	0.07	0.14	0.03	0.03	0.12	0.03	0.03	0.12	0.03
CO2	%	11.40	12.61	5.94	6.42	11.88	1.25	5.24	10.45	11.66	6.49	11.29	1.87	0.81	9.79	1.72	2.79	8.91	1.98

Appendix Table 6 Results of Chemical Analysis for Sampling Sediments (3)

Sample No.		94SDLC01 B	94SDLC06 A	94SDLC08 A+B	94SDLC09 0-10	94SDLC09 10-20	94SDLC09 41-47	94SDLC09 49-57	94SDLC09 64-74	94SDLC09 91-101	94SDLC09 113-123	94SDLC09 123-133	94SDLC09 136-146	94SDLC12 10-20	94SDLC12 35-45	94SDLC12 60-70	94SDLC13 10-20	94SDLC13 25-30	94SDLC13 35-40	94SDLC13 45-48	94SDLC13 60-70
SiO2	%	50.62	49.64	36.25	37.94	38.45	46.15	44.07	42.17	35.84	31.68	31.20	35.06	51.44	51.15	51.13	51.24	38.71	50.49	52.70	50.01
TiO2	%	1.34	1.20	0.55	0.59	0.61	0.42	0.61	0.56	0.49	0.43	0.42	0.48	0.75	0.74	0.66	0.74	0.58	0.68	0.76	0.73
Al2O3	%	15.12	15.26	11.41	11.89	12.64	8.57	12.84	11.28	10.32	9.07	8.64	9.76	14.45	14.15	12.66	14.19	11.69	14.11	14.50	13.93
Fe2O3	%	13.17	12.23	7.08	7.27	7.52	17.40	8.73	9.19	7.14	6.93	7.30	7.82	9.76	9.75	12.44	9.61	7.70	10.88	10.23	9.50
FeO	%	8.89	8.70	1.70	1.17	0.78	2.13	3.12	2.93	2.51	1.84	1.73	2.11	4.46	4.10	3.79	4.43	2.36	0.19	5.24	5.18
MnO	%	0.20	0.20	0.71	1.05	1.30	0.22	0.24	0.19	0.24	0.52	0.36	0.27	0.21	0.50	0.58	0.29	0.53	2.76	0.19	0.18
MgO	%	4.72	5.41	2.50	2.41	2.35	2.96	2.79	2.68	2.53	2.20	2.13	2.37	3.24	3.16	3.12	3.17	2.51	3.16	3.30	3.09
CaO	%	10.04	10.98	19.71	17.02	16.37	6.23	14.05	13.81	20.00	23.31	23.06	20.65	6.97	6.07	4.59	6.46	17.46	4.60	5.81	7.50
BaO	%	0.01	0.02	0.06	0.07	0.07	0.04	0.06	0.06	0.06	0.07	0.08	0.06	0.05	0.04	0.04	0.04	0.06	0.04	0.04	0.04
Na2O	%	3.64	3.50	2.72	2.98	2.81	3.24	3.11	3.16	2.24	2.20	1.87	2.10	3.89	4.09	3.78	4.20	3.14	3.80	4.18	4.18
K2O	%	0.63	0.66	0.87	1.23	1.20	1.87	1.20	1.42	0.66	0.61	0.43	0.59	1.70	2.05	2.01	1.84	1.26	2.20	1.60	1.65
P2O5	%	0.19	0.21	0.23	0.31	0.28	0.17	0.24	0.22	0.18	0.19	0.18	0.19	0.28	0.28	0.25	0.27	0.25	0.25	0.27	0.27
CO2	%	0.15	0.73	12.21	10.63	9.79	2.64	7.33	7.77	12.98	16.35	16.50	13.86	1.83	1.14	0.44	1.54	3.23	0.18	0.95	2.49
LOI	%	0.18	1.49	18.01	18.26	17.08	12.33	12.69	14.81	20.41	23.01	24.24	21.31	7.97	7.35	7.90	7.76	15.80	7.95	7.09	8.23
Total	%	99.86	100.80	100.10	101.02	100.68	99.60	100.63	99.55	100.11	100.22	99.91	100.66	100.71	99.33	99.16	99.81	99.69	100.92	100.67	99.31
Ag	ppm	0.02	0.02	<0.02	<0.02	<0.02	0.02	0.02	<0.02	0.02	<0.02	0.02	<0.02	<0.02	<0.02	0.04	<0.02	<0.02	<0.02	0.1	0.02
As	ppm	<0.2	1.4	8.8	19.0	24.6	21.0	12.4	11.4	6.0	31.8	37.2	24.0	3.4	7.0	13.2	3.6	14.0	21.4	2.2	10.4
Cu	ppm	68.6	111.0	89.0	107.5	112.0	65.8	83.4	79.0	107.0	87.2	58.4	65.0	98.8	88.0	50.2	96.4	88.4	79.2	106.5	98.4
Hg	ppm	20	10	20	80	40	40	30	40	30	90	40	40	10	10	60	10	20	30	70	50
Pb	ppm	2.5	7.5	16.0	12.5	13.0	7.0	9.5	8.5	11.5	12.0	12.5	12.0	6.5	5.0	5.0	6.0	13.5	5.0	8.5	8.0
Sb	ppm	<0.2	<0.2	0.4	0.4	0.2	0.2	<0.2	0.8	0.4	<0.2	<0.2	<0.2	<0.2	<0.2	<0.2	<0.2	0.2	0.6	1.6	<0.2
Zn	ppm	66	84	46	78	88	40	46	49	75	74	67	66	55	48	43	56	45	45	57	51
Ba	ppm	120	140	540	630	620	380	560	580	580	620	690	560	410	390	330	380	510	390	400	390
Cd	ppm	0.5	0.5	<0.5	0.5	0.5	<0.5	1.0	0.5	0.5	0.5	0.5	0.5	0.5	0.5	<0.5	0.5	<0.5	<0.5	0.5	1.0
Co	ppm	37	37	23	24	24	17	20	19	18	20	18	18	22	22	19	23	21	23	21	21
Cr	ppm	26	19	36	27	22	15	22	20	27	25	22	24	9	10	10	11	22	10	16	14
Mn	ppm	1400	1350	4650	6980	8510	1525	1655	1340	1630	3390	2400	1825	1455	3570	4010	2090	3540	>10000	1300	1320
Ni	ppm	12	18	20	38	44	11	10	14	18	25	24	19	6	3	4	10	19	5	6	6
P	ppm	890	890	1030	1420	1250	710	1030	960	840	870	830	840	1190	1230	1070	1200	1110	1080	1170	1180
Sr	ppm	216	255	701	706	658	352	676	575	706	800	784	703	401	383	305	385	652	313	347	423
Tl	ppm	<0.1	<0.1	0.1	0.8	1.2	0.1	0.1	0.1	0.2	0.1	0.1	0.2	0.1	0.2	0.1	0.2	0.4	0.2	0.1	0.1
V	ppm	325	287	168	175	175	144	211	194	213	148	131	153	173	182	164	176	176	167	198	185
Li	ppm	4	4	10	12	12	7	9	9	9	8	9	8	13	14	12	13	10	31	10	11
Cl	ppm	2300	5400	>10000	>10000	>10000	>10000	>10000	>10000	>10000	>10000	>10000	>10000	>10000	>10000	9100	>10000	>10000	7900	>10000	>10000
B	ppm	15	20	35	40	45	115	35	45	40	35	40	40	40	35	70	45	40	60	50	45
Rb	ppm	13	11	17	14	19	37	21	14	11	9	11	11	19	17	22	17	15	20	19	15
U	ppm	0.4	0.4	0.4	0.8	0.6	0.2	0.6	0.6	0.2	0.2	0.2	0.4	0.8	0.6	0.6	0.8	0.6	0.6	1.0	1.0
Total-S	%	0.047	0.060	0.081	0.097	0.094	0.054	0.085	0.088	0.094	0.104	0.097	0.088	0.097	0.098	0.078	0.093	0.720	0.059	0.225	0.241
SO4	%	<0.01	0.01	0.08	0.13	0.12	0.08	0.08	0.09	0.11	0.11	0.12	0.10	0.06	0.06	0.04	0.06	0.08	0.05	0.11	0.11
CO2	%	0.15	0.73	12.21	10.63	9.79	2.64	7.33	7.77	12.98	16.35	16.50	13.86	1.83	1.14	0.44	1.54	3.23	0.18	0.95	2.49

Appendix Table 6 Results of Chemical Analysis for Sampling Sediments (4)

Sample No.		94SDLC15	94SDLC15	94SDLC15	94SDLC15	94SDLC15	94SDLC18	94SDLC18	94SDCB01	94SDPG01	94SDPG01	94SDPG01	94SDPG01	94SDPG01	94SDPG01	94SDPG02	94SDPG02	94SDPG02	94SDPG02	94SDPG02	94SDPG05
		0-S	10-17	22-30	41-50	62-69	50-60GREEN	50-60MIX	MIX	A	B	D	E	F	G	A	B	C	D	E	A
SiO2	%	42.75	49.05	41.34	47.08	44.43	not/ss	20.14	25.50	40.98	50.71	39.51	35.55	39.06	41.99	51.62	47.55	49.43	44.59	50.01	28.87
TiO2	%	0.64	0.70	0.59	0.62	0.57	not/ss	0.08	0.26	0.62	0.96	0.35	0.54	0.51	0.62	0.74	0.75	0.75	0.57	0.63	0.10
Al2O3	%	13.20	17.99	14.29	16.60	14.26	not/ss	4.17	5.82	12.44	15.43	6.88	10.99	10.57	13.39	17.68	17.79	17.65	14.66	18.65	1.36
Fe2O3	%	7.81	8.42	8.15	8.58	8.13	not/ss	45.70	42.03	7.54	11.00	17.27	8.49	10.86	8.22	8.92	10.19	10.58	9.35	8.15	38.02
FeO	%	2.74	2.45	2.08	2.09	2.65	not/ss	0.52	0.49	2.06	1.53	1.18	1.47	2.21	1.47	2.39	2.23	3.52	2.91	2.38	0.29
MnO	%	0.30	0.19	0.29	0.21	0.23	not/ss	0.04	1.99	0.68	2.43	0.36	0.56	0.27	1.34	0.96	0.16	0.27	0.18	0.34	0.72
MgO	%	2.67	3.41	3.03	3.27	3.52	not/ss	1.34	1.83	2.45	3.21	2.61	2.37	2.58	2.74	3.48	3.71	4.70	4.92	3.23	1.22
CaO	%	15.08	9.85	15.77	10.71	13.56	not/ss	2.11	3.12	15.25	6.49	10.70	18.66	15.48	14.91	8.35	9.12	9.98	12.65	10.12	1.76
BaO	%	0.05	0.03	0.03	0.03	0.04	0.01	0.01	0.02	0.07	0.06	0.04	0.06	0.05	0.05	0.04	0.02	0.02	0.02	0.02	0.02
Na2O	%	2.90	3.33	2.67	3.30	3.03	not/ss	3.55	1.92	3.27	3.86	2.70	2.51	2.59	3.00	3.58	3.25	3.04	2.81	3.34	2.47
K2O	%	1.27	1.26	0.88	1.31	1.20	not/ss	0.15	0.74	1.53	2.92	1.60	0.85	1.16	1.38	1.86	1.24	1.19	1.10	1.12	0.58
P2O5	%	0.33	0.20	0.22	0.20	0.22	not/ss	0.90	1.04	0.34	0.54	0.17	0.22	0.20	0.25	0.24	0.19	0.17	0.17	0.19	1.76
CO2	%	8.03	1.54	7.96	3.04	5.76	not/ss	0.48	1.10	9.09	0.15	6.82	11.99	9.28	7.85	0.33	1.39	0.51	3.81	1.58	1.61
LOI	%	13.20	5.88	13.66	7.87	10.65	not/ss	19.72	16.32	15.35	3.40	16.78	19.20	16.82	13.12	2.73	6.85	1.84	9.02	5.10	23.42
Total	%	100.20	100.31	100.92	99.78	99.84	not/ss	97.91	100.59	100.52	101.01	98.97	100.00	100.15	101.01	100.20	100.82	99.62	100.04	100.90	100.30
Ag	ppm	0.02	<0.02	<0.02	<0.02	<0.02	<0.02	<0.2	<0.02	<0.02	<0.02	0.02	<0.02	0.02	0.06	<0.02	<0.02	<0.02	<0.02	<0.02	0.02
As	ppm	7.0	2.4	6.0	7.6	3.6	4100	>10000	3900	29.0	32.0	41.0	32.4	24.8	25.2	16.2	3.2	1.6	3.6	8.2	163.5
Cu	ppm	80.2	88.0	82.2	77.2	65.4	0.8	3.0	95.6	105.5	146.5	59.0	115.0	62.8	85.4	55.0	177.5	51.2	90.4	70.2	87.8
Hg	ppm	30	20	20	30	30	30	10	10	40	10	50	40	10	40	10	10	10	10	10	80
Pb	ppm	14.0	5.0	14.5	6.0	13.5	4.0	4.0	5.5	11.5	3.5	11.0	16.0	15.5	10.0	3.0	4.0	2.0	5.0	3.5	21.5
Sb	ppm	<0.2	<0.2	0.2	<0.2	<0.2	0.2	4	5.8	<0.2	0.4	0.8	<0.2	0.8	<0.2	<0.2	<0.2	<0.2	<0.2	<0.2	2
Zn	ppm	48	61	55	53	45	3	20	49	60	59	47	68	51	46	31	71	43	63	49	37
Ba	ppm	440	230	300	240	380	60	60	140	640	560	320	520	440	490	330	180	200	180	180	190
Cd	ppm	0.5	1.0	0.5	0.5	<0.5	<0.5	<0.5	<0.5	0.5	<0.5	1.0	0.5	0.5	<0.5	<0.5	0.5	1.0	0.5	0.5	0.5
Co	ppm	23	29	24	28	19	<1	1	75	23	30	21	25	20	26	32	28	35	31	29	41
Cr	ppm	39	26	31	26	60	88	40	46	22	21	13	27	22	15	18	30	37	103	18	9
Mn	ppm	2070	1430	1905	1605	1405	120	300	>10000	4550	>10000	2500	3770	1855	8740	6810	1210	2020	1285	2550	5480
Ni	ppm	19	14	20	20	20	4	8	32	28	25	18	21	17	15	15	14	17	27	14	12
P	ppm	1540	970	920	940	750	2880	3110	4470	1580	2430	800	1110	970	1210	1200	880	930	810	950	8350
Sr	ppm	695	739	742	743	574	117	139	246	644	499	411	718	609	713	582	652	691	490	697	366
Ti	ppm	0.2	0.1	0.1	0.1	0.2	<0.1	0.1	1.3	0.6	0.6	0.1	0.1	0.1	<0.1	0.1	0.1	0.1	<0.1	0.2	1
V	ppm	190	209	189	209	171	1990	856	317	174	318	111	165	189	205	229	227	261	228	175	195
Li	ppm	9	11	9	11	8	1	1	4	11	26	8	10	9	9	7	15	4	11	9	2
Cl	ppm	>10000	6700	>10000	8300	>10000	not/ss	>10000	8000	>10000	5100	>10000	>10000	>10000	9100	6200	5800	4200	9200	6000	>10000
B	ppm	50	34	55	50	45	not/ss	75	200	50	50	180	60	75	60	45	45	30	40	30	250
Rb	ppm	24	14	15	18	16	not/ss	<2	<2	24	33	32	14	17	17	21	17	19	18	11	<2
U	ppm	0.8	0.8	0.6	0.6	0.8	not/ss	1.0	14.2	0.6	1.0	<0.2	0.6	0.6	0.6	0.8	0.4	0.4	0.6	0.4	3.6
Total-S	%	0.099	0.062	0.154	0.132	0.098	not/ss	0.077	0.032	0.092	0.006	0.069	0.092	0.086	0.074	0.040	0.053	0.024	0.069	0.069	0.065
SO4	%	0.09	0.05	0.10	0.07	0.07	not/ss	0.08	0.03	0.11	0.03	0.07	0.10	0.07	0.07	0.01	0.04	0.02	0.04	0.06	0.07
CO2	%	8.03	1.54	7.96	3.04	5.76	not/ss	0.48	1.10	9.09	0.15	6.82	11.99	9.28	7.85	0.33	1.39	0.51	3.81	1.58	1.61

*not/ss : not sufficient sample

Appendix Table 7 Results of Microscopic Observation (Thin Section) (1)

					Volcanic rocks (fragments)																others		
					phenocrysts					Groundmass													
					Olivine	Augite	Hyperthene	Plagioclase	Fe-oxides	Olivine	Augite	Hyperthene	Plagioclase	Magnetite	Ilmenite	Apatite	Fe-Oxides	Todorokite	Birnessite	Glass	Foraminifer	Clay minerals	Scoria
1	94SBGC06	30-36	Fragments of basic rock and minerals	———						・	・	・	○	・		・	・	・					◎
2	94SBGC02	21-24	Fragments of basic rock and minerals	———							○	・	◎	・		・	・		◎		・		
			Augite basalt	intersertal texture		・		○															◎
3	94SBLC08	20-42	Fragments of basic rock and minerals	———							・	・	○	・					◎				
			Fragments of aphyric basalt	hyalopilitic texture															◎				
			fragments of basalt	vitric texture				○											◎				
			Hyperthene bearing augite andesite	intersertal texture		○	・	○											○				
			Fe-oxide with rock fragments	———													◎						
4	94SBBL09	14-15	Fragments of aphyric basalt	intersertal texture				・											◎				
			Fragments of augite basalt	intersertal to hyalopilitic texture		○		・											◎				
			Fragments of augite basalt to andesite	vitric to hyalopilitic texture		○		○											◎				
			Fragments of hyperthene bearing augite basalt	intersertal texture		○	・	○											◎				
5	94SBLC09	38-40	Fragments of basic rock and minerals	———									○							◎			◎
			Fragments of augite basalt	vitric texture		・		○											◎				
			Fragments of hyperthene bearing augite basalt	interserta to hyalopilitic texture		○	・	○											◎				
			Fe-hydrooxide with plagioclase and augite	———							・		・				◎		◎				
6	94SBLC13	UNDER	Pumice	———		・	・	○											◎				
			Scoria	———		・		○															
7	94SBGC15	28-29	Fragments of basic rock and minerals	———							○	・	○	・		・		○			○		◎
			Aphyric basalt	vitric to hyalopilitic texture															◎				
			Augite basalt	vitric to hyalopilitic texture			・	○											◎				
8	94SGGC16	32-33	Fragments of basic rock and minerals	———							○	・	○	・		・					○		◎
			Aphyric basalt	intersertal texture				・											◎				
			Porous aphyric basalt	vitric to hyalopilitic texture															◎				
9	94SDLC01	B	Porous aphyric hyperthene-augite basalt	variolitic to hyalopilitic texture				・			・	・	○						◎				
10	94SDLC03	D	Porous aphyric hyperthene-augite basalt	variolitic to hyalopilitic texture							・	・	○						◎				
11	94SDLC04	C	Porous aphyric hyperthene-augite basalt	variolitic to hyalopilitic texture							・	・	○						◎				
12	94SDLC05		Porous aphyric hyperthene-augite basalt	variolitic to hyalopilitic texture							・	・	○						◎				
13	94SDLC06	B	Porous aphyric hyperthene-augite basalt	variolitic to hyalopilitic texture							・	・	○						◎				
14	94SDCB01		Porous hyperthene-augite basalt	intersertal texture		◎	○	◎	・		○	○	◎				・		○				
15	94SDCB02		Hyperthene-augite basalt	intersertal texture		・	・	○			・	・	◎						◎				
16	94SDPG02	H	Hyperthene bearing augite basalt	variolitic to intersertal texture		○	・	○	・		○	・	◎	・	・				○				
17	94SDPG03	E	Hyperthene-augite andesite	vitric texture		○	・	○	・		・		・	・					◎				
18	94SDPG05	G	Porous aphyric hyperthene-augite basalt	variolitic to hyalopilitic texture		・	・	・			・	・	○						◎				
19	94SDPG05	C	Porous aphyric hyperthene-augite basalt	variolitic texture							○	・	◎						◎				
20	94SDPG07	B	Porous aphyric hyperthene-augite basalt	vesicular to hyalopilitic texture							・	・	○						◎				
21	94SDPG081	B	Hyperthene-augite basalt	intersertal(partly variolitic)texture		○	・	◎			○	・	○	・	・				・				

◎ : abundant ○ : common ・ : poor

Appendix Table 7 Results of Microscopic Observation (Polished Thin Section) (2)

					Volcanic rocks (fragments)															others		
					phenocrysts					Groundmass												
					Olivine	Augite	Hypersthene	Plagioclase	Fe-oxides	Olivine	Augite	Hypersthene	Plagioclase	Magnetite	Ilmenite	Apatite	Fe-Oxides	Todorokite	Birnessite	Glass	Foraminifer	Clay minerals	Scoria
1	94SDLC01	A	Fe-oxides(partly goethitized)														○						
2	94SDLC09	X-axis	Mn-oxides intergrowing in the pipe	nodular													·	·	·		○		○
3	〃	Y-axis	〃	nodular		·		·										·			◎		·
4	94SDLC10	A	Mn- and Fe- oxides with low refractivity	columnar-colloform, nodular				·									○	·	◎		·		·
5	94SDCB02	Mn	Fe-oxides	worm-like to feather-like													○						○
6	94SDPG01	H	Mn-oxides with both low and high refractivity	nodular, colloform crustified														·	◎				
7	94SDPG02	F	Mn-oxides	columnar-colloform, nodular														·	◎				○
8	94SDPG03	C	Mn- and Fe- oxides with medium to high refractivity	columnar-colloform, nodular		·		○									○	◎					○
9	〃	D	Mn- and Fe- oxides with medium to high refractivity	columnar-colloform, nodular		·		·									◎	◎					○

◎ : abundant ○ : common · : poor